Doctorate Program in Molecular Oncology
and Endocrinology
Doctorate School in Molecular Medicine

XX cycle - 2004–2007
Coordinator: Prof. Giancarlo Vecchio

Photodynamic therapy (PDT) induces a transient block of proteasome activity: implications of its combination with Aspirin

Angela Chiaviello

University of Naples Federico II
Dipartimento di Biologia e Patologia Cellulare e Molecolare
"L. Califano"

Administrative Location

Dipartimento di Biologia e Patologia Cellulare e Molecolare "L. Califano"
Università degli Studi di Napoli Federico II

Partner Institutions

Italian Institutions
Università di Napoli "Federico II", Naples, Italy
Istituto di Endocrinologia ed Oncologia Sperimentale "G. Salvatore", CNR, Naples, Italy
Seconda Università di Napoli, Naples, Italy
Università del Sannio, Benevento, Italy
Università di Genova, Genoa, Italy
Università di Padova, Padua, Italy

Foreign Institutions
Johns Hopkins School of Medicine, Baltimore, MD, USA
Johns Hopkins Krieger School of Arts and Sciences, Baltimore, MD, USA
National Institutes of Health, Bethesda, MD, USA
Ohio State University, Columbus, OH, USA
Université Paris Sud XI, Paris, France
Universidad Autonoma de Madrid, Spain
Centro de Investigaciones Oncologicas (CNIO), Spain
Universidade Federal de Sao Paulo, Brazil
Albert Einstein College of Medicine of Yeshiwa University, USA

Supporting Institutions
Università di Napoli "Federico II", Naples, Italy
Ministero dell'Istruzione, dell'Università e della Ricerca
Istituto Superiore di Oncologia (ISO)
Terry Fox Foundation, Canada
Istituto di Endocrinologia ed Oncologia Sperimentale "G. Salvatore", CNR, Naples, Italy
Centro Regionale di Competenza in Genomica (GEAR)

Faculty

Italian Faculty

Giancarlo Vecchio, MD, Co-ordinator
Salvatore Maria Aloj, MD
Francesco Beguinot, MD
Maria Teresa Berlingieri, PhD
Angelo Raffaele Bianco, MD
Bernadette Biondi, MD
Francesca Carlomagno, MD
Gabriella Castoria, MD
Angela Celetti, MD
Annamaria Cirafici, PhD
Mario Chiariello, MD
Vincenzo Ciminale, MD
Annamaria Colao, MD
Alma Contegiacomo, MD
Sabino De Placido, MD
Monica Fedele, PhD
Pietro Formisano, MD
Alfredo Fusco, MD
Massimo Imbriaco, MD
Paolo Laccetti, MD
Antonio Leonardi, MD
Barbara Majello, PhD
Rosa Marina Melillo, MD
Claudia Miele, PhD
Francesco Oriente, MD
Roberto Pacelli, MD
Giuseppe Palumbo, PhD
Silvio Parodi, MD
Giuseppe Portella, MD
Giorgio Punzo, MD
Antonio Rosato, MD
Massimo Santoro, MD
Giampaolo Tortora, MD
Donatella Tramontano, PhD
Giancarlo Troncone, MD
Bianca Maria Veneziani, MD
Giuseppe Viglietto, MD
Roberta Visconti, MD

Foreign Faculty

National Institutes of Health (USA)
Michael M. Gottesman, MD
Silvio Gutkind, PhD
Stephen Marx, MD
Ira Pastan, MD
Phil Gorden, MD

Johns Hopkins School of Medicine (USA)
Vincenzo Casolaro, MD
Pierre Coulombe, PhD
James G. Herman MD
Robert Schleimer, PhD

Johns Hopkins Krieger School of Arts and Sciences (USA)
Eaton E. Lattman, MD

Ohio State University, Columbus (USA)
Carlo M. Croce, MD

Albert Einstein College of Medicine of Yeshiwa University (USA)
Luciano D'Adamio, MD
Nancy Carrasco

Université Paris Sud XI (France)
Martin Schlumberger, MD

Universidad Autonoma de Madrid (Spain)
Juan Bernal, MD, PhD
Pilar Santisteban

Centro de Investigaciones Oncologicas (Spain)
Mariano Barbacid, MD

Universidade Federal de Sao Paulo (Brazil)
Janete Maria Cerutti
Rui Maciel

Photodynamic therapy (PDT) induces a transient block of proteasome activity: implications of its combination with Aspirin

"Non è il numero delle navi
o lo spessore della muraglia
che fanno la forza di una città,
ma la volontà dei suoi abitanti"

Tucidide

TABLE OF CONTENTS

LIST OF PUBLICATIONS

This dissertation is based upon the following publications:

Crescenzi E, Varriale L, Iovino M, **Chiaviello A**, Veneziani BM, Palumbo G. Photodynamic therapy with indocyanine green complements and enhances low dose cisplatin cytotoxicity in MCF-7 breast cancer cells. Mol Cancer Ther 2004; 3(5):537-44.

Crescenzi E, **Chiaviello A**[#], Canti G, Reddi E, Veneziani BM, Palumbo G. Low doses of cisplatin or gemcitabine plus Photofrin/photodynamic therapy: disjointed cell cycle phase-related activity accounts for synergistic outcome in metastatic non-small cell lung cancer cells (H1299). Mol Cancer Ther 2006; 5(3):776-85.
Chiaviello A is joint **first author**.

Coinu R, **Chiaviello A**[#]**,** Galleri G, Franconi F, Crescenzi E, Palumbo G. Exposure to modeled microgravity induces metabolic idleness in malignant human MCF-7 and normal murine VSMC cells. FEBS Lett 2006; 580(10):2465-70. # Chiaviello A is joint **first author**.

ABSTRACT

Photodynamic therapy (PDT) is a very attractive modality of cancer treatment especially in combination with other therapies. It is generally acknowledged that the principal cytotoxic effects of PDT is mediated by the production of reactive Oxygen species that directly damage sub-cellular components including membranes and proteins.

It has been shown that UPP system plays a pivotal role in the breakdown of the proteins that come unfolded in response to oxidative stress. To elucidate the role of UPP system in response to ROS-mediated damage, Photofrin-preloaded H1299 and A549 (respectively $p53^{-/-}$ and $p53^{+/+}$) were irradiated with halogen lamp equipped with bandpass filter using purposely sub-lethal dose (0.54 J/cm^2).

We have shown that the photodynamic treatment leads to a reversible decrease in proteasome activity, depending on ROS production, and to an increase in the accumulation of ubiquitinated proteins in both cell lines. PDT also resulted in an increase in the half life of various intracellular proteasome substrates as IκB and p27. We have also observed that the proteasome inhibition induces, 6 hours after the treatment, a significant accumulation of the cells in G_2 phase. In these conditions, this alteration of cell cycle profile of both cell lines was reverted at longer time while a complete recovery of clonogenic survival.

Considering that the prolongation of proteasome inhibition leads to cell death, we submitted the cells to a second photodynamic treatment during the proteasome activity lag phase. As expected, the second treatment prolonged this stall.

Since it has been demonstrated, that Aspirin may cause a block of proteasome activity with an undefined mechanism, we have investigated the possible implications for therapy deriving from a combined use of PDT with this non toxic drug. In our system we could demonstrate that the block of the proteasome activity upon Aspirin treatment, was concomitant with an accumulation of cells in the G_2 phase without apparent activation of apoptosis response and with restoration of their capacity to proliferate.

In order to inhibit the recovery of the clonogenic potential observed after single treatments (with PDT or Aspirin) we decided to test if the combination of the two treatment might have an additive effect, so favouring apoptotic response versus the recovery. It has been observed that the mode of administration of treatments (PDT followed by Aspirin or Aspirin followed by PDT) may determine the proteasomal activity. Indeed, an effective and prolonged stall is obtained only upon administration of Aspirin to cells previously submitted to photodynamic treatment. We could demonstrate that with this particular modality of treatment Aspirin sustains the PDT-dependent G_2 accumulation and concomitantly causes a decrease of clonogenic survival.

1. INTRODUCTION

1.1 Photodynamic therapy

Photodynamic therapy (PDT) is a minimally invasive therapeutic modality approved for treatment of many diffused human diseases, including macular degeneration, several dermatological disorders and cancer. Nowadays, PDT is finding increasing application for the treatment of lung, oesophageal, gynaecological, head and neck tumours. In particular PDT is considered the therapeutics treatment of choice of some precancerous lesions as Barrett's oesophagus, non-melanoma skin cancers and some forms of advanced cancers not otherwise easy to treat.

To now, PDT represents a very attractive modality of cancer treatment specially in combination with other conventional therapies as radio, immuno or chemo-therapy. Possibly this combined approach might consents the reduction of the drug dose and the side effects preserving the overall efficacy.

Historically, light has been used as therapy for more than three thousand years (Jain et al. 2002*)* but only at the end of the nineteenth century Niels Finsen used the word "phototherapy" to indicate the treatment of cutaneous tuberculosis with ultraviolet light (Ackroyd et al. 2001). The principle of photodynamic therapy (PDT) was first proposed about 100 years ago when researchers observed that a combination of light and certain chemicals could induce tissue-damage. In 1900 J. Prime, a neurologist, found that epilepsy patients who were treated with oral eosin developed dermatitis in sun-exposed areas. Later von Tappeiner and Jesionek treated skin tumours with eosin plus white light and demonstrated that this combination caused cell death. About thirty years after, Lipson and Baldes reported that the preparation of a non-toxic haematoporphyrin derivative (HPD) appeared to have a particular propensity to accumulate within neoplastic tissues. They, in fact, observed that injection of crude preparations of HPD led to fluorescence of neoplastic lesions visualized during surgery (Huettner et al. 2000). However, the clinical utility of PDT for tumour removal has been realised only in the 70's when Thomas Dougherty and co-workers showed that the topically administration of HPD and red light completely eradicated mammary and bladder tumour in mice.

Following the preliminary successes in the animal models , PDT was used in the human trials. Dougherty et al. treated with HPD-PDT 25 patients with a total of 113 primary or secondary skin tumours. A complete response was observed in 98 tumours, a partial response was observed in 13 tumours and 2 tumours were found to be treatment resistant (Dolmans et al. 2003).

1.2 Mechanism of PDT action

PDT is based on the systemic or local administration (by injection or by topical exposition to the skin) and the selective accumulation and/or retention of a photosensitizing agent (photosensitizer) in diseased tissue followed by irradiation with visible light of a wavelength matching the absorption spectrum of the photosensitizer.

Following the absorption of photons, the photosensitizer is promoted from its ground singlet to its excited singlet state, which, in turn, decays back to its ground state. Upon light activation, the photosensitizing agent transfers its excess energy to different substrates.
This phenomenon causes oxidative damage at in the immediate vicinities of the site in which photosensitizer accumulate. Importantly, a fraction of the excited singlet state molecules is transformed via intersystem crossing into the relatively long-lived (micro-to milliseconds) excited triplet state, which can either form free radicals or radical ions by hydrogen atom extraction or electron transfer to biological substrates (such as membrane lipids), solvent molecules or oxygen.
These radicals can interact with ground-state molecular oxygen to produce superoxide anion radicals, hydrogen peroxides and hydroxyl radicals. Such reaction is generally indicated as Type I reaction. Alternatively, from the excited triplet state the compound can transfer directly its energy to ground-state molecular Oxygen to form highly reactive singlet oxygen (ROS) (Fig. 1, Buytaert et al. 2007). Such reaction is generally indicated as Type II reaction.

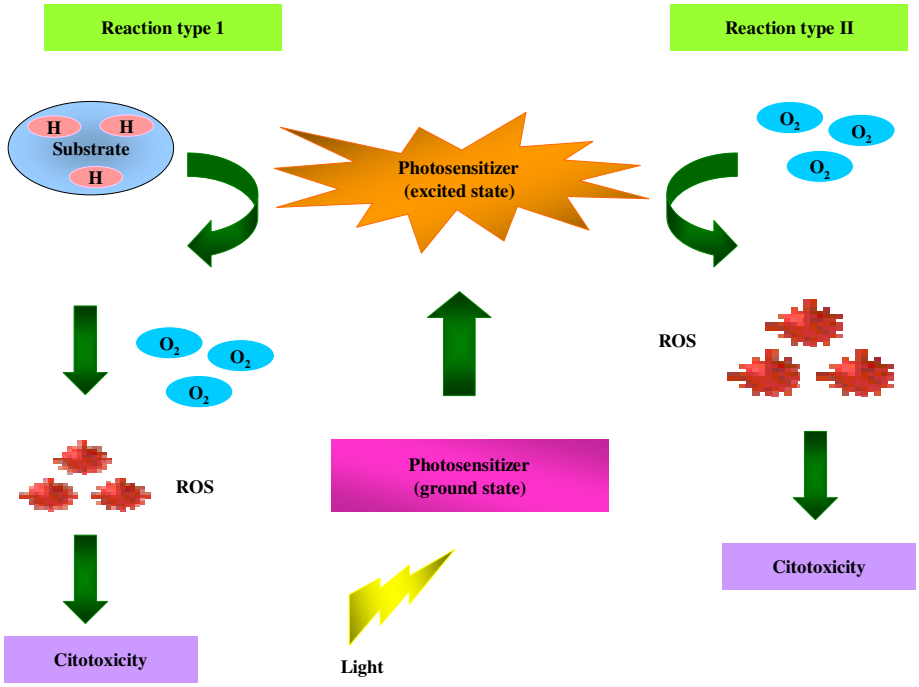

Figure 1: Mechanism of action of photodynamic therapy (PDT). PDT requires three elements: light, a photosensitizer and Oxygen. When the photosensitizer is exposed to specific wavelengths of light, it becomes activated from a ground to an excited state. As it returns to the ground state, it releases energy, which is transferred to Oxygen to generate ROS, such as singlet oxygen and free radicals, that mediate cellular toxicity.

Both these reactions occur simultaneously and while the ratio between them depends on the nature of the photosensitizer and the substrate molecules (Dougherty et al. 1998). Indeed, several direct and indirect evidences support a pivotal role for $^1O2$ in the molecular processes initiated by photo-activation (Niedre et al. 2002).

Photodynamic action induces damage only in cells that are proximal to the site of the ROS production (and consequently of photosensitizer localization) whereas surrounding tissues are poorly damaged. This is due to the fact that in biological system the half-life of singlet Oxygen is very short <0.04 μs, and, therefore, its radius of the action is less than 0.02 μm. The ROS that are produced during PDT have been shown to destroy target tissue by multifactorial mechanisms. In the case that the absorption of the exciting photons by the photosensitizer is followed by fluorescence emission, this event can be exploited for diagnostic purposes (Berg et al. 2005).

1.3 PDT's effect on tumour

It is now known that there are three main mechanisms by which PDT induces tumour destruction through direct ROS-mediated photodamage: a) direct cancer cell death b) destruction of the tumour-associate vasculature and c) possible activation of an immune response. The relative importance of each of these mechanisms on the tumour response has yet to be defined, although a combination of these processes. It is appears, however, that combination of all process is important in the long-term tumour control.

The photo-damage depends on many different factors. In particular it may result significant different in extent and cellular effect depending on the nature and dose of the sensitizer, the extra-cellular and/or intracellular localization, the time interval between the administration of the drug and light exposure, the light Dose (the total energy of exposed light across a sectional area of irradiated spot), the Fluence Rate of the light (the radiant energy incident per second across a sectional area of irradiated spot) and the Oxygen availability.

1.3.1 Direct tumour-cell killing

It is known that the PDT may have a direct effect on cancer cells and causing *in vivo* a decrease of the number of the clonogenic tumour cells (Henderson et al. 1985). Qualitatively, the photodynamic action may trigger apoptosis or may primer necrosis or autophagy. The balance between apoptosis and necrosis after PDT in vitro depends on several factors including the intracellular localization of photosensitizer and the light fluence (Oleinick et al. 2002).

The intracellular localization of photosensitizer depends on its chemical nature and this fact determines its sub-cellular distribution. The latter is finally responsible in ruling the cellular response to photodynamic damage (Noodt and al. 1999).

As already stated, the photo-generated singlet Oxygen, has a very short half-life and very limited diffusion capacity in biological systems. This implies that primary molecular targets of the photodynamic process must reside within few

nanometers from the dye. Generally, photoactive compounds that localize within mitochondria or ER promote apoptosis, within a certain threshold of oxidative stress, while activation of photosensitizer targeting either the plasma membrane or lysosomes can either delay or even block the apoptotic program predisposing the cells to necrosis (Oleinick et al. 2002). Therefore the localization of photoactive compounds depends also on the incubation time. In fact, several studies have demonstrated that the widely used photosensitizer Photofrin concentrates into different cellular compartments, according to incubation time. Photofrin accumulates in plasma membranes or cytoplasm upon brief incubation, and in the Golgi complex or RE upon prolonged incubation (Hsieh et al. 2003).
Indeed, some studies have reported on the re-localization of certain photosensitizers after irradiation suggesting that, besides the primary site, photodamage can be directed to other subcellular locations (Kessel 2002 and Marchal et al. 2007).
It is clear, the cellular response to PDT depends also on the light fluence. While apoptosis is the predominant mode of cell death when cells are photosensitized with low light doses, necrosis was observed at higher doses (Vantiegheman et al. 1998).
In recent time, a some papers have reported that sublethal photo-damage of a cell may trigger in its autophagy and promote cell survival (Buytaert et al. 2006). This is obtained by removing damaged organelles. Alternatively it may also promote cell death through excessive self-digestion or degradation of essential cellular constituents is generated (Gozuacik et al. 2004 and Tsujimoto et al. 2005).

1.3.2 Vascular damage

The viability of cancer cells depends on the amount of nutrients supplied by the blood vessels. In turn, formation and maintenance of blood vessels depend on growth factors produced by tumour or host cells (Carmeliet et al. 2000). Targeting the tumour vasculature is therefore one promising approach to cancer treatment.
PDT also has an effect on the tumour vasculature, whereby illumination and ROS production cause the shutdown of vessels and subsequently deprive the tumour of nutrients (Dolmans et al. 2002). It has been reported that PDT may induce vasculature collapse with consequent hypoxia of the neighbouring tissues and rapid thrombus formation in animal model. In particular, MV6401 (pyropheophorbide derivative) - a new photosensitizer - caused a biphasic vascular response following PDT. The most rapid response was vasoconstriction. This initial phase was followed three hours later by the formation of thrombus. Interestingly enough, these vascular effects were associated with a delay in tumour growth. Different studies with other photosensitizers, such Photofrin also reported vascular constriction, thrombus formation and inhibition of tumour growth (Fingar et al. 1997). On the other hand, expression of vascular endothelial growth factor (VEGF) and cycloxygenase (COX-2) — both potent angiogenic factors — were up-regulated during PDT (Ferrario et al. 2002). These effects were presumably due to the ROS formation and secondary hypoxia that was induced by PDT. Although most of these observation have been reported in the past, further

studies are required to definitively establish the long-term effects of PDT on tumour vasculature.

1.3.3 Immune response

In contrast to most cancer treatments that are prevalently immunosuppressive, PDT may exert a pro-inflammatory action. In this regard, several studies have demonstrated that PDT causes acute inflammatory and immune responses like expression of heat shock proteins, invasion and leukocyte infiltration of the tumour. In addition, PDT appears to increase the presentation of tumour-derived antigen to T cells (Castano 2006). PDT causes attraction of host leukocytes, lymphocytes, and macrophages into treated tumour tissue, by up-regulating the inflammatory cytokines interleukin (IL)-6 and IL-1 and by activating the neutrophil accumulation (Henderson et al. 1992; Korbelik 1996 and Gollnick et al. 1997).

In such regard it is of remarkable interest the observation that following sub-lethal photodynamic treatment of MCF-7 cells, the levels of HSP70 mRNA were increased (Nonaka et al. 2004). It is now known that HSP70, released from necrotic tumour cells, are non only able to inhibit tumour cell death by apoptosis but also to promote the formation of stable complexes with cytoplasm tumour antigens. These antigens can then either be expressed at the cell surface or escape intact from dying necrotic cells to interact with antigen-presenting cells (APCs) and stimulate an antitumour response (Castano et al. 2006).

Extra cellular HSP70 binds to high affinity receptors on the surface of APCs. This leads to the activation and maturation of dendritic cells, a process that enables the cross-presentation of peptide antigen cargo of HSP70 by the APCs to CD8 + cytotoxic T cells.

The release of HSP-bound tumour antigens that can easily be taken up by APC from PDT–induced necrotic tumour cells, may explain the efficiency of PDT in stimulating an immune response against tumours (Ahmad et al. 2004).

On the other hand, the evaluation of long term effects of Photofrin-PDT on tumour growth in normal Balb/C and immunodeficient mice showed that the tumour recurrence occurred more frequently in the immuno-compromised mice and that this effect was reversed by bone-marrow transplants from immuno-competent Balb/C donors. These results suggest that, whereas the direct effects of PDT can destroy the bulk of the tumour, the immune response may result very helpful in eliminating the survived cells (Korbelik et al. 1996).

Studies in this direction are actively going on to demonstrate such effect also in patients who received PDT.

Finally, recent experiments reported that a extracts from Photofrin/PDT treated cells could be used to vaccinate mice against the development of further tumours. Also this observation agrees with the hypothesis of a strong induction of tumour-specific immunity (Gollnick et al. 2002).

1.4 Photosensitezers

The most ideal photosensitizer would be a chemically pure drug with preferential uptake in tumour, rapid clearance from surrounding normal tissue, less skin photosensitivity, capacity to absorb light at longer wavelengths (to facilitate tissue penetration of the light), and minimal toxicity in dark.
In general, the photosensitizers used in human cancer therapy (including clinical trials) are intravenously infused but, in the case of patients with skin cancer, the topical application is an obvious alternative. The time between the injection and exposure to light may vary from drug to drug, according to the respective pharmacokinetic properties.

Most photosensitizers approved for use in humans in selected cases belong to the class of porphyrins and chlorines and include porfimer sodium, m-THPC, meta-tetrahydroxyphenylchlorin, verteporfin, and benzoporphyrin derivative monoacid ring A. Another important class of photosensitizer largely employed in dermatology (i.e., actinic keratosis) includes 5-aminolevulinic acid, methyl and benzyl aminolevulinate. In table 1 are shown several photosensitizers used in clinical trials or at preclinical stages.

Photosensitizers used in clinical and preclinical cancer studies				
Photosensitizer	***Trade name***	***Major Reported Uses***	***λ (nm)***	***Cellular localization***
Porfimer Na	Photofrin	Cervix, advanced and early lung, esophageal, bladder, superficial gastric, brain cancers.	~630	Golgi apparatus, Plasma membrane, ER
m-THPC	Foscan	Head and neck, (prostate, pancreas).	~650	ER, Mitochondria
BPD-MA, Verteporfin	Verteporfin	Basal-cell carcinoma	~690	Mitochondria, ER
5-ALA	Levulan	Basal carcinoma, head and neck, gynaecological cancer.	635	Mitochondria, Cytosol, membranes
Photosensitizers used in preclinical cancer studies and/or phase I-III clinical trials				
Mono-asparylchlorin e6 or Taloporfin Na, NPe6	Laserphyrin	Early endobronchial carcinoma. Preclinical studies.	664	Lysosomes, Endosomes
Disulphonate-Al-phtalo-cyanine	Photosens	Head and neck, other. Preclinical studies.	650 800	Golgi apparatus, Plasma
[5,10,15,20]-tetrakis-m-hydroxy phenyl-chlorin	SQN 400 mTHPBC	Liver metastasis. Preclinical studies.	740	ER
Pd-bact-pheophorbide	Tookad	Prostate (after radiation failure). Preclinical studies.	763	Mitochondria, Nucleus
2-[1-hexyloxyethyl]-2-devinyl pyropheophorbide	HPPH Photochlor	Esophageal cancers. Preclinical studies.	~665	Mitochondria
Photosensitizers used in preclinical cancer studies				
Sulphonated aluminum phthalocyanines	$ALPcS_n$	Animal studies, cell lines.	650 700	ER, Mitochondria
Hypericin		Cell lines	550-590	ER, Lysosomes
Indocyanine Green	ICG	Cell lines.	790	ER, Nucleus, Golgi apparatus

Table 1: The table show the most photosensitizers used in clinical trials or at preclinical stages and their sub-cellular localization (modified by Palumbo 2007).

1.5 Photofrin®

The development of Photofrin®, approved in 1993 in Canada for the treatment of bladder cancer, was a breakthrough in PDT research. Today this photosensitizer holds the largest number of approvals for clinical use.
In particular, Porfimer sodium is the most commonly photosensitizer used in Europe for the treatment of advanced stage lung cancer, in Japan for early-stage oesophageal, gastric and cervical cancer and in the United States for advanced oesophageal cancer (Almeida et al. 2004 and Dougherty 2002)

Photofrin® is a haematoporphyrin derivative. This is typically < 50% monomeric/dimeric porphyrins and > 50% oligomeric material. The latter fraction (porfimer sodium) has been partly purified in the commercial development of Porfimer sodium or Photofrin® (Fig. 2), which has been reported to be ~90% oligomeric material.

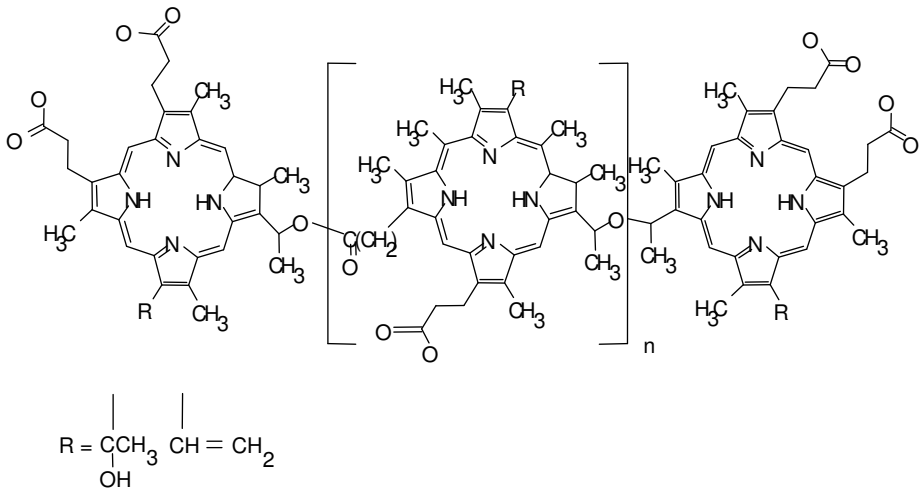

Figura 2: Photofrin®, the most popular photosensitizer used in PDT. Photofrin is a haematoporphyrin derivative. This is typically < 50% monomeric/dimeric porphyrins and > 50% oligomeric material. The latter fraction (porfimer sodium) has been partly purified in the commercial development of Porfimer sodium or Photofrin® which has been reported to be ~90% oligomeric material.

The advantages offered by Photofrin® include the possibility of using minimal drug and light doses (respectively 2.0 mg/kg and to 50 until 150 J/cm^2) and the good clearance from surrounding normal tissue (MÄkvy et al.1998). The drug, moreover, is not toxic and can be administered repeatedly, without consequences for the neoplastic patient.
Photofrin®, however, causes long-lasting cutaneous photosensitivity, as it is absorbed by the skin. For this reason, patients who have been treated with Porfimer sodium have to avoid sunlight for long time (Sibata et al. 2001).

However, there are some drawbacks with this photosensitizer because it is a mix of about 60 different compounds and therefore it is difficult to reproduce its

composition. In addition, Photofrin® is activated at λ 630 nm. At this wavelength the light scarcely penetrates human tissues and so is not suitable for non-superficial cancers.

Although, these latter observations have prompted researcher to discover and assay new photosensitizers, Photofrin® remains the most popular in PDT.

1.6 Subcellular targets of PDT

Because of the limited migration of $^1O_2$ from the site of its formation, sites of initial cell and tissue damage of PDT are closely related to the localization of the sensitizer (Peng et al. 1996). Although sensitizers can accumulate in different cellular compartment, the preferential sites are represented by the mitochondria and the endoplasmic reticulum (Table 1, Almeida et al. 2004).

1.6.1 Mitochondrial damage

It is now known that most photosensitizers localize in the mitochondria, and that, exerting their primary action there, rapidly induce apoptosis (Kessel 1998). The very early event after PDT treatment is the cytochrome c release from mitochondria (Ferri et al. 2001). Several studies showed, in fact, that in HeLa and in leukaemia cells treated with benzoporphyrin derivative (BDP) and Pc4, respectively, and light, cytochrome c, released into the cytosol immediately after exposure to light, activated caspases (Granville et al. 1998; Varnes et al. 1999). Studies based on different cell models and various sensitizers targeting mitochondria have shown that the cytocrome C release may rely on the induction of permeabilization of mitochondrial membranes probably due to variations of intracellular Ca^{2+} .

The released cytochrome C acts by forming a complex named apoptosome, that ultimately is responsible of activation of caspase 3, the final step of the apoptotic process. Furthermore, it was demonstrated that several sensitizers can activate caspase 8, and in turn caspase 3, by means of multimerization of the FAS/TNF receptor induced by singlet oxygen (Moore 2000).

Recently, numerous research groups has focused their studies on the function of Bcl-2 family in PDT in consideration of their relationship with mitochondria. The Bcl-2 family can be subdivided in two groups based on their role in apoptotic cell death: Bcl-2, Bcl-XL, Mcl-1 that have anti-apoptotic activity and Bax, Bak, Bid that are pro-apoptotic factors.

Bcl-2 is a protein, which is found in the outer membrane of the mitochondria, as well as in the endoplasmic reticulum and the nuclear envelope. It is known that over-expression of Bcl-2 can cause resistance to chemo-therapeutic drugs and radiations. In contrast the role of Bcl-2 in PDT is ambiguous.

It has been shown that the over-expression of Bcl-2 inhibited the DNA fragmentation and apoptosis in the Chinese hamster ovary cell lines (CHO) loaded with Pc4 and irradiated by the prevention of cleavage of pro-caspase 3 and 9 (Granville et al. 1999). The regulatory role of Bcl-2 in PDT has also been confirmed by trasfecting antisense Bcl-2 sequence in a retroviral vector into a

human gastric adenocarcinoma cell line. In this case a remarkable decrease of cell viability was observed.
It has also been reported that the event that protects the cells irradiated from apoptosis is a phosphorylation event of Bcl-2 at Ser 70, mediated by the action of CDK-1, during G2/M arrest (Vantieghem et al. 2002).

Very interestingly, it has been reported that PDT causes *in vivo* and *in vitro* a down-regulation of Bcl-2 antiapoptotic activity. Such down-regulation has been possibly explained assuming that Bcl-2 undergoes a conformational change or even an oxidative damage by PDT produced ROS (Castelli et al. 2004 and Moore 2000). In whole, these studies clearly indicate that PDT may induce specific post-traslational modification in Bcl-2 which may be a direct target of the photogenerated ROS or a down stream effectors of signal transduction.

1.6.2 Endoplasmic reticulum damage

In eukaryotes, the role of endoplasmic reticulum (ER) is linked to two specific functions: a) Ca^{2+} storage and signalling and b) folding, remodeling and sorting of newly synthesized proteins. Disturbances in any of these functions can lead to ER stress. It is now known that the ER stress may determine changes in protein folding and subsequent activation of the unfolded protein response (UPR).

The UPR is a primarily pro-survival response activated to reduce the accumulation and aggregation of unfolded or misfolded proteins and to restore normal ER functioning prevalently by the induction of molecular chaperones (Schroder et al. 2005). However, if ER stress persists, the UPR can activate a cell death program, which generally converges into the caspase-activation cascade.

The cellular stress in fact may trigger the activation of ER trans-membrane stress receptors: ER kinase (PERK), activating transcription factor 6 (ATF6) and inositol requiring enzyme 1 (IRE1). This event directs the translation of certain genes, such as that encoding for activating transcription factor 4 (ATF4) that may promote cell survival, through the induction of genes involved in restoring ER homeostasis, or favour apoptosis, through the induction of the transcription factor C/EBP homologous protein (CHOP). Importantly, the induction of CHOP leads to the down-regulation of expression of Bcl-2, which favours cytochrome c efflux and mitochondrial apoptosis. On other hand, the activation of RE stress receptors (and in particular of IRE1) may determine the recruitment of TRAF-2 in a complex to activate caspase 12 or the activation of JNK (c-Jun N-terminal kinase) and p38-MAPK, key molecules in the modulation of apoptosis induction.

Recent data indicate that following PDT, different heat shock proteins as well as the ER chaperones, GRP78/Bip, calreticulin, calnexin are induced in a time dependent manner (Mak et al. 2004).
In addition, it has been also demonstrated that several photosensitizers may cause the induction of CHOP, activation of the ER stress-mediated caspase-12 and apoptosis (Grebenova et al. 2003).
A recent genome-wide analysis in hypericin-PDT exposed bladder cancer cells (T24 cells) revealed that proximal molecular sensors and effectors of the UPR are induced in a coordinated manner (Buytaert E et al. 2007).

These studies uncover that perturbations in the ER caused by accumulation of photo-oxidated/misfolded proteins can persistently activate the UPR pathway. Hence the functional impact of the UPR on the modulation and efficiency of PDT-induced cell death in cancers should be further evaluated both *in vitro* as well as *in vivo*.

1.7 Ubiquitin- Proteasome pathway

The ubiquitin-proteasome pathway (UPP) strictly controls the degradation of most cellular proteins (~80%) in eukaryotes. It consists of two systems that work together: the ubiquitin-conjugating system and the proteasome (Fig. 3, Glickman et al. 2002). UPP plays a critical role in degradation of key signalling molecules that promote cell cycle progression, cellular adhesion, proliferation and induction of anti-apoptotic pathways *(*Voges et al. 1999). Accordingly, the proteasome is an attractive target for the cancer therapy. Recently, it has been shown that UPP system play a pivotal role in the degradation of many short lived functional proteins and in the breakdown of the proteins that come unfolded in response to oxidative damages. The reactive oxygen species, in fact, can promote the partial unfolding of the proteins, exposing hydrophobic domains to proteolytic enzymes constituting the proteasome core (Fribley et al. 2004*).*

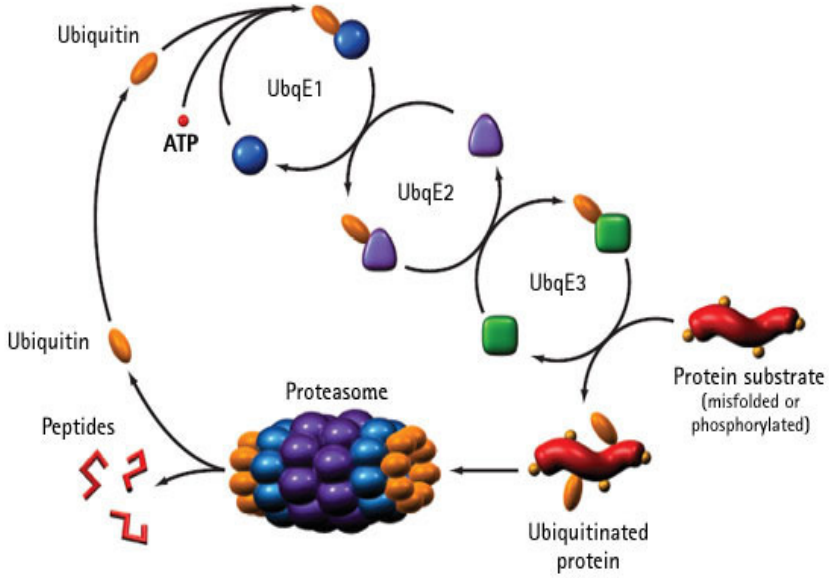

Fig 3: In the ubiquitin-proteosome degradation pathway, Ub is first covalently ligated to target proteins by a multi-enzymatic system consisting of Ubiquitin-activating (E1), Ubiquitin-conjugating (E2), and the Ubiquitin-ligating (E3) enzymes. Ubiquitinated protein is then escorted to the 26S proteasome where it undergoes final degradation and the ubiquitin is released and recycled

1.8 Mechanism of UPP action

The UPP is characterized by a cascades of controlled steps and represents a system finely conserved in the evolution.

The intracellular proteins are targeted for degradation by the conjugation of multiple molecules of ubiquitin (Ub). This process occurs through a multi-enzymatic system consisting of a Ub-activating (E1), Ub-conjugating (E2), and Ub-ligating (E3) enzymes, which act in a sequential manner and allowing the protein recognition by the proteasome (Adams 2003). The proteasome is a large multi-subunit protease complex that rapidly catalyzes the degradation of the Ubiquitin-tagged proteins (Ubiquitin is recycled the in an ATP dependent fashion, Almond et al. 2002). The proteasome is localized in the nucleus and cytosol and consists of two multisubunit functional components: a single catalytic 20S core and two regulatory 19S flanking regions.

The 20S core is comprised of four stacked rings (two outer α-rings and two inner β-rings), each comprising seven distinct but structurally related subunits termed α1-7 and β1-7, to form a cylindrical structure. The proteolytic activity is confined to the β–subunits (β1, β2 and β5), at the center of 20S core, and is characterized by 3 enzymatic activities: chymotrypsin-like, trypsin-like, and post-glutamyl peptide hydrolase-like. After the progressive degradation of the tagged protein, the protein substrate is release as small peptides (from 3 to 22 amino acids).

The regulatory 19S unit of the proteasome contains the polyubiquitin-binding sites and the isopeptidase activity necessary for the cleavage and release of Ubiquitin to the protein substrate. It also contains six different ATPases that unfold the protein substrate and facilitate its degradation.

1.9 Pharmacological inhibitors of proteasome system

It has been shown that the deregulation of UPP system is involved in the cell malignant transformation. Several studies on patient-derived chronic lymphocytic leukaemia (CLL) cells, in fact, have demonstrated that they are characterized by 3-fold higher levels of chymotrypsin-like proteasome activity than normal lymphocytes (Masdehors et al. 2000). It is now known that low levels of some, as p27 or p21, that are normally degradated by UPP system, are associated to worse prognosis (Zhan et al. 2002 and Spataro et al. 1997). On other hand, it has been shown that the fibroblasts transformed with *ras* and *c-myc* resulted up to 40-fold more susceptible to apoptosis than normal human lymphoblasts if treated with the peptidyl aldehyde MG-132, a proteasome inhibitor (Orlowski et al. 1998 and Guzman et al. 2002). It is been shown that the selective citotoxicity of proteasome inhibitors on cancer cells is probably due by the presence of intact checkpoints in the normal cells which allow the recover the damage.

Recently numerous synthetic and biologic drugs, that inhibit the UPP activity, have been identified. These inhibitors act prevalently on the core particle by binding irreversibly or reversibly the active sites with different activities. They include the already cited synthetic peptide aldehydes MG-132, and Lactacystin, Epoxomicin and the class of peptide boronic acids (Adams 2003).

Many of these compounds, however, while having a poor metabolic stability bind too tightly to their substrate. To date, the most promising proteasome inhibitor is the class of peptide boronic acids. These compounds are extremely selective for the proteasome by blocking the chymotrypsin-like activity but in a reversible manner. Within this class of peptides, the dipeptidyl boronic acid have the advantage of a relatively low molecular weight and simplicity of synthesis. The water-soluble dipeptidyl boronic acid Bortezomib is an extremely potent (K_i= 0,6 nM), reversible and selective proteasome inhibitor. It binds the proteasome with very high affinity and dissociates slowly, conferring stable but reversible proteasome inhibition (Kisselev et al. 2001).
Accordingly, Bortezomib (Velcade®) is the first proteasome inhibitor approved to the Food and Drug Administration for treatment of multiple myeloma.

One the first indications of potential use of Bortezomib in cancer treatment, was the results obtained screening 60 cell lines derived from multiple human tumours at National Cancer Institute (Bethesda, MD, USA). This screening indicated that Bortezomib potently inhibited the growth at very low concentration (~ 7 nM) inducing G_2-M cell cycle arrest and apoptosis (Ling et al. 2002 and Frankel et al. 2000).

The precise mechanism by which proteasome inhibitors induce cell death are yet to be fully established. However, it has been demonstrated the stabilization of several important proteins, often dysregulated in many human malignancies, are controlled by the proteasome including the inhibitor of the tumour suppressor p53, the cyclin and cyclin-dependent kinase inhibitors p21 and p27 and the nuclear factor NFκB (IκB) (Almond et al. 2002*).*

The control of NF- κB pathway by the inhibition of proteasome system is of particular interest in the cancer treatment. More recent evidence supports, in fact, the role of this nuclear transcription factor in tumorigenesis, in the suppression of apoptosis, in the enhancement of tumour cell invasiveness and metastasis, and in the induction of angiogenesis (Orlowski et al. 2002).

Under normal circumstances, NF−κB is sequestered in the cytoplasm and rendered inactive by its association with the inhibitor protein IκB that blocks its nuclear translocation. Furthermore, when the cells are stimulated by stress, the critical serine residues on IκB may be phosphorylated and the protein becomes a target for ubiquitination and degradation by the proteasome system. This event causes the traslocation of NFκB to the nucleus and the subsequent transcription of genes encoding for stress response enzymes, cell adhesion molecule, pro-inflammatory cytokine and anti-apoptotic proteins as Bcl-2. (Chen et al. 2000). The proteasome inhibition stabilizes, therefore, the complex IκB / NF−κB which renders NF−κB transcriptionally silent (Fig. 4).

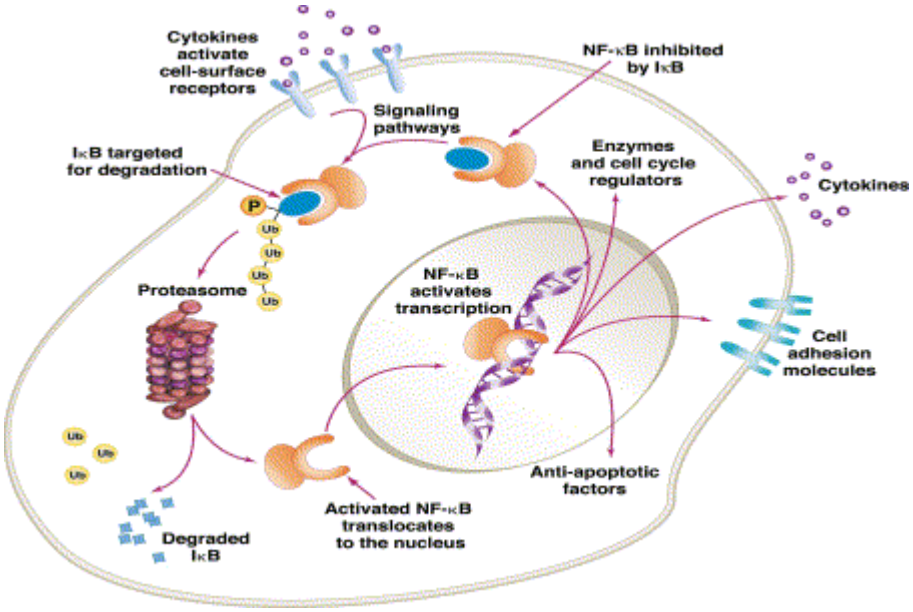

Fig. 4: NF-κB initiates pro-survival pathways. NF-κB is a pivotal regulatory protein, activating the transcription of a number of genes, including growth factors, angiogenesis factors, cell adhesion molecules, and anti-apoptotic factors. In quiescent cells, NF-κB is located in the cytoplasm and is bound to an inhibitor protein, IκB. When the cell is stimulated by stress, growth factors, radiation, etc., IκB is degraded by the proteasome and NF-κB becomes free to translocate to the nucleus, where it activates transcription. Proteasome inhibition stabilizes the IκB–NF-κB complex, which renders NF-κB transcriptionally silent (from Adams J 2003).

Accordingly, the expression of the "super-repressor" IκB in which critical serines are mutated to alanines (and cannot therefore be phosphorylated) prevents its proteasome-mediated degradation. In addition NF−κB remains sequestered in the cytoplasm, thereby mimicking the impact of proteasome inhibitors on this pathway. In a murine xenograft model of head and neck squamous cell carcinoma, expression of an IκB super-repressor, or treatment with Bortezomib, led to inhibition of tumour growth and angiogenesis and to down-regulation the vascular endothelial growth factor and NF−κB dependent pro-angiogenic cytokines (Sunwoo et al. 2001)

Recently it has been demonstrated that the combination of proteasome inhibitor with a chemotherapeutic agent may increase the overall anti-tumour efficacy. The use of Irinotecan or Gemcitabine combined with Bortezomib in pancreatic and colon cancer (LoVo) xenograft models, in fact, determined tumour regression, although neither Irinotecan, Gemcitabine nor Bortezomib had striking activity as single agent for these typically refractory cancers (Cusack et al. 2001). The reason for this additive activity is not clear. It is now known that the most of chemotherapeutic approaches as the treatment with antineoplastic drugs, i.e Irinotecan and Gemcitabine, or radiations may induce an up-regulation of NF−κB,

a transcriptional factor that initiates pro-survival pathways. In such regard, the use of Bortezomib, that alone causes a down-regulation of NF−κB, may provide an additional anti-tumour effect in cells that, constitutively or in response to traditional antineoplastic approaches, express high levels of this nuclear transcription factor.

1.10 A new inhibitor of proteasome system: Aspirin

Historically, the anti-inflammatory drugs had their origin in the unexpected discovery that several plants and their extracts may apply for the treatment of fever and inflammation. In the mid-19th century it has been developed the chemistry of salicylates and subsequently the acetyl-salicylic acid or aspirin.

The clinical utility of non-steroidal anti-inflammatory drugs (NSAIDs) results from their ability to inhibit the activity of cyclooxygenase (COX). COX is important in the transformation of arachidonic acid into prostanoids, prostaglandins and thromboxane A2 (Vane 1971). NSAIDs include not only Aspirin, first-generation non-selective inhibitors of both COX-1 and COX-2, but newer second-generation drugs that inhibit primarily COX-2. The two functional isoforms of COX, termed COX-1 and COX-2, play important roles. In particular, the activity of COX-2 is crucial in stress responses.

Recently, It has been shown that COX-2 is hyper-expressed in colon as well as in other human cancers (neck, breast, lung tumours). Several, but not all, epidemiological studies have reported a reduction in colon cancer incidence associated with the use of aspirin. (Giovannucci et al. 1995).

It is been recently demonstrated that low doses of Aspirin induces a proteasome dysfunction preventing the degradation of several substrates as p27, p21 and IκB. In particular the failed degradation of IkB may block the nuclear translocation and transactivation of NF-kB and the transcription of pro-survival genes.

Because the proteasome system is involved in the degradation of many short-lived proteins that are required for cell survival, it is clear that the dysfunction of this pathway may promote cell death. In fact, the block of proteasome system by Aspirin or other pharmacological inhibitors, promotes cell death by apoptosis in different human cell lines (Dikshit et al. 2006).

Several studies have demonstrated that the inhibition of proteasome activity causes apoptosis by two mechanisms: caspases activation (Bellosillo et al. 1998), and/or down-regulation of anti-apototic proteins, such as Bcl-2 (Zhang et al. 2000).

It has been demonstrated that Aspirin-mediated apoptosis in several cell lines may also depend on the arrest of cell cycle, probably because the large accumulation of proteins, such as p27 or p21 (Luciani et al. 2007). The inhibition of proteasome system, however, is related to the direct inhibition of the enzymatic activity or to the indirect inhibition of the various proteasome subunits. Further studies are however required to establish the molecular mechanism of proteasome inhibition by Aspirin in cancer.

2. AIM OF THE STUDY

Photodynamic therapy (PDT) is a minimally invasive therapeutic modality approved for treatment of many diffused human diseases including cancer. In fact, PDT is finding increasing application for the treatment of different tumours. Several observations from our own as well as other groups, indicate that photodynamic therapy acts on tumours through direct ROS-mediated photodamage. This action involves oxidative effects on cellular components including proteins. It has been shown that UPP system plays a pivotal role in the breakdown of the proteins that come unfolded in response to oxidative stress.

The aim of this work is to clarify the role of UPP system in response to ROS-mediated photodamage in cells. Since it has been demonstrated, that Aspirin may cause a block of proteasome activity, we have investigated the possible implications for therapy deriving from a combined use of PDT with Aspirin. To this purpose two lung cancer cell lines (H1299 and A549), notoriously resistant to conventional antineoplastic treatments, were selected.

3. MATERIAL AND METHODS

3.1 Cell Cultures

The H1299 human non–small cell lung cancer cell line was obtained from American Type Culture Collection (Rockville, MD). They were cultured in RPMI 1640, 2 mmol/L L-glutamine, 10 mmol/L HEPES, 1 mmol/L sodium pyruvate, 4,500 mg/L glucose, 1,500 mg/L sodium bicarbonate, 100 Ag/mL streptomycin, 100 units/mL penicillin, and 10% FCS. The H1299 cells are $p53^{-/-}$.

The A549 human non–small cell lung cancer cell line was obtained from American Type Culture Collection (Rockville, MD). They were cultured in Ham's F12K, 2 mmol/L L-glutamine, 1,500 mg/L sodium bicarbonate, 100 units/mL penicillin and 10% FCS. All media and cell culture reagents were purchased from Life Technologies (San Giuliano Milanese, Italy). The A549 cells are $p53^{+/+}$.

3.2 Materials

The Photofrin (the Hematoporphyrin derivative Porfimer sodium) used in this work was supplied as freeze-dried powder (lot no. 162A6-06; Axcan Pharma, Mont-Saint- Hilaire, Quebec, Canada). Its absorption spectrum consists of various peaks within the visible region. A Photofrin stock solution was prepared by dissolving the powder in water containing 5% glucose to obtain a final concentration of 2.5 mg/mL. This solution was stored in aliquots at -20°C in the dark. Before measurements, appropriate aliquots of this solution were diluted to the desired concentration.

Cells were routinely irradiated by a broadband light delivered with a PTL-Penta apparatus (Teclas, Sorengo, Switzerland) consisting of a halogen lamp (Osram 250 W, 24 V Osram, Munich, Germany) equipped with a bandpass filter (>80% transmittance in the 510 to 590 nm spectral region). The light was delivered through an 8-mm bundle of optical fibers placed at a distance from the cell plates that ensures uniform illumination of the entire cell monolayer. The fluence rate at the level of the cell monolayer was fixed at 6 mW/cm^2 and the light dose used was fixed at 0.54 J/cm^2.

Acetylsalicylic acid (Aspirin or ASA) used in this work was supplied as powder by Sigma Aldrich (St Louis USA). An Aspirin stock solution was obtained by its dissolution in TRIS 1 M pH 8,8 to a final concentration of 110 mmol/l. Before the use, appropriate aliquots of this solution were diluted to the desired concentration.

Cycloheximide used in this work was supplied as powder by Sigma Aldrich (St Louis USA). The Cycloheximide is an inhibitor of protein biosynthesis that blocks the translation of messenger RNA on cytosolic, 80 S ribosomes, but does not inhibit organelle proteine synthesis. The Cycloheximide stock was obtained by its dissolution in water to a final concentration of 100 mg/ml.

The proteasome inhibitor MG-132 was obtained from Calbiochem, La Jolla, CA. MG-132 is a peptide aldehyde that inhibits ubiquitin-mediated proteolysis by binding to and inactivating 20S and 26S proteasomes (Rock et al. 1994).

A stock solution of 150 µg/ml of this reagent (Z-leu-leu-CHO) was prepared in normal medium containing 7.5 µL per ml dimethylsulfoxide (DMSO).

The Dithiothreitol (DTT), efficient radical oxygen scavenger, was obtained from Sigma Aldrich (St Louis USA). A stock solution was prepared in water and conserved to -20 °C. Before use appropriate aliquotes were diluted.

3.3 Drug treatments

In individual experiments 400000 cells were incubated at 37°C in the dark with 2.5 µg/mL of Photofrin for 16 hours before irradiation or with Aspirin for 24 hours or 48 hours. In combined treatment the cells were incubated respectively with Aspirin (0-24 hours) and Photofrin (8-24 hours) or with Photofrin (8-24 hours) and, after irradiation, with Aspirin for 24 hours.

The effect of mono-therapy with PDT or with Aspirin or combined therapy were evaluated at the times indicated elsewhere by: a) by Trypan Blue and MTS assay, to check the cell viability, b) by Colony Forming Assay, to test the capacity to form colonies, c) by cytofluorimetry, to determine the cell distribution and ROS amount, d) by Western Blot, to analyze protein expression patterns.

3.4 MTS assay

Cell viability was assayed using CellTiter 96 Aqueous One Solution Non–Radioactive Cell Proliferation Assay (Promega, USA). According to the supplier, 5x 10^4 cells were seeded into 96-well plates, incubated with Aspirin (0, 5.0, 10.0 mm/L) for 24 or 48 hours. The cells subjected to PDT treatment were treated with Photofrin for 16 hours and then irradiated. Each culture condition was analyzed in triplicate. The absorbance values at 492 nm were corrected by subtracting the average absorbance from the control wells containing ‘‘no cells”.

3.5 Colony-forming efficiency

Colony forming efficiency assay was assayed in triplicate by seeding in 6 – well plates, 2 x10^4 cells which have survived to the various treatments: a) Aspirin 0 and 10 mmol/L b) PDT 0.54 J/cm^2 c) Aspirin followed by PDT d) PDT followed Aspirin. After 8 to 10 days, colonies (> 50 cells) were stained with 1% methylene blue in 50% ethanol.

3.6 Flow Cytometry

Dishes (10 cm) containing 4 x 10^5 H1299/ A549 cells were incubated for 24 hours at 37 ° C in 7 mL complete medium (controls) or in medium supplemented with Photofrin (2.5 µg/mL) alone or associated with Aspirin (5 e 10 mm/L) for 24 hours. Cells were exposed to single and/or combined treatments as described above and were then detached from the dishes by trypsinization, suspended in serum rich medium, centrifuged, washed twice with 1 mL PBS, and resuspended for storage (20°C) in 95% ethanol. Before analysis, fixed cells were washed twice, centrifuged, and resuspended in 1 mL PBS containing 1 µg RNase and 100 µg propidium iodide (Crescenzi et al. 2004). Samples were stored in the dark for 20 minutes at room temperature before final readings.

The cellular orange fluorescence of Propidium Iodide was detected in a linear scale using a flow cytometer (FACScan, Becton Dickinson, Mountain View, CA) equipped with an excitation laser line at 488 nm. About 30,000 events (i.e., fluorescence readings, corresponding to not less than 20,000 cells) were recorded for each sample. The cell cycle was examined after monotherapy and combined treatment at the indicated times. Data were analyzed with ModFit/LT (Verity Software, Topsham, ME).

3.7 Measurement of ROS production

Reactive oxygen species were detected with H_2DCFDA (Calbiochem). H_2DCFDA diffuses into the cells where it is converted into a non-fluorescent derivative (H2DCF) by endogenous esterases. H_2DCFDA is oxidized to green fluorescent DCF in the presence of intracellular ROS (Caro et al. 1996). Cells before PDT were washed and incubated at 37 °C in serum-free medium alone or in the presence of DTT 1 mM. After 30' the cells were incubated in the presence of H2DCFDA in serum-free medium. After 30' the cells were washed with Hank's, irradiated, detached by trypsinization and resuspended in phosphate-buffered saline, then analyzed immediately by flow cytometry using a FACScan Cell Scanner (BD Biosciences).

3.8 Western Blot Analysis

Total cell protein preparations were obtained by lysing cells in 50 mmol/L Tris (pH 7.5), 100 mmol/L NaCl, 1% NP40, 0.1% Triton, 2 mmol/L EDTA, 10 Ag/mL aprotinin, and 100 Ag/mL phenylmethylsulfonyl fluoride. Protein concentration was routinely measured with the Bio-Rad protein assay (Bradford 1976). Polyacrylamide gels (10–15%) were prepared essentially as described by Laemmli (Laemmli 1971). Molecular weight standards were from New England Biolabs (Beverly, MA).

Proteins separated on the polyacrylamide gels were blotted onto nitrocellulose filters (Hybond-C pure, Amersham Italia, Milan, Italy). Filters were washed and stained with specific primary antibodies and then with secondary antisera conjugated with horseradish peroxidase (Bio-Rad; diluted 1:2,000). Filters were developed using an electro-chemiluminescent Western blotting detection reagent (Amersham Italia) and quantified by scanning with a Discover Pharmacia scanner equipped with a Sun Spark Classic Workstation. The anti-Bcl-2 (100), p27 (C-19); Ikb (C-15) and actin (C-2) antibodies were from Santa Cruz Biotechnology (Santa Cruz, CA). Anti-tubulin (MCA77G) was from Serotec.

3.9 Cycloheximide experiments

H1299 cells were plated onto 100 mm cell culture dishes and an the following day, cells were incubated with Photofrin for 16 hours then washed twice and incubated with 40 μg of Cycloheximide. After three hours the cells were washed, irradiated and replaced in a fresh complete medium. Cells collected at each time point (1, 2, 3 and 6 hours) were then processed for immunoblotting using antibodies against IκB. Anti-Tubulin antibody has been used to normalize.

3.10 Immunoprecipitation

Dishes (10 cm) containing 4 x 10^5 H1299 cells were incubated for 24 hours at 37° C in 7 mL complete medium (controls) or in medium supplemented with Photofrin (2.5 μg/mL) for 16 hours or in medium containing 10 μM of MG-132 for 3 hours. Cells were exposed to photodynamic therapy (0.54 J/cm^2) as described above. Total cell protein preparations were obtained by lysing cells in RIPA buffer (1% Nonidet P40, 0.1% SDS, 0.5% sodium deoxycholate), 10 Ag/mL aprotinin, 100 Ag/mL phenylmethylsulfonyl fluoride, and phosphatase inhibitors (Sigma). Protein concentration was routinely measured with the Bio-Rad protein assay (Bradford 1976).To cell lysate sample was added 20 μl of anti-IκB (N-19) antibody, incubated overnight at 4°C, and gently mixed on a suitable shaker. The sample was treated with 40 μl of γ binding Sepharose, incubated overnight at 4°C, washed twice with RIPA buffer. Proteins separated on the polyacrylamide gels were blotted onto nitrocellulose filters (Hybond-C pure, Amersham Italia, Milan, Italy). Filters were washed and stained with anti-Ub (C-15) antibody and then with secondary antisera conjugated with horseradish peroxidase (Bio-Rad; diluted 1:2,000). Filters were developed using an electro-chemiluminescent Western blotting detection reagent (Amersham, Italia) and quantified by scanning with a Discover Pharmacia scanner equipped with a Sun Spark Classic Workstation.

3.11 Statistical analysis

All the data were expressed as mean ± SD. Significance was assessed by Student's *t* test for comparison between two means. P values of less than 0.05 were considered statistically significant.

4. RESULTS AND DISCUSSION

4.1 PDT induces ROS- mediated cell death

Several studies in vitro have demonstrated that PDT induce cell death in many cell lines. Investigations from our own as well as other groups evidenced that PDT may cause apoptosis or necrosis depending on many factors including the intracellular localization of photosensitizer and the light fluence (Oleinick et al. 2002 and Dennis et al. 2003). In this work we used two human cell lines, namely H1299 and A549, both derived from human non-small cell lung cancer (NSCLC) cells that differ for the key protein p53 which is null ($^{-/-}$) in the former and wild-type ($^{+/+}$) in the latter strain. Moreover, the A549 human lung adenocarcinoma cells are particularly resistant to conventional antineoplastic therapy (i.e. chemotherapy, radiation) while presenting high basal levels of NF-κB.

To have some insight on the molecular mechanism determining the increased susceptibility to PDT stress-induced cell death, we checked the radicals oxygen species (ROS) production at different light doses in the H1299 and A549 cell lines. As shown in Figure 5 when the light fluence increase from 0 to ~ 1.40 J/cm2, the ROS production is enhanced proportionally in both cell lines.

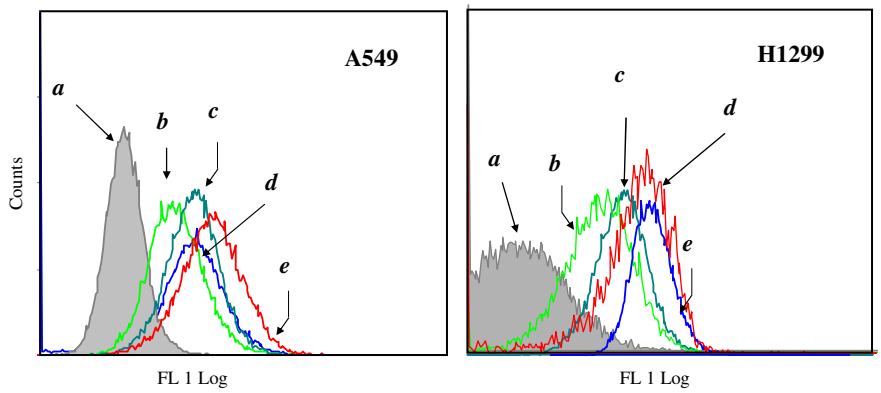

Figure 5: PDT induces ROS accumulation. H1299 and A549 cell lines were incubated with Photofrin (16 hours) then washed and incubated with 5 μM of H_2DCFDA in free serum medium. After 30' the cells were irradiated with different light doses (a, b, c, d, e from 0 to 1.40 J/cm2). The reactive oxygen species (ROS) were determined by cytofluorimetry.

The preliminary experiments consisted in assaying the effective role of reactive oxygen species (ROS). This has been done by comparing the viability, by MTS assay, of cells irradiated directly or pre- treated with 1 mM Dithiothreitol (DTT). As shown in Figure 6, DTT protects A549 (upper panel) and H1299 (lower panel)

cells from death. These data suggest that the cell death in both cell lines was due to an accumulation of ROS.

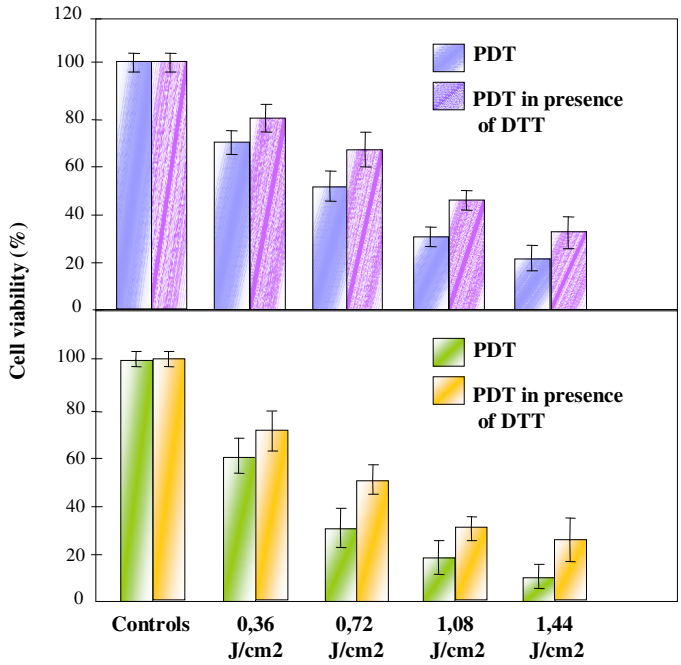

Figure 6: PDT induces ROS- mediated cell death. H1299 (upper panel) and A549 (lower panel) were irradiated and/or pre- treated with 1 mM Dithiothreitol (DTT). The cell viability was assessed by MTS assay 24 hours after treatment. Data are mean ± S.D. from three experiments.

4.2 Sub-lethal photodynamic treatment reversibly inhibits the proteasome function

The cytotoxic effects of PDT are mediated by the production of reactive oxygen species (ROS). Due to the high reactivity and unspecific choice of substrate, such species exert their harmful effects on the cell at the site where they are generated: in the nucleus they damage DNA, in the membranes fatty acids and in the cytoplasm target proteins. At low concentrations as 2.5 µg/mL and less than 24 hs of incubation, Photofrin is mostly concentrated in the cytoplasm (Hsieh YJ et al. 2003). In these conditions the major photodynamic effects concerns the cytosolic proteins.

Several in vitro studies have shown that the UPP system plays a major role in the breakdown of abnormal proteins that result from an oxidative stress. In fact, it is known that oxidation may damage and even irreversibly denature proteins. The resulting unfolded molecules are rapidly tagged with ubiquitin and successively degraded by the proteasome machinery (Fribley et al. 2004).

To explore the mechanism of stress response induced by a sub-lethal photodynamic treatment in the H1299 and A549 cell lines we analyzed the

expression profile of proteins, like as p27, IκB factor and Bcl-2. Such proteins are routinely processed by proteosomal degradation. In our experience, within two hours following the irradiation the expression levels of the proteins p27, IκB and Bcl-2 significantly increases (Fig.7). Such raise amounts to ~1.3-1.4 folds over the control. After two hours, however, the proteins expression levels tend to fade and return to the original (or lesser) value.

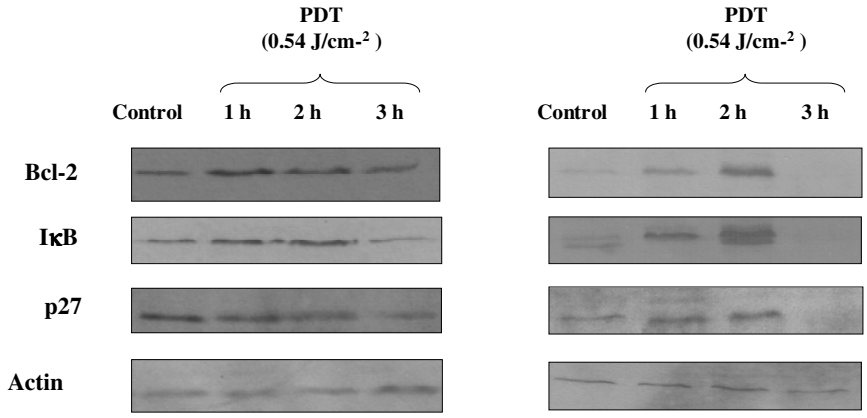

Figure 7: Sub-lethal photodynamic treatment reversibly inhibits the proteasome function. H1299 (right panel) and A549 (left panel) were incubated with Photofrin for 16 hours then irradiated (0,54 J/cm^2). The extraction of total proteins was performed 1, 2, 3 hours after PDT. The expression of Bcl-2, IκB and p27 was evaluated by Western Blot. Both panels show an increase of expression extended up two hours followed by fading or disappearance at longer time ≥ 3 hours. Anti- Actin antibody has been used to normalize.

While no earlier observations have been reported to now concerning p27 and IκB behaviour upon photodynamic treatment with Photofrin, the increase in the expression of Bcl-2 within the first two hours appears in contrast with previous observations (Ferrario et al. 2005). Other authors describe a direct Bcl-2 damage by photodynamic treatment with various photosensitizers (Xue et al. 2001 and Usuda et al. 2003), different photosensitizer concentrations and/or other experimental conditions (Ferrario et al. 2005).

Our findings suggest that Photofrin-PDT, at a dose of 0.54 J/cm^2, induces a transient stall of proteasome activity (< 3hs) in H1299 and A549 cell lines.

Within this window of light fluences, the H1299 and A549 viability remains at appreciable levels and does not noticeably change within 6 hours (decrease of ~ 30% respect to the control). It is noteworthy that in both cases at three hours post irradiation the proteasome appears to reactivate its function. The same result is obtained at higher (1.25 J/cm^2) (Fig. 8) while at lower energy (0.18 J/cm^2) the proteasome block is not even observed (not shown). The behaviour of A549 cells is fully super imposable to that of H1299 cells.

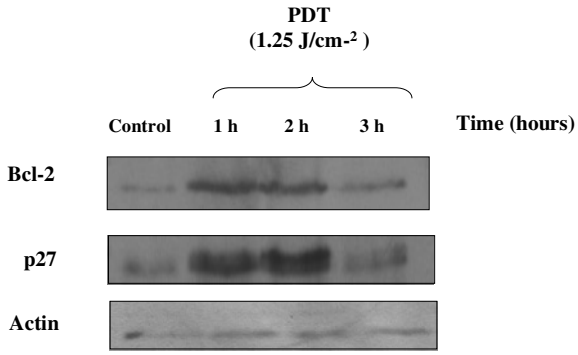

Fig. 8: High energy causes a transient block of proteasome activity. H1299 was incubated with Photofrin for 16 hours then irradiated at high energy (1,25 J/cm^2). The extraction of total proteins was performed 1, 2, 3, hours after the photodynamic treatment. The expression of Bcl-2 and p27 was evaluated by Western Blot. An increase of both proteins was shown at short time compared with the control. Anti-Actin antibody has been used to normalize.

4.3 PDT in presence of radicals oxygen scavengers is not able to inhibit proteasome activity

It has been demonstrated that the severity of cell damage, caused by different stimuli as radiation or chemotherapy, depends on the amount of ROS generated within the cell. A large production of ROS induces, in fact, the death of cancer cells by apoptosis or necrosis while small ROS production can activate other cellular pathways. To verify whether the increased production of ROS was responsible of the transient stall of proteasome activity, the cells subjected to Photofrin-PDT were pre-incubated with 1 mM Dithiotreithol (DTT) (fig. 9).

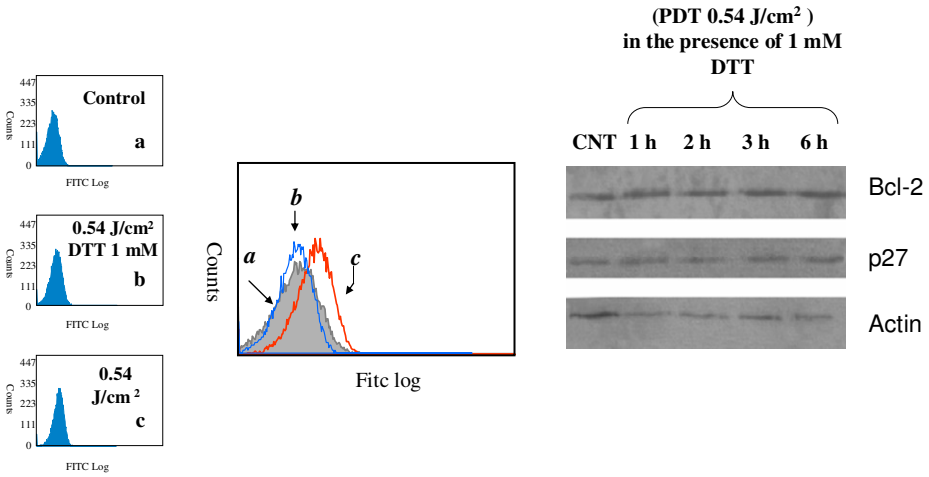

Figure 9: Dithiotreithol (DTT) effect on proteasome activity. H1299 cell line was pre-treated with DTT (1 mM) then irradiated. The extraction of total proteins was performed 1, 2, 3, 6 hours after the PDT. The expression of Bcl-2 and p27 was evaluated by Western Blot. The right panel shows that DTT abolished the proteasome stall. Left panel show confirmed that, at the same conditions, the cells pre-incubated with DTT are characterized by a decrease of ROS amount.

DTT is an efficient scavenger of oxygen radicals. The expression levels of target proteins was evaluated by western blot; the ROS levels were determined by flow cytometry. It is interesting that in these conditions the transient accumulation of Bcl-2, p27 and IκB proteins was no longer observed (as shown in Fig. 9). These results demonstrate that an effective inhibition of ROS formation prevented proteasome stall. Similar results were obtained by using another reducing agent as N-acetylcysteine (NAC), at a dose of 1 mM (not shown).

4.4 Photodynamic treatment increases the ubiquitination level of proteins

To investigate the mechanism of the proteasome malfunction, we evaluated the ubiquitination profile of the cells after photodynamic treatment. It has been shown, in fact, that the inhibition of proteasome function leads to an increased levels of ubiquitinated proteins. In general, when the cell is extensively damaged and/or when the injury concerns the external membrane, it rapidly proceeds to necrosis. When the damage is not such as to kill immediately, cells may recover in full, may decide to proceed toward apoptosis or activate an autophagic program. Depending on the intensity and location of an oxidative stress all these fates may be evoked. In any case, however, a number of cellular proteins will result irreversibly denatured as result of the oxidative stress.
The intracellular protein denaturation asks for the activation of cellular defence systems including ubiquitination of all those proteins that can not be rescued.

Our findings suggest that Photofrin-PDT at the dose of 0,54 J/cm^2 affects the ubiquitination profile of proteins extracted from irradiated cells as shown in Figure 10.

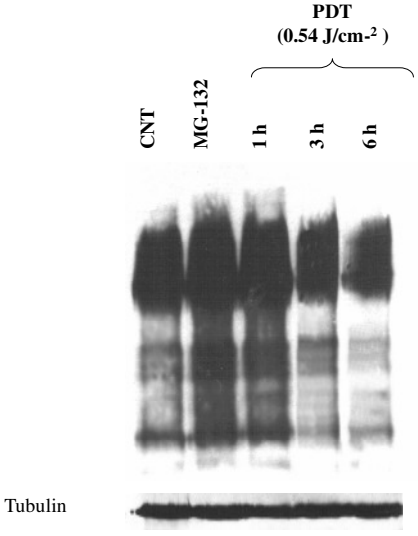

Figure 10: Photodynamic treatment increases the accumulation of ubiquitinated proteins. H1299 was incubated with Photofrin for 16 hour with 10 μM of MG-132 for 3 hours. After PDT (0.54 J/cm^2) the proteins extracted were immunoprecipitated with anti-IκB and ubiquitin-conjugated IκB was detected by Western blotting. Anti-Tubulin antibody has been used to normalize.

We observed that the accumulations of the ubiquitinated proteins is induced within two hours after the photodynamic treatment. It is noteworthy that, in these conditions, the ubiquitination profile is similar to that obtained by treating the cells with a known and specific pharmacological proteasome inhibitor, namely MG-132.
According with previous observation, three hours post incubation the ubiquitination profile is changed back to that of non- irradiated cells (control). It is also interesting that, following PDT at the indicated conditions, the protein ubiquitination machinery is preserved while the non-lysosomal proteasome-mediated protein digestion is ineffective.
The observation that after PDT the levels of ubiquitinated protein were increased has been required further investigations.

To this aim, the cells were incubated for three hours with 40 μg of Cycloheximide (CHX), a molecule that inhibits *de novo* protein biosynthesis before irradiation. After three hours the cells were washed, irradiated and replaced in a free-drug medium. Cells collected at each time point (1, 2, 3 and 6 hours) were then processed for immunoblotting using antibodies against IκB. As shown in Figure 11, the PDT treatment caused an increase in the accumulation of IκB, whose cytoplasmatic concentration is regulated by proteasome system.

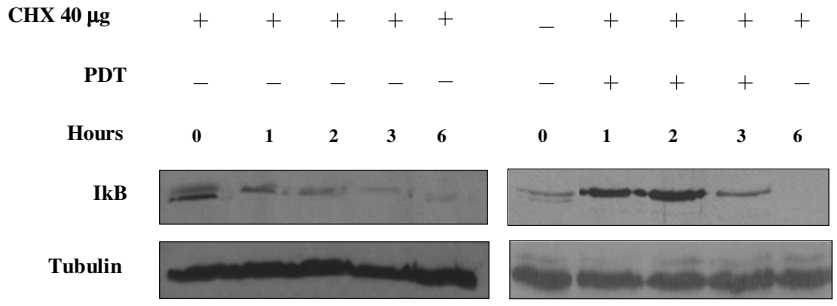

Figure 11: **Photodynamic therapy increases the stability of IκB.** H1299 cells was incubated for three hours with 40 μg of Cycloheximide (CHX) before irradiation. After three hours the cells were washed, irradiated and replaced in a free-drug medium. Cells collected at each time point (1, 2, 3 and 6 hours) were then processed for immunoblotting using antibodies against IκB. Anti-Tubulin antibody was used to normalize.

Such increase is due to the concomitant block of non-lysosomal protein degradation and the progressive (but not instantaneous) slowing down protein synthesis rate. As expected, three hours from exposure to light, IκB expression patterns changes back returning to the original profile. Accordingly, the up-regulation of the proteins studied does not depend on de novo synthesis.

4.5 Proteasomal inhibition induces G_2-M cell cycle arrest in photodamaged cells

The increased accumulation of some proteins whose destiny is regulated by proteasome system might result in the cell cycle arrest and apoptosis.
While no observations have been reported to now concerning cell cycle arrest mediated by proteasome inhibition after PDT, several studies have highlighted the relationship between the modifications of cell cycle profile and the treatment with pharmacological proteasome inhibitors.

To evaluate the effect of PDT on cell cycle distribution, both H1299 and A549 were irradiated and analyzed by flow cytometry 6 hours after the treatment. Our findings suggest (Fig. 12, panels b-e) that PDT affects the cell cycle profile in both cell lines. The photodynamic treatment promotes the accumulation of H1299 and A549 in the G_2 phase of the cell cycle.

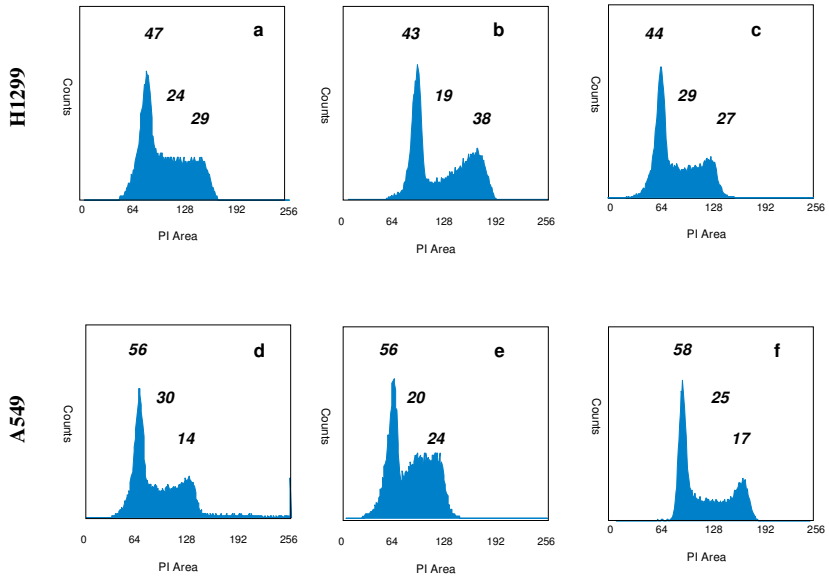

Figure 12: H1299 and A549 were incubated with Photofrin for 16 hours then irradiated. The cell cycle distribution was determined after 6 hours (panels b-e) and within 24 hours (panels c-f) after treatment, by cytofluorimetry. The cell cycle profile of controls were indicated in the panel a (H1299) and d (A549). Numbers, percentage of cells in G_1, S, G_2 phase.

To further investigate the effect of cell cycle arrest in H1299 and A549 cell lines, the cell cycle distribution within 24 hours after PDT has been evaluated. As shown in Figure 12 (panels c-f), the accumulation of the cells in G_2 was reduced and was accompanied by a re-establishment of the original profile (control) within 24 hours. In such regard, we evaluated the capacity of these cells to re-start proliferation. To this purpose, H1299 and A549 cell lines were irradiated, extensively washed and incubated in a fresh complete medium. After 8 days, the capacity of these cells to refurbish the normal proliferation and form colonies was

investigated. As shown in Figure 13**,** consistent with the re-establishment of normal cell cycle distribution, both cell lines recovery quite in full their ability to form colonies.

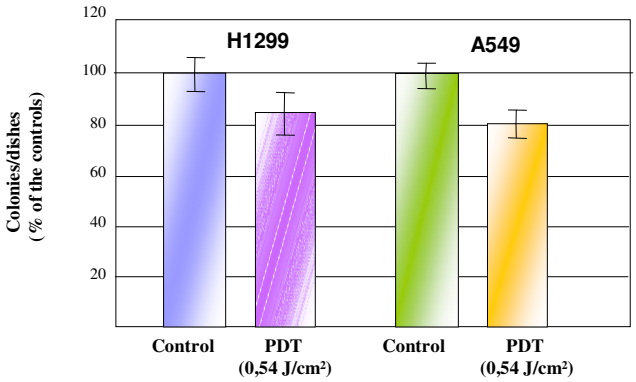

Figure 13: Effect of PDT on clonogenic survival. Triplicate samples of H1299 and A549 cells were incubated with Photofrin for 16 hours then irradiated. After 8 days, colonies were stained with methylene blue. Data are mean ±S.D. from three independent experiments.

Even the protein expression profile returns to the original patterns, as we already shown in a previous work (Crescenzi et al. 2006).

In conclusion, these data showed that the PDT treatment in both cell lines causes within 6 hours a significant accumulation of the cells in G_2 cell cycle phase. Furthermore, the altering of the expression profile and cell cycle were reverted within 24 hours after photodynamic treatment.

4.6 A second PDT treatment does not stabilize the proteasome stall.

We have shown that following PDT the proteasome activity is arrested for about two hours. We decided to study the effects of a second irradiation (at the same light dose) exactly at two hours after the first exposure to the light. The expression profiles of key proteins was evaluated by western blot 1, 2, 3 hours after to the second treatment. As shown in Figure 14**,** although the second treatment prolonged the proteasome inhibition, this block appeared reversible. Furthermore, the stall of proteasome activity was reversible and the cells restored their capacity to proliferate. These data show that a second treatment is not able to sustain the block of the proteasome system. Also in such case the cells recover their capacity to proliferate.

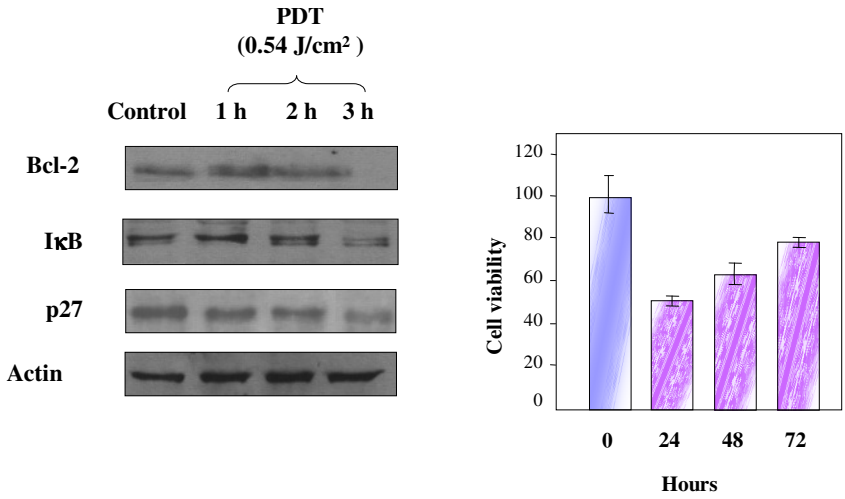

Figure 14:Effect of a second PDT treatment on proteasome activity. H1299 cell line was irradiated, washed and incubated for two hours. In this interval the proteasome system was fully blocked. After two hours the cells were subjected to a second photodynamic treatment at the same dose (0,54 J/cm^2). The proteins expression profiles was evaluated by Western Blot 1, 2, 3 hours after to the second treatment. The cell viability was determined by MTS Assay 24, 48, and 72 hours after the second treatment.

4.7 Aspirin reduces H1299 and A549 cells viability

To investigate the effect on proliferation of Aspirin, the H1299 and A549 carcinoma lung cancer cells were treated with Aspirin for 24 or 48 hours at two different concentrations (5 and 10 mM) as shown in Fig. 15.

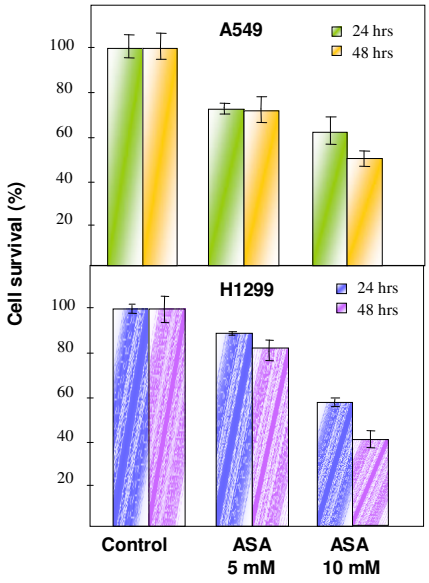

Figure 15: Aspirin (ASA) reduces NCI-H1299 and A549 cell viability. A549 (upper panel) and H1299 (lower panel) were treated with 5 and 10 mM of Aspirin (ASA) and incubated for 24 or 48 hours. The cell viability were assessed by MTS assay 24 hours after the treatment. Data are mean ±S.D. from three independent experiments

It appears that Aspirin treatment induced a concentration-dependent reduction in the viability of both cell lines as judged by MTS assay (fig. 15).

However, even after 48 hours of treatment with 10 mM Aspirin, the number of viable cells remained still elevated (~ 40%) and did not really change also at concentrations above 10 mM (not shown). It appears that 10 mM Aspirin inhibits transiently cell proliferation but it is not fully toxic to cells.

4.8 Aspirin at high concentration may induce G_2 accumulation

The arrest in cell proliferation observed upon Aspirin treatment of both cell lines requires the activation of specific cell cycle checkpoints. Previous observations on HCT116 have reported that low concentrations of Aspirin (≤5 mM) may induce a cell cycle arrest in G1 phase (Goel et al. 2003). However, Subbegowda et al. 1998 showed that the human colon cell lines, treated with high doses of Aspirin (> 5 mM), were able to bypass G_1/S checkpoint and favour G_2/M arrest. To unravel the relationship between Aspirin and cell responses, we analyzed the cell cycle profiles of H1299 and A549 treated for 6 or 24 hours with 10 mM Aspirin.

We report that, after 6 h incubation, both H1299 and A549 accumulated in S, while at longer incubation (24 hours) we observed a significant ammassing of cells in the G2 phase (amounting to ~ 37 % in H1299 and ~ 27 % in A549, respectively, Fig. 16).

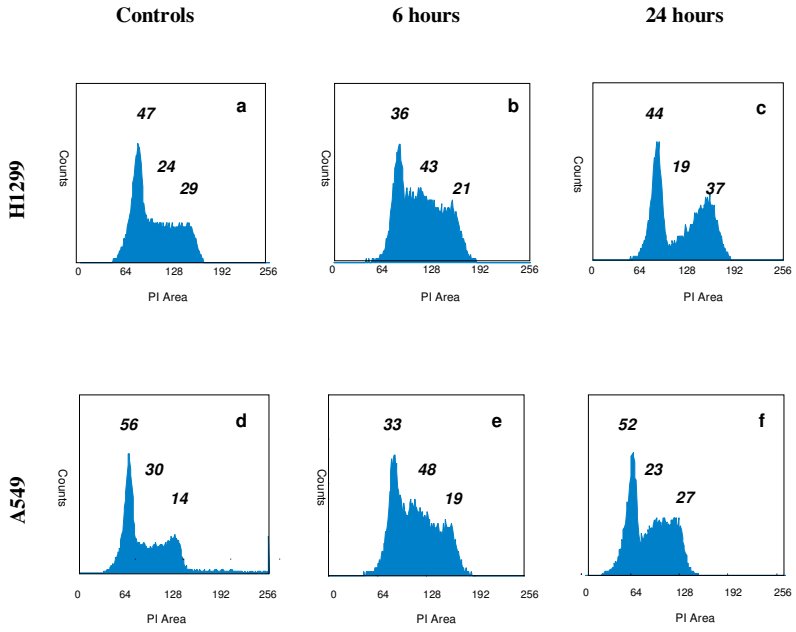

Figure 16: Effects of Aspirin (ASA) on cell cycle profile. H1299 and A549 were incubated with 10 mM of Aspirin for 6 (panels b-e) or 24 (panels c-f) hours. The cell cycle distribution was determined by cytofluorimetry. Numbers, percentage of cells in G_1, S, G_2 phase.

In the latter conditions the number of cells populating the sub-G_1 phase was rather small suggesting that the G_2 arrest was not accompanied by apoptosis.

Concomitantly, H1299 and A549 cell lines were assayed for viability by means of a clonogenic survival assay to detect the capacity of cells to recover the normal proliferation rate and form colonies. These data showed that both cell lines restored their full ability to form colonies (Fig. 17).

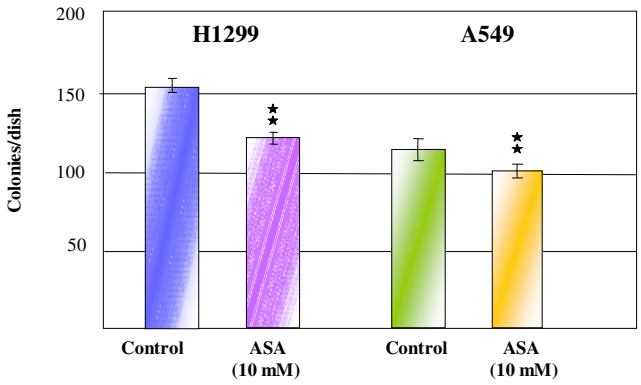

Figure 17: Effect of Aspirin (ASA) on clonogenic survival. Triplicate samples of H1299 and A549 cells were incubated with 10mM Aspirin (ASA) for 24 hours and replated in drug-free medium. After 8 days, colonies were stained with methylene blue. Columns, mean of three independent experiments. Statistical analysis was by unpaired Student's t test: **, $p < 0.002$; ***, $p < 0.0001$.

In conclusion, these data suggest that high concentrations of Aspirin induce two divergent effects in H1299 and A549 cells. At 6 hours cells from both lines, appear to accumulate in the S phase, while at longer times a significant G_2-M arrest is observed without apparent increase in apoptosis. Release of these cells in Aspirin-free medium rapidly restores their capacity to proliferate and to form colonies.

4.9 Even Aspirin may determine a reversible arrest of proteasome activity.

Recently, Diskshit et al. 2006 have demonstrated that the Aspirin treatment causes proteasome inhibition and apoptosis in Neuro 2a and HeLa cells. To evaluate the ability of Aspirin to affect the proteasome system in H1299 and A549 cells, these were treated for 1, 2, 3 and 6 hours with 10 mM Aspirin, washed and then lysed to extract the proteins. The expression profile of proteins that normally undergo proteosomal degradation like as p27, IκB was obtained by Western Blot analysis. A significant accumulation of these target proteins was rapidly observed within the first two hours of treatment with 10 mM Aspirin (Fig. 18 right panel). At longer times, however the same proteins were progressively disappearing. Now we demonstrate that Aspirin increases the ubiquitination level of IκB (Fig. 18 left panel). Even such stall, however, is not sustained for long since the cells re-start to proliferate if released in drug-free medium as discussed before (Fig. 17).

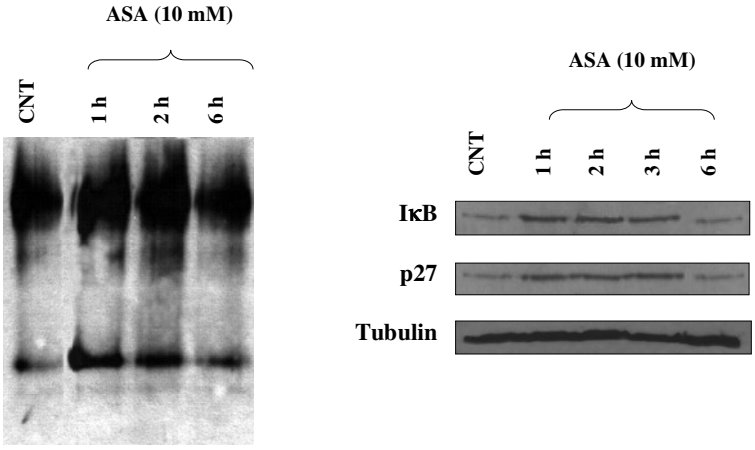

Figure 18: Aspirin (ASA) may determine a reversible arrest of proteasome activity. H1299 cells was treated with ASA 10 mM for 1, 2, 3, 6 hours then lysed to extract the proteins. The expression profile of p27 and IκB was obtained by Western Blot analysis. The antibody anti-tubulin was used to normalized. An increase of both proteins was shown within two hours compared with the control (right panel). The proteins extracted were immunoprecipitated with anti-IκB and ubiquitin-conjugated IκB was detected by Western blotting. An increase of ubiquitynation level of IκB was observed (left panel).

4.10 Aspirin sustains the PDT-dependent G_2 accumulation.

As already observed, the treatment with Aspirin or PDT of H1299 and A549 cell lines cell lines caused in both cases an accumulation of cells in G_2. We have now investigated the effects of the combined treatment (PDT + Aspirin). To this purpose both cell lines were incubated with Photofrin for 16 hours then washed and irradiated (0.54 J/cm2). Immediately after photodynamic treatment these cells were incubated with 10 mM of Aspirin for 24 hours and then analyzed by flow cytometry. As shown in Figure 19 (upper panel), the combined treatment (PDT followed by aspirin) sustains G_2/M accumulation with concomitant depletion of G1 phase in both cell lines.

When we have inverted the order of treatment (Aspirin followed by PDT) a different result was obtained. In this case, H1299 and A549 cell lines were incubated with Aspirin (for 24 hours) and Photofrin (16 hours) then washed and immediately irradiated at the same light dose as before. Cells were replaced in fresh medium and analyzed 24 hours later by flow cytometry. As shown in Figure 19 (lower panel), the accumulation of the cells in G_2 observed upon individual treatments (Aspirin or PDT) was significantly reduced, the entire profile resembling that of the controls.

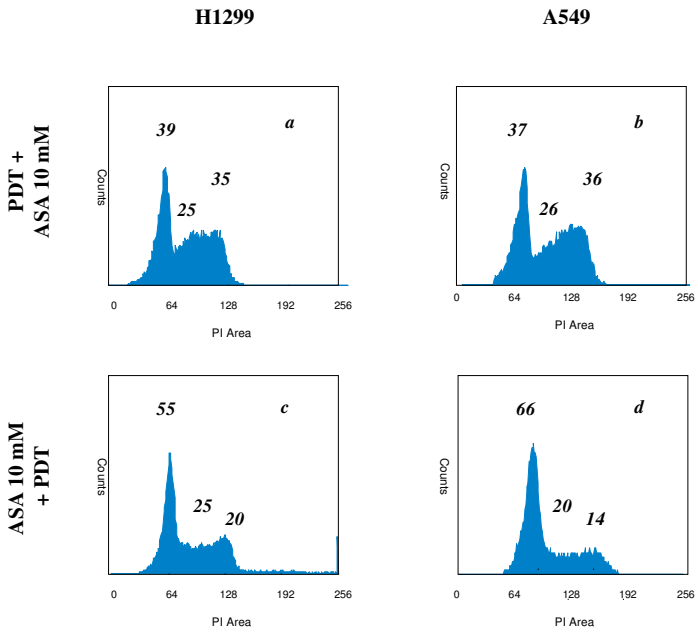

Figure 19: Aspirin sustains the PDT-G_2 arrest. H1299 and A549 were irradiated (0.54 J/cm^2). Immediately after photodynamic treatment were incubated with 10 mM of Aspirin for 24 hours and then analyzed by flow cytometry (upper panel). H1299 and A549 cell lines were incubated with Aspirin (for 24 hours) and Photofrin (16 hours) then irradiated at the same light dose. Cells were replaced in fresh medium and analyzed 24 hours later by flow cytometry (lower panel).

When the clonogenic assay was performed on cells under the two different regimens, we obtained results in agreement with cytofluorimetric data. In fact, as shown in Figure 20, cells that received Aspirin following PDT were not able to restore their clonogenic potential. Such behaviour may find explanation in the findings of Podhaisky et al. 1997 who demonstrated how Aspirin is able to regulate the proteins deputed to the protection against oxidative stress modulating ferritin expression. The ferritin is an iron-binding protein that, in addition to other functions, plays also an important role during oxidative stress by preventing iron-mediated formation of oxygen radicals. Another possibility is that Aspirin may directly scavenge the oxygen radicals (Bellosillo et al.1998).

In such conditions PDT becomes ineffective and Aspirin is destroyed. As shown in Figure 20**,** both cell lines pre-treated with Aspirin are characterized by a normal capacity of establishing new colonies. In this case the effect of Aspirin is clearly additive in respect to that caused by PDT. The whole set of data suggests that the modality of treatment is important and is by no mean equivalent.

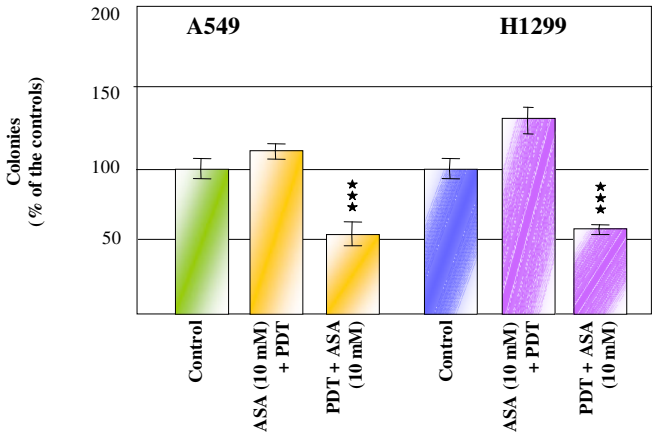

Figure 20: Effect of combined treatments on clonogenic survival. Cells were incubated for 24 hours with 10 mM of Aspirin then irradiated or subjected to PDT then incubated with 10 mM of Aspirin for 24 hours. The cells were replated in drug-free medium. After 8 days, colonies were stained with methylene blue. Columns, mean of three independent experiments. Statistical analysis was by unpaired Student's *t* test: **, $p < 0.002$; ***, $p < 0.0001$.

5. CONCLUSIONS

Photodynamic therapy (PDT) is a minimally invasive therapeutic modality approved for treatment of many diffused human diseases, including macular degeneration, several dermatological disorders and cancer. Nowadays, PDT represents a very attractive modality of cancer treatment specially in combination with other conventional therapies as radio, immuno or chemo-therapy.

In the present study we show that PDT leads to a reversible decrease in proteasome activity and a significant modification of cell cycle profile in two human non–small cell lung cancer cell lines. In both cases, the alteration of cell cycle profiles was reverted within 24 hours. In addition, cells recovered completely the clonogenic survival.

Since it has been demonstrated, that Aspirin may cause a block of proteasome activity with a mechanism that still awaits full clarification, we have investigated the possible implications for therapy deriving from a combined use of PDT with this non toxic drug. Our data suggest that Aspirin may sustain the PDT G_2-accumulation and concomitantly causes a decrease of clonogenic survival. Furthermore, a positive therapeutic effect is observed only when Aspirin administration follows the photodynamic treatment.

In conclusion, appropriate doses of photosensitizer and light combined with low doses of a non toxic drug represent a promising strategy of treatment in cancer.

In principle, combinations of PDT with non-toxic drugs, as Aspirin, would not only destroy cancer cells more efficiently but, being essentially side-effects-free, would also result more acceptable to patients.

6. ACKNOWLEDGEMENTS

I thank *Prof. Giuseppe Palumbo* who gave me the possibility to work in his laboratory and to learn that the science is passion and dedication.

I would like to thank *Prof. Giancarlo Vecchio* who let me attend this Doctorate program under his supervision.

Thanks to *Dr.ssa Roberta De Mattia* who was a friend and collegue, a rare gift…

Thanks to *Dr.ssa Ilaria Postiglione* and all the member of Palumbo's Lab for the hours spent in joyful atmosphere.

Thanks to my sister *Debora* for encouragements daily received.

I lovely thank *Gaetano* for his presence in my life.

Finally I would like to thank my *parents* who gave me the opportunity to follow my way.

7. REFERENCES

Ackroyd R, Kelty C, Brown N and Reed M. The history of photodetection and photodynamic therapy. Photochem Photobiol 2001; 74: 656–69.

Adams J. The proteasome: structure, function and role in the cell. Cancer Treatment Rev 2003; 29: 3-9.

Ahmad M, Rees RC and Ali SA. Escape from immunotherapy: possible mechanisms that influence tumour regression/progression. Cancer Immunol Immunother 2004; 53: 844-54.

Almeida RD, Manadas BJ, Carvalho AP, Duarte CB. Intracellular signaling mechanisms in photodynamic therapy. Biochimica et Biophysica Acta 2004; 1704: 59– 86.

Almond JB, Cohen GM. The proteasome: a novel target for cancer chemotherapy. Leukemia 2002; 16: 433–43.

Almond JB, Cohen GM. The proteasome: a novel target for cancer chemotherapy. Leukemia 2002; 16: 433–43.

Bellosillo B, Piqué M, Barragán M, Castaño E, Villamor N, Colomer D, Montserrat E, Pons G, Gil J. Aspirin and salicylate induce apoptosis and activation of caspases in B-cell chronic lymphocytic leukemia cells. Blood 1998;92(4):1406-14.

Berg K, Selbo PK, Weyergang A, Dietze A, Prasmickaite L, Bonsted A, Engesaeter BO, ngell-Petersen E, Warloe T, Frandsen N, Hogset A. Porphyrin-related photosensitizers for cancer imaging and therapeutic applications. J Microsc 2005; 218 :133–47.

Bradford M. A rapid and sensitive method for the quantitation of microgram quantities of protein utilizing the principle of protein-dye binding. Anal Biochem 1976; 72: 248–54.

Buytaert E, Callewaert G, Hendrickx, Scorrano L, Hartmann D, Missiaen L, Vandenheede JR, Heirman I, Grooten J, Agostinis P. Role of endoplasmic reticulum depletion and multidomain proapoptotic BAX and BAK proteins in shaping cell death after hypericin-mediated photodynamic therapy. FASEB J 2006; 20: 756–58.

Buytaert E, Dewaele M, Agostinis P. Molecular effectors of multiple cell death pathways initiated by photodynamic therapy. BBA 2007; 1776: 86-107.

Carmeliet P and Jain RK. Angiogenesis in cancer and other diseases: from genes to function to therapy. Nature 2000; 407: 249–57.

Caro A. and Puntarulo S. Effect of in vivo iron supplementation on oxygen radical production by soybean roots. Biochim Biophysi Acta 1996; 1291(3): 245-51.

Castano AP, Mroz P, Hamblin MR. Photodynamic therapy and antitumour immunity. Nature Review of Cancer 2006; 6: 535- 45.

Castelli M, Reiners JJ, Kessel D. A mechanism for the proapoptotic activity of ursodeoxycholic acid: effects on Bcl-2 conformation. Cell Death Differ 2004; 11: 906–14.

Chen C, Edelstein LC, Gelinas G. The Rel/NF-kB family directly activates expression of the apoptosis inhibitor Bcl-x(L). Mol Cell Biol 2000;20: 2687-95.

Crescenzi E, Varriale L, Iovino M, Chiaviello A, Veneziani BM, Palumbo G. Photodynamic therapy with indocyanine green complements and enhances low-dose cisplatin cytotoxicity in MCF-7 breast cancer cells. Mol Cancer Ther 2004; 3: 537–44.

Cusack JC, Liu R, Houston M, Abendroth K, Elliott PJ, Adams J, Baldwin AS Jr. Enhanced chemosensitivity to CPT-11 with proteasome inhibitor PS-341: implications for systemic Nuclear Factor- Kappa B inhibition. Cancer Res 2001; 61:3535-40.

Dikshit P, Chatterjee M, Goswami A, Mishra A, Jana NR. Aspirin induces apoptosis through the inhibition of proteasome function. J Biol Chem 2006; 281(39): 29228-35.

Dolmans DE, Fukumura D, Jain RK. Photodynamic therapy for cancer. Nat Rev Cancer 2003; 5:380-7.

Dolmans DE, Kadambi A, Hill JS, Waters CA, Robinson BC, Walker JP, Fukumura D, Jain RK. Vascular accumulation of a novel photosensitizer, MV6401, causes selective thrombosis in tumour vessels after photodynamic therapy. Cancer Res 2002; 62:2151-56.

Dougherty TJ, Gomer CJ, Henderson BW, Jori G, Kessel D, Korbelik M, Moan J, Peng Q. Photodynamic therapy. J Natl Cancer Inst 1998; 90: 889–905.

Dougherty TJ. An update on photodynamic therapy applications. J Clin Laser Med Surg 2002; 20: 3 –7.

Ferrario A, Fisher AM, Rucker N, Gomer CJ. Celecoxib and NS-398 enhance photodynamic therapy by increasing in vitro apoptosis and decreasing in vivo inflammatory and angiogenic factors. Cancer Res 2005; 65(20): 9473-8.

Ferrario A, von Tiehl K, Wong S, Luna M, Gomer CJ. CycloOxygenase-2 inhibitor treatment enhances photodynamic therapy-mediated tumour response. Cancer Res 2002; 62: 3956–61.

Ferri KF, Kroemer G. Organelle-specific initiation of cell death pathways. Nat Cell Biol 2001; 3: 255–63 .

Fingar VH, Wieman TJ, Haydon PS. The effects of thrombocytopenia on vessel stasis and macromolecular leakage after photodynamic therapy using Photofrin. Photochem Photobiol 1997; 66: 513–17.

Frankel A, Man S, Elliott P, Adams J, Kerbel RS. Lack of multicellular drug resistance observed in human ovarian and prostate carcinoma treated with proteasome inhibitors PS-341. Clin Cancer Res 2000; 6: 3719-28.

Fribley A, Zeng Q, Wang CY. Proteasome inhibitor PS-341 induces apoptosis through induction of endoplasmic reticulum stress-reactive oxygen species in head and neck squamous cell carcinoma cells. Mol Cell Biol 2004 ; 24: 9695-704.

Giovannucci E, Egan KM, Hunter DJ, Stampfer MJ, Colditz GA, Willet WC and Speizer FE. Aspirin and the risk of colorectal cancer in women. N Engl J Med 1995 Sep 7;333(10):609-14 N Eng J Med 1995; 333: 609-14.

Glickman MH, Ciechanover A. The ubiquitin-proteasome proteolytic pathway: destruction for the sake of construction. Physiol Rev 2002; 82: 373–428.

Goel A, Chang DK, Ricciardiello L, Gasche C, Boland CR. A novel mechanism for aspirin-mediated growth inhibition of human colon cancer cells. Clin Cancer Res 2003; 9(1): 383-90.

Gollnick SO, Liu X, Owczarczak B, Musser DA, Henderson BW. Altered expression of interleukin 6 and interleukin 10 as a result of photodynamic therapy in vivo. Cancer Res 1997; 57: 3904–9.

Gollnick SO, Vaughan L, Henderson BW. Generation of effective antitumour vaccines using photodynamic therapy. Cancer Res 2002; 62: 1604–08.

Gozuacik D and Kimchi A. Autophagy as a cell death and tumour suppressor mechanism. Oncogene 2004; 23: 2891–906.

Granville DJ, Carthy CM, Jiang H, Shore GC, Mcmanus BM, Hunt DW. Rapid cytochrome c release, activation of caspase 3, 6 7 and 8 followed by Bap31 cleavage in HeLa cells treated with photodynamic therapy. Febs Letters 1998; 437: 5-10.

Granville DJ, Jiang H, An MT, Levy JT, McManus BM, Hunt DW. Bcl-2 over-expression blocks caspase activation and downstream apoptotic events instigated by photodynamic therapy. Br J Cancer 1999; 79: 95– 100.

Guzman ML, Swiderski, CF, Howard DS, Grimes BA, Rossi RM, Szilvassy SJ and Jordan CT. Preferential induction of apoptosis for primary human leukemic stem cells. Proc Natl Acad Sci USA 2002; 99: 16220–25.

Henderson BW and Dougherty TJ. How does photodynamic therapy work? Photochem Photobiol 1992; 55:145–57.

Henderson BW, Waldow SM, Mang TS, Potter WR, Malone PB, Dougherty TJ. Tumour destruction and kinetics of tumour cell death in two experimental mouse tumours following photodynamic therapy. Cancer Res 1985; 45: 572–76.

Hsieh YH, Wu CC, Chang CJ, Yu JS. Subcellular localization of Photofrin determines the death phenotype of human epidermoid carcinoma A431 cells triggered by photodynamic therapy: when the plasma membranes are the main targets. Journal of cellular physiology 2003;194: 363-75.

Huettner CS, Zhang P, Van Etten RA and Tenen DG. Reversibility of acute B-cell leukaemia induced by BCR–ABL1. Nature Genet 2000; 24: 57–60.

Jain M, Arvanitis C, Chu K, Dewey W, Leonhardt E, Trinh M, Sundberg CD, Bishop JM, Felsher DW. Sustained loss of a neoplastic phenotype by brief inactivation of MYC. Science 2002; 297:102–104.

Kessel D and Luo Y. Mitocondrial photodamage and PDT induced apoptosis. J Photochem Photob 1998; 42: 89-95.

Kessel D. Relocalization of cationic porphyrins during photodynamic therapy. Photochem Photobiol Sci 2002; 1: 837–40.

Kisselev AF, Goldberg AL. Proteasome inhibitors: from research tools to drug candidates. Chem Biol 2001; 8: 739-58.

Korbelik M, Krosl G, Krosl J, Dougherty GJ. The role of host lymphoid populations in the response of mouse EMT6 tumour to photodynamic therapy. Cancer Res 1996; 56: 5647–52 .

Korbelik M. Induction of tumour immunity by photodynamic therapy. J Clin Laser Med Surg 1996; 14: 329-34.

Laemmli UK. Cleavage of structural proteins during the assembly of the head of bacteriophage T4. Nature 1971; 227: 680–5.

Ling YH, Liebes L, Ng B. PS-341, a novel proteasome inhibitor, induces Bcl-2 phosphorylation and cleavage in association with G2-M phase arrest and apoptosis. Mol Cancer Ther. 2002; 1: 841–49.

Luciani MG, Campregher C, Gasche C. Aspirin blocks proliferation in colon cells by inducing a G1 arrest and apoptosis through activation of the checkpoint kinase ATM. Carcinogenesis 2007; 28(10): 2207-17.

Mak NK, Li KM, Leung WN, Wong RN, Huang DP, Lung ML, Lau YK, Chang CK. Involvement of both endoplasmic reticulum and mitochondria in photokilling of nasopharyngeal carcinoma cells by the photosensitizer Zn-BC-AM. Biochem Pharmacol 2004; 68: 2387–96.

MÄkvy P, Messmann H, Regula J, Conio M, Pauer M, Millson CE, MacRobert AJ, Bown SG. Photodynamic therapy for gastrointestinal tumours using three photosensitizers - ALA induced PPIX, Photofrinand MTHPC: a pilot study. Neoplasma 1998; 3: 157-61.

Marchal S, Francois A, Dumas D, Guillemin F, Bezdetnaya L. Relationship between subcellular localisation of Foscan and caspase activation in photosensitised MCF-7 cells. Br. J. Cancer 2007; 96: 944–51.

Masdehors P, Merle-Beral H, Maloum, K, Omura S, Magdelenat H and Delic J. Deregulation of the ubiquitin system and p53 proteolysis modify the apoptotic response in B-CLL lymphocytes. Blood 2000; 96: 269–74.

Moore ACE. Signaling pathways in the cell death and survival after photodynamic therapy. J Photochem and Photobiol 2000; 57: 1-13.

Niedre M, Patterson MS, Wilson BC. Direct near-infrared luminescence detection of singlet Oxygen generated by photodynamic therapy in cells in vitro and tissues in vivo. Photochem Photobiol 2002; 75: 382–91.

Nonaka M, Ikeda H, Inokuchi T. Inhibitory effect of heat shock protein 70 on apoptosis induced by photodynamic therapy in vitro. Photochem Photobiol 2004; 79:94-98.

Noodt BB, Berg K, Stokke T, Peng Q, Nesland JM. Different apoptotic pathways are induced from various intracellular sites by tetraphenylporphyrins and light. Br J Cancer 1999; 7972–81.

Oleinick NL, Morris R and Belichenko I. The role of apoptosis in response to photodynamic therapy: what, where, and how. Photochem photobiol Sci 2002; 1: 1-21.

Orlowski RZ and Baldwin AS. NF-kB as a therapeutic target in cancer. Trends Mol Med 2002; 8: 385–89.

Orlowski RZ, Eswara JR, Lafond-Walker A, Grever MR, Orlowski M and Dang CV. Tumour growth inhibition induced in a murine model of human Burkitt's lymphoma by a proteasome inhibitor. Cancer Res 1998; 58: 4342–8.

Peng Q, Moan J, Nesland JM. Correlation of subcellular and intratumoural photosensitizer localization with ultrastructural features after photodynamic therapy. Ultrastruct Pathol 1996; 20: 109–29.

Podhaisky HP, Abate A, Polte T, Oberle S, Schröder H. Aspirin protects endothelial cells from oxidative stress--possible synergism with vitamin E. FEBS Lett. 1997; 417(3):349-51.

Rock KL, Gramm C, Rothstein L, Clark K, Stein R, Dick L, Hwang D, Goldberg AL: Inhibitors of the proteasome block the degradation of most cell proteins and the generation of peptides presented on MHC class I molecules. Cell 1994; 78: 767-771.

Schroder M, Kaufman RJ. ER stress and the unfolded protein response. Mutat Res 2005; 569: 29–63.

Sibata CH, Colussi VC, Oleinick NL, Kinsella TJ. Photodynamic therapy in oncology. Expert Opin Pharmacother 2001; 2: 917–27.

Spataro V, Toda T, Craig R, Seeger M, Dubiel W, Harris A L and Norbury C. Resistance to diverse drugs and ultraviolet light conferred by overexpression of a novel human 26 S proteasome subunit. J Biol Chem 1997; 272: 30470–75.

Subbegowda R, Frommel TO. Aspirin toxicity for human colonic tumour cells results from necrosis and is accompanied by cell cycle arrest. Cancer Res. 1998; 58(13):2772-6.

Sunwoo JB, Chen Z, Dong G, Yeh N, Crowl Bancroft C, Sausville E, Adams J, Elliott P and Van Waes C. Novel proteasome inhibitor PS-341 inhibits activation

of nuclear factor- kB, cell survival, tumour growth, and angiogenesis in squamous cell carcinoma. Clin Cancer Res 2001; 7: 1419–28.

Tsujimoto Y and Shimizu S. Another way to die: autophagic programmed cell death. Cell Death Differ 2005; 12: 1528–34.

Usuda J, Chiu SM, Murphy ES, Lam M, Nieminen AL, Oleinick NL. Domain-dependent photodamage to Bcl-2. A membrane anchorage region is needed to form the target of phthalocyanine photosensitization. J Biol Chem. 2003; 278: 2021-9.

Vane JR. Inhibition of prostaglandin synthesis as a mechanism of action for aspirin-like drugs. Nat New Biol 1971; 231(25): 232-5.

Vantieghem A, Assefa Z, Vandenabeele P, Declercq W, Courtois S, Vandenheede JR, Merlevede W, de Witte P, Agostinis P. Hypericin- induced photosensitization of HeLa cells leads to apoptosis or necrosis. Involvement of cytochrome c and procaspase-3 activation in the mechanism of apoptosis. FEBS Lett 1998; 440: 19–24.

Vantieghem A, Xu Y, Assefa Z, Piette J, Vandenheede JR, Merlevede W, de Witte PAM, Agostinis P. Phosphorylation of Bcl-2 in G2/M phase arrested cells following photodynamic therapy with hypericin involves a CDK1-mediated signal and delays the onset of apoptosis. J Biol Chem 2002; 2043- 48.

Varnes ME, Chiu SM, Xue LY, Oleinick NL. Photodynamic therapy-induced apoptosis in lymphoma cells: translocation of cytochrome c causes inhibition of respiration as well caspase activation. Biochem Biophys Res Commun 1999; 6: 28-35.

Voges D, Zwickl P, Baumeister W. The 26S proteasome: a molecular machine designed for controlled proteolysis. Annu Rev Biochem 1999; 68: 1015-68.

Xue LY, Chiu SM, Oleinick NL. Photochemical destruction of the Bcl-2 oncoprotein during photodynamic therapy with the phthalocyanine photosensitizer Pc 4.Oncogene 2001; 20: 3420-7.

Zhan F, Hardin J, Kordsmeier B, Bumm K, Zheng M, Tian E, Sanderson R, Yang Y, Wilson C, Zangari M, Anaissie E, Morris C, Muwalla F, van Rhee F, Fassas A, Crowley C, Tricot G, Barlogie B and Shaughnessy J J. Global gene expression profiling of multiple myeloma, monoclonal gammopathy of undetermined significance and normal bone marrow plasma cells. Blood 2002; 99: 1745–57.

Zhang L, Yu J, Park B H, Kinzler KW and Vogelstein B. Role of BAX in the apoptotic response to anticancer agents.Science 2000; 290: 989-92.

FEBS Letters 580 (2006) 2465–2470

Exposure to modeled microgravity induces metabolic idleness in malignant human MCF-7 and normal murine VSMC cells

Rita Coinu[b,1], Angela Chiaviello[a,1], Grazia Galleri[b], Flavia Franconi[c], Elvira Crescenzi[a], Giuseppe Palumbo[a,*]

[a] *Dipartimento di Patologia e Biologia Cellulare e Molecolare/IEOS CNR, Università di Napoli Federico II, Via S. Pansini, 5, I-80131 Naples, Italy*
[b] *Dipartimento di Scienze Fisiologiche Biochimiche e Cellulari, Università di Sassari, Sassari, Italy*
[c] *Dipartimento di Scienze del Farmaco, Università di Sassari, Sassari, Italy*

Received 24 February 2006; accepted 27 March 2006

Available online 7 April 2006

Edited by Veli-Pekka Lehto

Abstract **We investigated the effect of modeled microgravity (MMG) on normal vascular smooth muscle cells (VSMC) and neoplastic human breast cancer cells (MCF-7). In both cell types, MMG induced partial arrest in G_2M and increased p14-3-3, HSP70, HSP60 and p21 expression. Cells synchronized by 24 h starvation reentered the normal cycle within 24 h if released in complete medium and exposed to normal gravity, but not if exposed to MMG. Similarly, MMG prevented VSMC and MCF-7 cells from overcoming growth arrest and re-synthesizing DNA. This study shows that cells adjust their metabolic rate in response to MMG.**

Keywords: Modeled microgravity; Cell cycle; Cell metabolism

1. Introduction

Microgravity induces adverse and metabolic effects in animals, humans and cellular systems [1–4]. We have evaluated the effects of microgravity on cell proliferation, glucose uptake, amino acid uptake and incorporation into proteins in neoplastic human breast cancer cells (MCF-7) and normal murine vascular smooth muscle cells (VSMC). Although these cells originate from different tissues and different species and have a distinct differentiation status, both are p53-positive and require similar culture conditions. In addition, both cell types have insulin receptors, which suggest that their metabolic activities depend on culture nutrients, including the insulin normally present in fetal calf serum (FCS). As transformed cells, MCF-7 require constant refurbishment to meet their energy requirements and are hence highly dependent on glucose metabolism for growth, whereas muscle cells depend on amino-acid metabolism (protein synthesis and breakdown). Therefore, glucose uptake and amino acid uptake and utilization studies conducted in these cells under conditions of microgravity may reveal derangements of metabolism induced by space-related stress.

2. Materials and methods

2.1. Cell cultures

Human breast cancer MCF-7 cells were grown in DMEM-5% FCS^+ at 37 °C in a humidified atmosphere as previously reported [5]. VSMC were harvested from aortas of young male rats (Sprague Dawley) by the media explant technique and cultured in DMEM-10% FCS^+ as described elsewhere [6]. Serum starvation (in modified Krebs Ringer phosphate solution in the presence of 0.025% albumin) is designated "FCS^-". [^{3}H]-thymidine, 2-deoxy-D-[^{14}C]-glucose and [^{35}S]-methionine were purchased from Amersham (Milan, Italy). Concentration of proteins extracted from cells was measured as according to Bradford [7].

2.2. Modeled microgravity

Six flasks containing 1.5×10^5 MCF-7 cells or VSMC, at time 0 were filled with FCS^+ media and capped. Three (MCF-7 or VSMC) flasks were placed in a temperature-controlled room (37 °C) on a running random positioning machine (RPM; Dutch Space, The Hague, NL); the remaining three flasks were fasten to the edge of the RPM and served as controls (see below). Samples and controls were left to grow for 48 h in modeled microgravity (MMG).

2.3. Normal gravity

Cells grown on the RPM are subjected to changes in gravity and mechanical stress due to the vibration of the machine. Therefore, we fasten the control flasks to the edges of the RPM. All control cells considered hereafter are those subjected to mechanical stress only.

2.4. DNA synthesis, glucose uptake, methionine uptake and incorporation into neo-synthesized proteins

2.4.1. DNA synthesis. These assays were carried as described previously [5]. MCF-7 or VSMC (normally 1.5×10^5 cells) were incubated with ~1 μCi/ml of [^{3}H]-thymidine as detailed in the legends to Figs. 1B and 4, respectively, then rinsed three times with cold PBS, and fixed in cold 10% trichloroacetic (TCA) acid. The precipitates were washed with ethanol and dried by evaporation. The precipitates were washed and solubilized in NaOH: a portion was used to determine protein concentration [7]; the remaining part was neutralized with HCl and counted by liquid scintillation. Incorporation was calculated as counts per minute (cpm) per mg of protein and expressed as percentage of control. Three separate experiments have performed. Each experiment was done using triplicate samples.

2.4.2. Glucose uptake. VSMC and MCF-7 cells were plated at a density of 1.5×10^5 cells and grown in FCS^+ medium. Cells were cultured for about 24 h, transferred to a temperature-controlled room (37 °C) and exposed to MMG in a RPM for 48 h. They were then washed and starved for 5 h in modified Krebs Ringer phosphate solution. Incubation (37 °C)

*Corresponding author.
E-mail address: palumbo@unina.it (G. Palumbo).

[1] R.C. and A.C. contributed equally to this work.

Abbreviations: MMG, modeled microgravity; VSMC, vascular smooth muscle cells; FCS, fetal calf serum; RPM, random positioning machine; MCF-7, neoplastic human breast cancer cells; NG, normal gravity

0014-5793/$32.00
doi:10.1016/j.febslet.2006.03.078

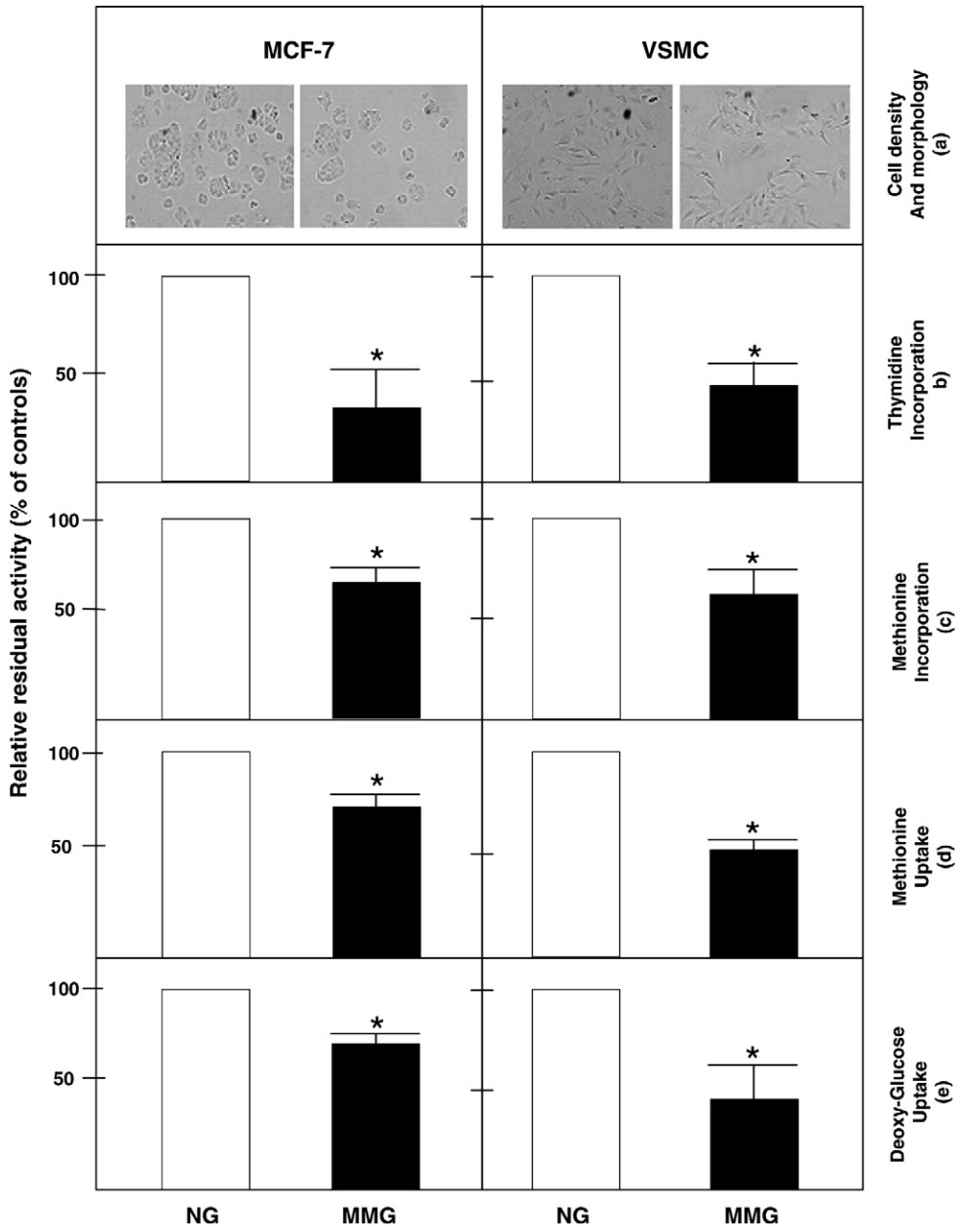

Fig. 1. Panel a: MCF-7 cells (left) and VSMC (right) after 48 h of growth in NG and MMG. Panel b: Incorporation of [^{3}H]-thymidine into DNA in MCF-7 (left) and VSMC cells (right) exposed to MMG (close bars) and NG (open bars). Panels c and d: [^{35}S]-methionine uptake and TCA-precipitable material in MCF-7 (left) and VSMC cells (right) exposed to NG and MMG. Panel e: Uptake of 2-deoxy-[^{14}C]-glucose in MCF-7 (left) and VSMC (right) exposed to NG and MMG. Data are calculated by dividing the measured cpm per mg of protein and were expressed as % of respective controls to allow the results of three experiments to be pooled and analyzed collectively. Statistical significance in each experiment was estimated with the *t* test, where $P < 0.05$ was considered statistically significant.

was continued for 30 min after the addition of 2-deoxy-D-[^{14}C]-glucose and 0.17 mM glucose as carrier [5]. Next, cells were washed and solubilized in NaOH and the protein concentration determined [7]. Finally [^{14}C]-deoxy-glucose radioactivity was counted by liquid scintillation. Uptake was calculated as counts per minute (cpm) per mg of protein and expressed as percentage of control. Three separate experiments have performed. Each experiment was done using triplicate samples.

2.4.3. Methionine uptake and incorporation. Amino acid uptake was determined in triplicate by measuring the uptake of [^{35}S]-methionine under normal gravity (NG) or MMG. After 36 h of MMG, cells were removed from the RPM, washed, repositioned on the RPM, and starved for 12 h with modified Krebs Ringer phosphate solution in the presence of 0.05% albumin. Incubation (37 °C) was continued for 30 min after the addition of [^{35}S]-methionine (12.5 μCi/flask). Next, cells were thoroughly washed and solubilized in NaOH. The solution was divided in three parts: a portion was used to determine protein concentration [7], a portion was used to count total radioactivity (free plus incorporated into proteins), a portion was used to measure protein-associated radioactivity after precipitation with TCA as described elsewhere [8]. Results (counts per minute per mg of total protein) are expressed as percentage of controls. Three similar experiments have performed. Each experiment was done using triplicate samples.

2.5. Statistical analysis and presentation of data

Thymidine incorporation, methionine incorporation/uptake and glucose uptake were expressed as % of respective controls to allow the results of multiple experiments to be pooled and analyzed collectively. Statistical significance was estimated with the T-test. A *P* value of less than 0.05 was considered statistically significant.

2.6. Flow cytometry – polyacrylamide gel electrophoresis and Western blotting

At least 20 000 events were collected for each sample. Samples prepared as described by Crescenzi et al. [5] were routinely run in quadruplicate in an Excalibur Cytofluorimeter (Becton Dickinson, Mountain View, CA).

Total cell protein preparations, the materials and the detailed procedure used for electrophoresis and Western blotting (WB) on nitrocellulose filters, including the antibodies (primary and secondary) are as previously reported [9]. In brief, after staining with Red Ponceau, suitable filters (i.e., those displaying a uniform level of staining in all lines) were developed using an electro chemiluminescent WB detection reagent (Amersham) and quantified by scanning with a Discover Pharmacia scanner equipped with a Sun Spark Classic Workstation. The protein extracts, obtained by three flasks were individually analyzed by WB. Results are representative of three experiments.

2.7. Cell starvation, cycle arrest and recovery

Dishes containing $\sim 4 \times 10^4$ MCF-7 or VSMC cells were incubated for 24 h at 37 °C in 7 ml of complete medium. 24 h after attachment, cells were washed and starved with modified Krebs Ringer phosphate solution in the presence of 0.05% albumin for 24 h, at which time the cell cycle was arrested. To determine the time required for cells to reenter the cycle, cell cycle arrested cells were released in complete medium and analyzed by cytofluorimetry at 4, 8, 12 and 24 h. The effect of MMG on MCF-7 and VSMCs capacity to reenter the cycle, was estimated by cytofluorimetry, whereas the recovery of original proliferation rate, was evaluated by [^{3}H]-thymidine incorporation experiments.

Cell cycle. Recovery after cell synchronization. Synchronized MCF-7 cells (seeded at a density of $\sim 1.5 \times 10^5$ cells/flask) were obtained by starvation in FCS$^-$ medium. Thirty-six hours later, flasks were drained, refilled with FCS$^+$ medium, divided into two groups of three flasks each and exposed, respectively, to MMG or NG (controls) for 24 h. Cells were then fixed and analyzed by cytofluorimetry.

[^{3}H]-thymidine incorporation. Recovery from cell synchronization. To evaluate recovery from cell synchronization, six flasks containing $\sim 2.0 \times 10^5$ attached MCF-7 cells (time 0) were starved for 30 h by exposure to FCS$^-$ for 24 h. Once cells were synchronized, FCS$^-$ medium was replaced with FCS$^+$ medium containing 1 μCi/ml [^{3}H]-thymidine. Three flasks were kept under NG, and three were put on the RPM, and incorporation was measured 15 h later. In a different experiment, six flasks containing $\sim 2.0 \times 10^5$ VSMC cells were released in FCS$^-$ and exposed to MMG for 24 h. Cells were then released in FCS$^+$ medium containing 1 μCi/ml [^{3}H]-thymidine, divided in two groups (three in NG and three in MMG) and incubated for an additional 10 h before final assessment of thymidine incorporation. Each experiment, with MCF-7 and VSMC was performed twice, in identical conditions as above.

Table 1
Cell cycle of MCF-7 cells and VSMC exposed to NG and to MMG for 24 h

	MCF-7		VSMC	
	NG	MMG	NG	MMG
$G_{0/1}$	63.4 ± 0.14	64.4 ± 4.0	70.4 ± 1.5	67.5 ± 1.5
S	27.7 ± 1.4	18.4 ± 2.5	23.7 ± 1.34	17.7 ± 2.2
G_2/M	8.9 ± 1.5	17.2 ± 2.8	5.9 ± 0.14	14.8 ± 0.7

Average of three measurements.

3. Results and discussion

We have comparatively analyzed two cell lines, namely VSMC (normal) and MCF-7 (transformed) cells to understand how and to what extent weightlessness alters cellular properties

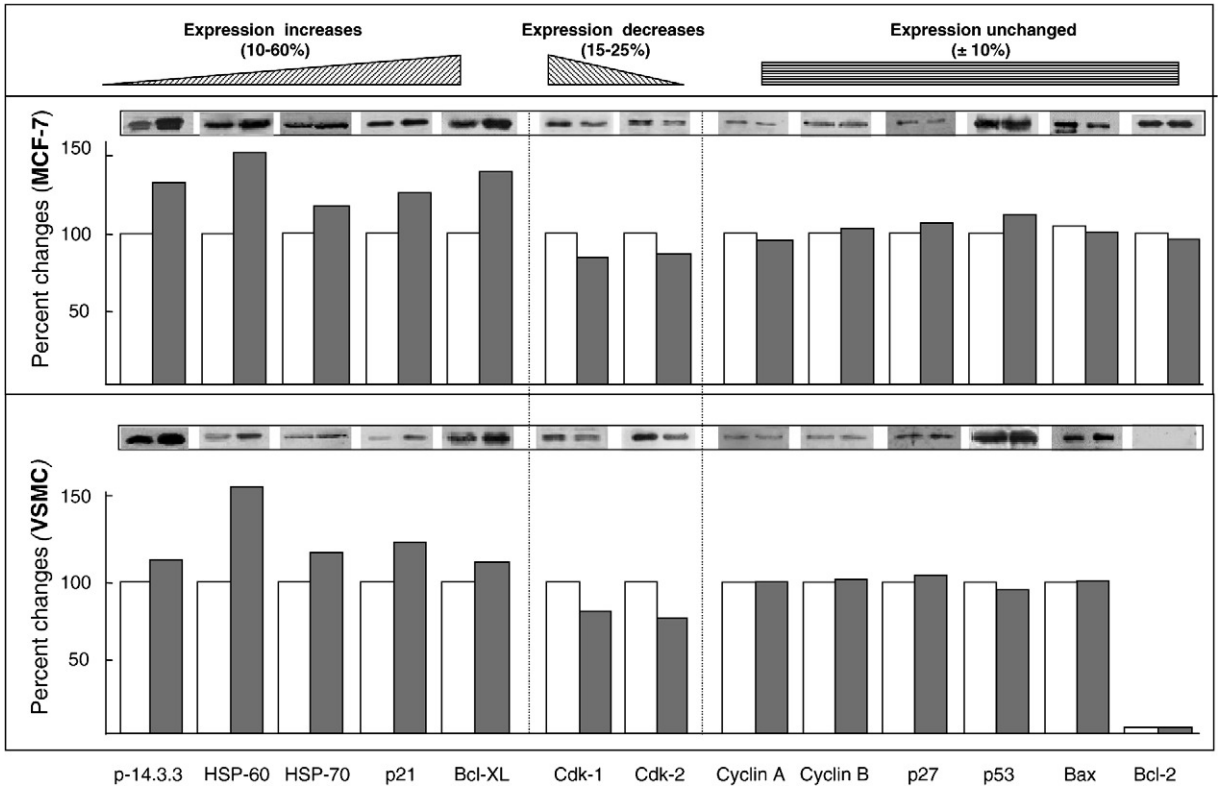

Fig. 2. Each histogram, obtained by digital densitometry, compares the expression of the marked protein in MMG (closed bars) versus the NG conditions (controls, open bars). Density of controls was arbitrarily set at 100. Upper panel refers to MCF-7 cells; lower panel to VSMC cells. Filter staining with Red Ponceau has been used as indicator of uniform protein transfer, while actin (not shown), has been used as loading control. The representative WB inserts show the profile of the indicated proteins in MMG and NG conditions. Although multiple experiments and scans have been performed, all data may be considered only denotative of an apparent increasing (left), decreasing (center) or unchanging (right) trend in the particular protein expression.

including basal proliferation rate (thymidine incorporation), glucose uptake and methionine uptake/incorporation, cell cycle profiles and the expression of several proteins.

3.1. Cell growth and proliferation

Proliferation was much lower in MCF-7 cells and in VSMC exposed to MMG versus NG (Fig. 1, panel a). Moreover, [^{3}H]-thymidine incorporation was significantly ($P < 0.05$) lower in MCF-7 cells (~70%) and in VSMC (~50%) exposed to MMG (Fig. 1, panel b). As found in free-floating Jurkat cells [10], MMG caused both cell types to slightly accumulate in G_2/M (Table 1). This partial remodeling of the cell cycle was associated with reduced cell proliferation. Prolonged MCF-7 mitosis during MMG is not a new finding and has been attributed to weightlessness-induced alteration of microtubules [4]. Also Meyers et al. [11] found that MMG alters proliferation rate, and reported that MMG, by decreasing integrin/MAPK signaling, contributes to reduced osteoblastogenesis during differentiation of human mesenchymal stem cells. Similarly, Plett et al. [12] demonstrated that MMG causes alterations of human hematopoietic progenitor cells.

3.2. Cellular metabolic activity

Fig. 1 shows also the effects in both MCF-7 and VSMC cells of MMG as compared to NG on some metabolic cellular activities. It appears that the incorporation of methionine into TCA-precipitable materials (panels c), its cellular uptake (panels d) and the deoxy-glucose uptake (panels e), are neatly reduced. All the differences noted were statistically significant ($P < 0.05$).

3.3. Protein expression

Protein expression has been quantitated by digital densitometry of three independent experiments. As may be noticed by the bars in Fig. 2 (see additional details in the legend), MMG-exposed MCF-7 cells (upper panel) express increased levels of HSP60 (~50%), Bcl-XL (~35%) and p14-3-3 protein (~30%); even p21 and HSP70 appear to be elevated, although to a lesser extent. Densitometry indicated possibly lower levels of both Cdk-1 and -2 (~15%). Similarly MMG did not (or very imperceptibly) affect the expression of p53, Bax, Bcl-2, p27 and Cyclins or PARP (not shown). As shown in lower panel of the same figure, MMG-exposed VSMC cells appear to express increased levels of HSP60 (>50%) and, to a lesser extent, of p21 (~25%), HSP70 (~20%), p14-3-3 (~20%) and Bcl-XL (~15%). Cyclin kinases appear to decrease of ~20%, while cyclins, p53, p27, Bax and also Bcl-2 (which indeed is already undetectable in control VSMC cells) appear to remain unchanged. Even in this case, PARP was not affected (not shown).

The increased expression of the constitutive proteins HSP-60, in particular, and, to a lesser extent, HSP-70 is obscure,

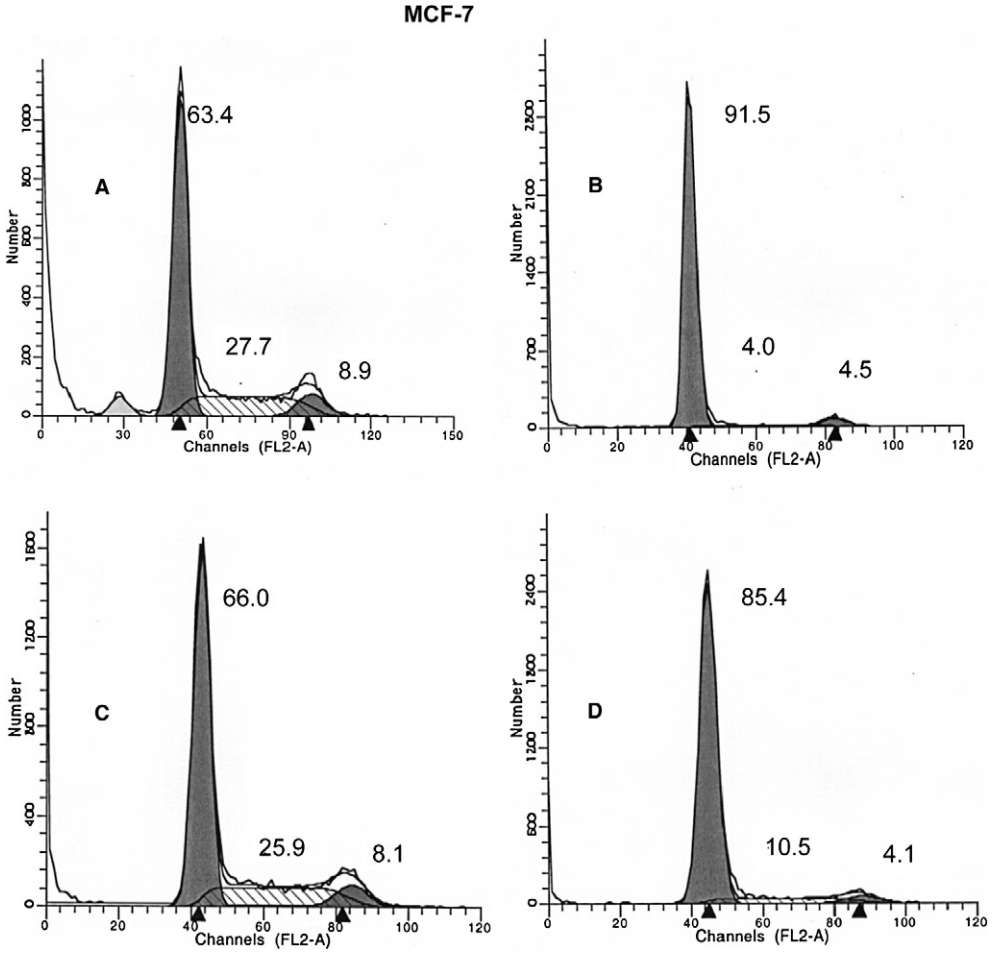

Fig. 3. MCF-7 growing in FCS$^+$ in NG (a); cells starved in FCS$^-$ for 24 h under NG (b); cells starved for 24 h (as before) and released in FCS$^+$ for a further 24 h under NG (c); cells starved for 24 h and released in FCS$^+$ for a further 24 h under MMG (d). Data shown are representative of triplicate samples.

although the two proteins may work in tandem to facilitate the refolding process after damage [13]. It is possible that MMG drives cells beyond their normal activity. This metabolic disturbance, accompanied by a modest, albeit reproducible increase in p21 and Bcl-XL expressions, negatively influences cell proliferation. Similarly, MMG affected appreciably the expression of p14-3-3 (especially in MCF-7). This protein is important for such vital regulatory processes as mitogenic signal transduction and cell cycle control [14]. In agreement with the cell cycle profiles, which lacked signs of apoptosis, the profiles of the pro-apoptotic proteins BAX and PARP (not shown) are unchanged as compared to controls.

Since digital densitometry integrates bands produced on films by chemiluminescent signals, which are intrinsically semi-quantitative, the data should be regarded with some caution: nonetheless, they are not in contrast with our metabolic and cytofluorimetric findings (see below) and previous observations made by others [10,11].

3.4. Effect of MMG on synchronized cells

We used two strategies, both based on a "stop and go" approach, to determine whether MMG affects proliferation rate. This requires preliminary synchronization of cells by serum starvation (*stop*) followed by re-nourishing of cells in FCS-containing medium (*go*) in MMG or NG (Fig. 3, panel a, controls). In one strategy we examined the original cell cycle profile, and in the other we evaluated restoration of the propensity to synthesize DNA by examining [^{3}H]-thymidine incorporation.

Cell cycle. Exposure of MCF-7 cells for 24 h to a FCS$^-$ solution caused cell cycle arrest and complete (~92%) synchronization in G_1 (Fig. 3, panel b). Upon release in FCS$^+$ medium, these cells resumed normal cycling activity, and the original profiles were restored after exposure to NG for 24 h (Fig. 3, panel c). This was not the case of cells exposed to MMG for 24 h. In this case >90% of cells arrested by starvation in G_1 did not progress (Fig. 3, panel d). This result indicates that MMG can hamper the normal cycling of the malignant fast-proliferating MCF-7.

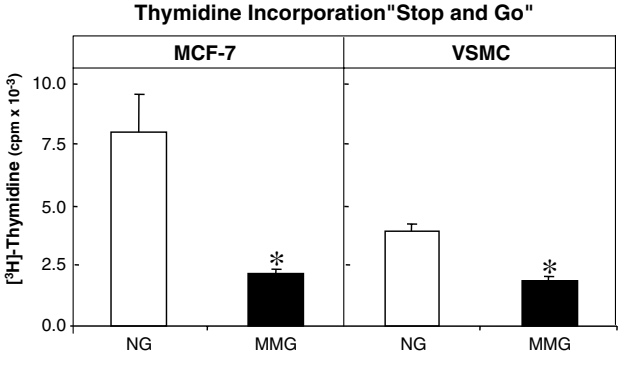

Fig. 4. Stop and go experiments. Two separate experiments have been performed on both cell type (MCF-7, left; VSMC, right). Each individual experiment was performed using three samples and three controls. The data reported in the chart depict the best estimate (weighted average) of each pair of experiments. Initial cell synchronization was obtained by serum deprivation (stop). [^{3}H]-thymidine incorporation was measured following release of cells in FSC$^+$ medium (go). Open bars refer to NG and close bars to MMG. The observed differences were statistically significant ($P < 0.05$). See Section 2 for further details.

[^{3}H]-thymidine incorporation. To determine whether MMG affects DNA synthesis, we examined fast growing MCF-7 cells and the normal slow proliferating VSMC. MCF-7 cells were synchronized by simple starvation for 24 in NG, whereas the slow proliferating VSMC cells were synchronized by starving cells exposed to MMG for 24 h.

The best estimates of two experiments, based on the weighted average of the determinations are reported in Fig. 4, indicated that DNA synthesis was reduced by ~4-fold (MCF-7, left panel) and ~2-fold (VSMC, right panel) in cells exposed to MMG. In both cases, the differences of the means are statistically significant ($P < 0.05$).

In conclusion, our results show that MMG alters the cytofluorimetric profile and slows down fundamental metabolic activities (glucose uptake, methionine uptake/incorporation and thymidine incorporation) in normal and transformed cells. MMG did not affect significantly the expression of most proteins that are related to the cell cycle and apoptosis, whereas it altered the expression of stress proteins. The large increase in the expression of HSP-60 and a minor increase in HSP-70 and 14-3-3 protein, suggest that transformed and normal cell lines are able to "sense" the altered conditions of gravity. We hypothesize that cells respond to stress by putting the proliferative and metabolic machinery on "stand by". MMG-promoted quiescence is demonstrated in both cell lines by the cell cycle profiling data and thymidine incorporation after synchronization. MMG alters the hydrodynamics of nutrient fluids (buoyancy and convection), that, in turn, affects the cell environment and cell–cell interactions. These changes, responsible for previously reported alterations in cell morphology [4,10] and in metabolic activity in animals [1] may explain also our results. It remains to be established whether or not these effects are fully or partially reversible, if are transient and if they may represent potential danger to human health in space, particularly in the presence of other hazards such as cosmic radiation.

Acknowledgements: G.P. is personally indebted to the Responsible of the RPM facility in Sassari for his generosity. All Authors thank Gavino Campus for the skilled technical support, Jean A. Gilder for text editing and the MoMa project (ASI, Rome, Italy) for funding.

References

[1] Pamnani, M.B., Mo, Z., Chen, S., Bryant, H.J., White, R.J. and Haddy, F.J. (1996) Effects of head down tilt on hemodynamics, fluid volumes, and plasma Na–K pump inhibitor in rats. Aviat. Spac. Environ. Med. 66, 928–934.
[2] Hughens-Fulford, M. and Lewis, M.L. (1996) Effects of microgravity on osteoblast growth activation. Exp. Cell Res. 224, 103–109.
[3] Carlsson, S.I., Bertilaccio, M.T., Ballabio, E. and Maier, J.A. (2003) Endothelial stress by gravitational unloading: effects on cell growth and cytoskeletal organization. Biochim. Biophys. Acta 1642, 173–179.
[4] Vassy, J., Portet, S., Beil, M., Millot, G., Fauvel-Lafève, F., Karniguian, A. and Gasset, G. (2001) Effect of weightlessness on cytoskeleton architecture and proliferation of human breast cancer cell line MCF-7. FASEB J. 15, 1104–1106.
[5] Crescenzi, E., Varriale, L., Iovino, M., Chiaviello, A., Veneziani, B.M. and Palumbo, G. (2004) Photodynamic therapy with indocyanine green complements and enhances low-dose cisplatin cytotoxicity in MCF-7 breast cancer cells. Mol. Cancer Ther. 3, 537–544.
[6] Owens, G.K., Loeb, A., Gordon, D. and Thompson, M.M. (1986) Expression of smooth muscle specific alfa isoactin in cultured SM cells: relationships, growth and cytodifferentiation. J. Cell Biol. 102, 343–352.

[7] Bradford, M. (1976) A rapid and sensitive method for the quantitation of microgram quantities of protein utilizing the principle of protein-dye binding. Anal. Biochem. 72, 248–254.
[8] Consiglio, R., Rengo, S., Liguoro, D., Riccitiello, F., Formisano, S., Palumbo, G. and Di Jeso, B. (1998) Inhibition by glass-ionomer cements of protein synthesis by human gingival fibroblasts in continuous culture. Arch. Oral Biol. 43, 65–71.
[9] Varriale, L., Coppola, E., Quarto, M., Veneziani, B.M. and Palumbo, G. (2002) Molecular aspects of photodynamic therapy: low energy pre-sensitization of hypericin loaded human endometrial carcinoma cells enhances photo-tolerance, alters gene expression and affects cell cycle. FEBS Lett. 512, 287–290.
[10] Lewis, M.L., Reynolds, J.L., Cubano, L.A., Hatton, J.P., Lawless, B.D. and Piepmeier, E.H. (1998) Spaceflight alters microtubules and increases apoptosis in human lymphocytes (Jurkat). FASEB J. 12, 1007–1018.
[11] Meyers, V.E., Zayzafoon, M., Gonda, S.R., Gathings, W.E. and McDonald, J.M. (2004) Modeled microgravity disrupts collagen I/integrin signaling during osteoblastic differentiation of human mesenchymal stem cells. J. Cell Biochem. 93, 697–707.
[12] Plett, P.A., Abonour, R., Frankovitz, S.M. and Orschell, C.M. (2004) Impact of modeled microgravity on migration, differentiation, and cell cycle control of primitive human hematopoietic progenitor cells. Exp. Hematol. 32, 773–781.
[13] Minowada, G. and Welch, W.J. (1995) Perspectives clinical implications of the stress response. J. Clin. Invest. 95, 3–12.
[14] Fu, H., Subramanian, R.R. and Masters, S.C. (2000) 14-3-3 Proteins: structure, function and regulation. Annu. Rev. Pharmacol. Toxicol. 40, 617–647.

Low doses of cisplatin or gemcitabine plus Photofrin/photodynamic therapy: Disjointed cell cycle phase-related activity accounts for synergistic outcome in metastatic non–small cell lung cancer cells (H1299)

Elvira Crescenzi,[1] Angela Chiaviello,[1] Gianfranco Canti,[2] Elena Reddi,[3] Bianca Maria Veneziani,[1] and Giuseppe Palumbo[1]

[1]Dipartimento di Biologia e Patologia Cellulare e Molecolare ''L. Califano'' and Istituto di Endocrinologia ed Oncologia Sperimentale/Consiglio Nazionale delle Ricerche, Università di Napoli Federico II, Naples, Italy; [2]Dipartimento di Farmacologia, Università di Milano, Milan, Italy; and [3]Dipartimento di Biologia, Università di Padova, Padua, Italy

Abstract

We compared the effects of monotherapy (photodynamic therapy or chemotherapy) versus combination therapy (photodynamic therapy plus a specific drug) on the non–small cell lung cancer cell line H1299. Our aim was to evaluate whether the additive/synergistic effects of combination treatment were such that the cytostatic dose could be reduced without affecting treatment efficacy. Photodynamic therapy was done by irradiating Photofrin-preloaded H1299 p53/p16-null cells with a halogen lamp equipped with a bandpass filter. The cytotoxic drugs used were *cis*-diammine-dichloroplatinum [II] (CDDP or cisplatin) and 2′,2′-difluoro-2′-deoxycytidine (gemcitabine). Various treatment combinations yielded therapeutic effects (trypan blue dye exclusion test) ranging from additive to clearly synergistic, the most effective being a combination of photodynamic therapy and CDDP. To gain insight into the cellular response mechanisms underlying favorable outcomes, we analyzed the H1299 cell cycle profiles and the expression patterns of several key proteins after monotherapy. In our conditions, we found that photodynamic therapy with Photofrin targeted G_0-G_1 cells, thereby causing cells to accumulate in S phase. In contrast, low-dose CDDP killed cells in S phase, thereby causing an accumulation of G_0-G_1 cells (and increased p21 expression). Like photodynamic therapy, low-dose gemcitabine targeted G_0-G_1 cells, which caused a massive accumulation of cells in S phase (and increased cyclin A expression). Although we observed therapeutic reinforcement with both drugs and photodynamic therapy, reinforcement was more pronounced when the drug (CDDP) and photodynamic therapy exert disjointed phase-related cytotoxic activity. Thus, if photodynamic therapy is appropriately tuned, the dose of the cytostatic drug can be reduced without compromising the therapeutic response. [Mol Cancer Ther 2006;5(3):776–85]

Introduction

Although chemotherapy is the leading treatment for most types and stages of cancers, photodynamic therapy is an effective anticancer procedure for selected tumors (1). This procedure involves administration of a tumor-localizing photosensitizing agent that when activated by light of a specific wavelength mediates cell destruction via the production of singlet oxygen. Photodynamic therapy has been shown to have few or no side effects in patients with Barrett's esophagus (high-grade dysplasia and early carcinoma) and in selected cases of early squamous cell carcinoma (2). One of the most widely used photosensitizing drugs is the hematoporphyrin-derivative Photofrin. This nontoxic substance has been used for photodynamic therapy for ~8 years and is the only one widely approved for human therapy. On exposure of Photofrin-loaded cells to visible light, intracellular toxic oxygen species (singlet oxygen, $^1O_2$) are generated that can trigger cell apoptosis or necrosis (3, 4).

Anticancer drugs target several cellular components and activate responses that go from cell repair to cell death. However, chemotherapy is effective only at high doses, because, at low doses, tumor cells may repair damage and resume their original high proliferation rate (5). *Cis*-diammine-dichloroplatinum [II] (CDDP or cisplatin) and 2′,2′-difluoro-2′-deoxycytidine (gemcitabine) are widely used in the management of various cancers. By forming adducts in DNA, CDDP inhibits DNA replication and chain elongation, which accounts for its antineoplastic activity. In clinical practice, CDDP is often combined with other drugs. Synergy between CDDP and other chemotherapeutic agents occurs by various pathways: increased intracellular drug accumulation, enhanced binding to DNA, and decreased DNA repair (6). Gemcitabine is a deoxycytidine analogue that is effective against solid tumors, including non–small cell lung cancer. After transport into the cell,

Received 10/14/05; revised 12/23/05; accepted 1/12/06.

Grant support: Ministero dell'Istruzione, dell'Università e della Ricerca-COFIN program and Agenzia Spaziale Italiana (Rome, Italy).

The costs of publication of this article were defrayed in part by the payment of page charges. This article must therefore be hereby marked advertisement in accordance with 18 U.S.C. Section 1734 solely to indicate this fact.

Note: E. Crescenzi and A. Chiaviello contributed equally to this work.

Requests for reprints: Giuseppe Palumbo, Dipartimento di Biologia e Patologia Cellulare e Molecolare ''L. Califano,'' Università di Napoli Federico II, Via S. Pansini 5, 80131 Naples, Italy. Phone: 39-81-7463249; Fax: 39-81-7701016. E-mail: palumbo@unina.it

doi:10.1158/1535-7163.MCT-05-0425

gemcitabine requires phosphorylation by deoxycytidine kinase to exert biological activity (7, 8). The enzyme responsible for this reaction is also the rate-limiting step in gemcitabine activation (8). It has been suggested that the combination of photodynamic therapy and conventional cancer treatments may become a workable anticancer strategy (9).

The aim of our study was to identify photodynamic therapy/chemotherapy combinations in which the dose of the most toxic compound could be decreased without a loss of efficacy. To this aim, we examined the response of H1299 human lung metastatic non–small cell lung cancer cells (cell viability, cell cycle, and protein expression) to moderately toxic doses of CDDP or gemcitabine with Photofrin/photodynamic therapy, administered separately and in appropriate combinations.

Materials and Methods

Cell Cultures

The NCI-H1299 human non–small cell lung cancer cell line was obtained from American Type Culture Collection (Rockville, MD). They were cultured in RPMI 1640, 2 mmol/L L-glutamine, 10 mmol/L HEPES, 1 mmol/L sodium pyruvate, 4,500 mg/L glucose, 1,500 mg/L sodium bicarbonate, 100 μg/mL streptomycin, 100 units/mL penicillin, and 10% FCS. The medium was changed every 3 days. All media and cell culture reagents were purchased from Life Technologies (San Giuliano Milanese, Italy). NCI-H1299 cells are p53−/− and p16−/−. All treatments, individual and in combination, were done in triplicate samples in tissue culture dishes (35 mm) in which 5×10^4 cells were routinely seeded. A larger number of cells (4×10^5) were seeded for cell cycle measurements and for protein extraction for Western blotting purposes. The effects of monotherapy with drugs or photodynamic therapy or combined therapy (drugs + photodynamic therapy) were evaluated (*a*) by trypan blue assays (to check residual cell viability), (*b*) by analyzing cell cycle profiles (to determine the cell distribution in the various conditions), and (*c*) by analyzing expression patterns (Western blots) of specific proteins involved in the control of cell growth and survival.

Cytotoxic Drugs

CDDP was obtained from Sigma-Aldrich Srl (Milan, Italy). A stock solution was obtained by dissolving CDDP in DMSO to obtain a final concentration of 40 mmol/L. Aliquots were stored at −20°C until used. Gemcitabine chlorhydrate (Gemzar) was supplied as dry powder by Eli Lilly SpA (Sesto Fiorentino, Italy). A stock solution (67 mmol/L) was obtained by dissolving gemcitabine in an isotonic solution (0.9% NaCl). Aliquots were stored at −20°C until used.

Photosensitizer

The Photofrin (the hematoporphyrin derivative Porfimer sodium) used in this work was supplied as freeze-dried powder (lot no. 162A6-06; Axcan Pharma, Mont-Saint-Hilaire, Quebec, Canada). Its absorption spectrum consists of various peaks within the visible region. A Photofrin stock solution was obtained by dissolving the powder in water containing 5% glucose to obtain a final concentration of 2.5 mg/mL. This solution was stored in aliquots at −20°C in the dark. Before measurements, appropriate aliquots of this solution were diluted to the desired concentration. Except for ''dark toxicity assays,'' Photofrin was always used at a concentration of 2.5 μg/mL. All treatments involving Photofrin were done on triplicate. Cells were exposed to 2.5 μg/mL Photofrin for 16 hours before irradiation.

Chemotherapy and Chemotherapy Schedule

Usually, 5×10^4 H1299 cells were seeded in 35-mm tissue culture dishes and exposed to the cytotoxic substances (individual or combined with photodynamic therapy) 24 hours later. This procedure was carried out in triplicate. Normally, 4×10^5 cells were used for cell cycle measurements and protein extraction for Western blotting. To obtain CDDP/gemcitabine dose-response curves, culture dishes were treated with CDDP (2.5–12 μmol/L) or gemcitabine (2–12 nmol/L) and kept at 37°C for 24 hours. After incubation, cells were washed and released into fresh medium. Cell viability was evaluated with the trypan blue assay (as detailed in ref. 10) 24 hours later, counting between 15 and 30 cells per field. Two sets of data were collected for each drug. In combination experiments, after incubation with the drug (0–24 hours) and Photofrin (8–24 hours), cells were washed, placed in a colorless saline solution (Hank's), and immediately irradiated. After irradiation, cells were placed in fresh complete medium, and cells negative to trypan blue staining were counted 24 hours later (see Fig. 1). Residual viability was expressed as percentage of trypan blue–negative cells versus untreated controls.

Photodynamic Therapy and Photodynamic Therapy Schedule

Cells were irradiated by a broadband light delivered with a PTL-Penta apparatus (Teclas, Sorengo, Switzerland). This apparatus consists of a halogen lamp (Osram 250 W, 24 V Osram, Munich, Germany) equipped with a bandpass filter (>80% transmittance in the 510 to 590 nm spectral region; bandwidth ~40 nm at 50% of the peak) corresponding approximately to one of the Photofrin absorption peaks. The emission spectrum was measured with a Macam SR9910 spectroradiometer (Macam Photometrics, Livingston, Scotland, United Kingdom). The light was delivered through an 8-mm bundle of optical fibers placed at a distance from the cell plates that ensures uniform illumination of the entire cell monolayer. The fluence rate at the level of the cell monolayer was fixed at 6 mW/cm^2 and irradiations were done with light doses of up to 1.8 J/cm^2. We invariably used a Photofrin concentration of 2.5 μg/mL. At a fluence of 0.54 J/cm^2, photodynamic therapy monotherapy reduced H1299 cell viability to ~50% that of treated but not irradiated cells (controls). Doses between 0.18 and 0.54 J/cm^2 were used in the combination experiments. Because only a few cells survived combined therapy with fluences >0.54 J/cm^2, higher fluences were not considered. In brief, after incubation, cells were washed

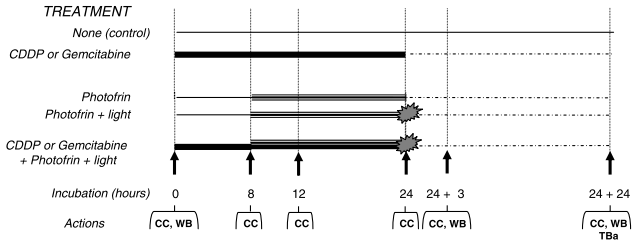

Figure 1. Single-agent and combination treatment schedule. For single-agent CDDP or gemcitabine treatments, cells were incubated with chemotherapeutic drugs for 8, 12, or 24 h, washed, and analyzed immediately and after 3 h. Cells exposed to drugs for 24 h were also analyzed 24 h after washing and release into fresh medium. Before photodynamic therapy, cells were incubated for 16 h with Photofrin in the dark. For combination treatments, cells were treated with CDDP or gemcitabine at prefixed concentrations, and Photofrin was added 8 h later. The samples were washed and analyzed immediately or released in fresh medium and analyzed 24 h later. *CC,* cell cycle; *WB,* Western blot; *TBa,* trypan blue assay; *star,* light turned on.

extensively, placed in colorless Hank's solution, exposed to light, and analyzed by cytofluorimetry either immediately or after exposure to fresh medium for a further 24 hours. Similarly, cell extracts obtained ~3 or 24 hours after irradiation were used to obtain protein profiles (Western blots). Residual cell viability was assessed by trypan blue assay after cells have been placed in fresh medium for 24 hours (Fig. 1).

Flow Cytometry

Dishes (10 cm) containing 4×10^5 H1299 cells were incubated for 24 hours at 37°C in 7 mL complete medium (controls) or in medium supplemented with Photofrin (2.5 μg/mL) alone or associated with CDDP (2.5 μmol/L) or gemcitabine (4 nmol/L). Cells were exposed to photodynamic therapy as described above and were then detached from the dishes by trypsinization, suspended in serum-rich medium, centrifuged, washed twice with 1 mL PBS, and resuspended for storage (−20°C) in 95% ethanol. Before analysis, fixed cells were washed twice, centrifuged, and resuspended in 1 mL PBS containing 1 μg RNase and 100 μg propidium iodide (11). Samples were stored in the dark for 20 minutes at room temperature before final readings. The cellular orange fluorescence of propidium iodide was detected in a linear scale using a flow cytometer (FACScan, Becton Dickinson, Mountain View, CA) equipped with an excitation laser line at 488 nm. About 30,000 events (i.e., fluorescence readings, corresponding to not less than 20,000 cells) were recorded for each sample. The cell cycle was examined after monotherapy and combined treatment at the indicated times (see Fig. 1). Data were analyzed with ModFit/LT (Verity Software, Topsham, ME).

Median Effect Analysis

We used the median effect analysis (12) together with the combination index (CI) to ascertain synergy and the additivity/antagonism of photodynamic therapy and chemotherapy. The median effect analysis derives directly from the mass action law and does not depend on a reaction mechanism. The reference equation is $F_a / F_u = (D / Dm) * m$, where F_a is the affected fraction, F_u is the unaffected fraction, D is the dose, Dm is the median dose (50%, for instance), and m is a coefficient related to the shape of the dose-response curve ($m = 1$, hyperbolic; $m > 1$, sigmoidal; $m < 1$, negatively sigmoidal). The shape is easily determined from the dose-effect curve from which Dm is directly estimated. The CI for treatments that are not mutually exclusive (i.e., that unequivocally have different modes of action) can be calculated by (13): $CI = (D)_1 / (D_x)_1 + (D)_2 / (D_x)_2 + [(D)_1(D)_2] / [(D_x)_1(D_x)_2]$, in which $(D)_n$ is the dose of the nth drug (or of light) needed to obtain a given effect in the combination and $(D_x)_n$ is the dose of the same drug (or light) necessary to obtain the same effect when used alone. Chou and Talalay (12) defined synergism as a more than expected additive effect, where the additive effect is designated CI equal to unity. Thus, for mutually exclusive agents that have totally independent modes of action, $CI < 1$, $CI = 1$, and $CI > 1$ indicate synergy, additive effect, and antagonism, respectively. We thus constructed several dose-response curves at a constant fluence and at a constant drug concentration.

Western Blot Analysis

Total cell protein preparations were obtained by lysing cells in 50 mmol/L Tris (pH 7.5), 100 mmol/L NaCl, 1% NP40, 0.1% Triton, 2 mmol/L EDTA, 10 μg/mL aprotinin, and 100 μg/mL phenylmethylsulfonyl fluoride. Protein concentration was routinely measured with the Bio-Rad protein assay (14). Polyacrylamide gels (10–15%) were prepared essentially as described by Laemmli (15). Molecular weight standards were from New England Biolabs (Beverly, MA). Proteins separated on the polyacrylamide gels were blotted onto nitrocellulose filters (Hybond-C pure, Amersham Italia, Milan, Italy). Filters were washed and stained with specific primary antibodies and then with secondary antisera conjugated with horseradish peroxidase (Bio-Rad; diluted 1:2,000). Filters were developed using an electrochemiluminescent Western blotting detection reagent (Amersham Italia) and quantified by scanning with a Discover Pharmacia scanner equipped with a Sun Spark Classic Workstation. The anti-Bcl-2 (100), Bcl-XL (S-18), Bax (N-20), p21 Cip1 (C-19), cyclin A (C-19), Cdk2 (M2), HSP60 (N-20), HSP70 (K-20), and actin (C-2) antibodies were from Santa Cruz Biotechnology (Santa Cruz, CA). Anti-caspase-3 (Ab-3), human (mouse), was from Calbiochem (San Diego, CA).

Results and Discussion

The metastatic non–small cell lung cancer H1299 carcinoma cell line does not express p53 or p16 INK4a. Although sensitivity to photodynamic therapy is not altered in human tumor cells after p53 abrogation (16), inactivation of the p53 and p16 INK4a pathways does not completely abrogate stress responses in carcinoma cells (17).

We evaluated if Photofrin/photodynamic therapy plus CDDP or gemcitabine induces an additive or even a synergistic effect, our aim being to determine whether the

dose of the cytostatic drug can be reduced. To identify the most effective doses of the components of combination therapy, we analyzed (*a*) the response of Photofrin-treated H1299 cells to increasing light doses, (*b*) the response of cells to increasing concentrations of CDDP or gemcitabine, and (*c*) the response of cells to combined therapy in selected conditions.

We first tested low CDDP (≤2.5 μmol/L) and gemcitabine (between 2 and 8 nmol/L) concentrations and mild photodynamic therapy conditions (Photofrin concentration, 2.5 μg/mL; light fluence, 0.18–0.54 J/cm^2). However, we focused on a concentration of 2.5 μmol/L for CDDP and 4 nmol/L for gemcitabine, and the fluence of choice was 0.54 J/cm^2. These drug concentrations caused a near 50% mortality when used alone. Higher concentrations (>5 μmol/L CDDP or >8 nmol/L gemcitabine) were not compatible with photodynamic therapy at a fluence of 0.54 J/cm^2, because no (CDDP) or only a few cells (gemcitabine) survived this combined treatment. Fluctuations of the lamp, which make it difficult to measure fluence accurately within the short irradiation time (<30 seconds), precluded the use of lower fluences (<0.2 J/cm^2).

We evaluated Photofrin-induced toxicity in the absence of light (''dark toxicity'') in 5 × 10^4 cells seeded in 35-mm tissue culture dishes and treated 24 hours later with 0, 2.5, 4, 8, 10, and 25 μg/mL Photofrin. Sixteen hours later, cell viability was evaluated by the trypan blue and 3-(4,5-dimethylthiazol-2-yl)-2,5-diphenyltetrazolium bromide assays (data not shown). We compared the viability of normally growing cells (100%) versus Photofrin-treated but not light-sensitized cells. Cell viability decreased in a dose-dependent fashion starting with 3.0 μg/mL Photofrin, and 25 μg/mL Photofrin reduced cell viability by a factor >5. With 2.5 μg/mL Photofrin, toxicity did not exceed 5%; hence, we used this dose in the photodynamic therapy experiments.

Individual Treatments

Because photodynamic therapy was applied to cells treated for 24 hours with CDDP or gemcitabine, we first determined the cycle stage of cells on irradiation. To this end, we incubated H1299 cells with 4 nmol/L gemcitabine or 2.5 μmol/L CDDP for 0 (controls), 8, 12, and 24 hours. The cells were then washed and immediately fixed for cytofluorimetry. Gemcitabine rapidly induced depletion of G_2-M cells and hence an accumulation of G_1 cells; 12 hours later, almost all cells were in S phase (Table 1). Therefore, when photodynamic therapy was applied, gemcitabine-exposed (4 nmol/L) cells were mostly in S phase. CDDP, on the contrary, caused cell accumulation in S phase followed by cell synchronization in G_1. Therefore, on photodynamic therapy, the S and G_2-M phases were partially emptied. After cells were withdrawn from CDDP- or gemcitabine-containing medium and placed in complete medium, they reentered the normal cycle within 24 hours (see also Fig. 1).

The two cytostatic drugs dose-dependently affected cell viability (Fig. 2). At 2.5 μmol/L, CDDP reduced cell viability by ~50% versus controls, and with 12 μmol/L CDDP, cell viability approached 0. Similarly, 4 nmol/L gemcitabine reduced cell viability by ~50%, and 10 nmol/L gemcitabine reduced it to <20% of control values. Cell viability was not completely abolished even at much higher gemcitabine concentrations (data not shown).

Table 1. Cytofluorimetric profiles of H1299 cells at 0 and 8, 12, and 24 hours of treatment with CDDP (2.5 μmol/L) or gemcitabine (4 nmol/L)

Phase	Control	CDDP (2.5 μmol/L)			Gemcitabine (4 nmol/L)		
	0 h	8 h	12 h	24 h	8 h	12 h	24 h
G_0-G_1	47.3	40.2	39.0	**64.9**	57.6	56.5	18.1
S	39.4	51.0	51.3	28.5	42.4	43.4	**81.9**
G_2-M	13.3	8.8	9.7	6.6	0	0.1	0

NOTE: Values are expressed as percent. Note the specific effects at 24 hours (bold).

The photodynamic therapy experiments were done in triplicate with 5 × 10^4 H1299 cells seeded in 35-mm tissue culture dishes. Twenty-four hours after seeding, the cells were incubated with Photofrin (2.5 μg/mL) for 16 hours, washed thrice with HBSS, and irradiated with increasing doses of light (see below). Cells were released into drug-free complete medium and left to grow for ~3 or 24 hours. At nontoxic Photofrin concentrations (i.e., 2.5 μg/mL), photodynamic therapy dose-dependently affected the magnitude of cell injury (Fig. 3). When light fluence increased from 0 to ~1.40 J/cm^2, cell viability decreased proportionally. No cells survived a fluence of 1.80 J/cm^2 (data not shown). At 0.54 J/cm^2, cell viability was reduced by ~50%. We used this sublethal dose in combination experiments with cytotoxic drugs. Unless indicated otherwise, all experiments reported hereafter were conducted with cells incubated for 16 hours with 2.5 μg/mL Photofrin and irradiated with a light fluence of 0.54 J/cm^2.

Combined Effects

Because we aimed at using the lowest drug concentration possible, we tested CDDP concentrations between 0.5 and 2.5 μmol/L and gemcitabine concentrations between 2 and 8 nmol/L while maintaining fluence at 0.54 J/cm^2. Very few cells treated with low concentrations of CDDP or gemcitabine survived fluences above 0.54 J/cm^2. However, within the concentration range tested, gemcitabine did not kill all H1299 cells (Fig. 2). Thus, for gemcitabine, we evaluated the effects caused by a fixed fluence on cells incubated with drug concentrations between 2 and 8 nmol/L and the effects caused by fixed drug concentrations (i.e., 4 and 8 nmol/L) and light fluences of 0.18, 0.28, 0.36, and 0.54 J/cm^2. We evaluated the efficacy of combined therapy by calculating the CI as detailed in the next paragraph and as reported in Table 2A (fixed fluence, 0.54 J/cm^2; CDDP between 0.25 and 2.50 μmol/L), Table 2B (fixed fluence, 0.28 J/cm^2; gemcitabine between 2 and 8 nmol/L), and Table 2C (fluence between 0.18 and 0.54 J/cm^2, gemcitabine 4 nmol/L). The most striking results were obtained with a light fluence of 0.54 J/cm^2 combined

with 2.5 μmol/L CDDP or 4 nmol/L gemcitabine. Individually, photodynamic therapy, CDDP, and gemcitabine reduced cell viability to 50 ± 7%, whereas photodynamic therapy combined with CDDP or gemcitabine reduced cell viability to 8 ± 2% and 14 ± 4%, respectively (Fig. 4).

Median Effect Analysis

Using the Chou and Talalay method (12) and the equations developed by Mack et al. (13), we calculated the CI and show that the effects of combined therapy at a fixed light fluence (0.54 J/cm^2) are additive within the range of CDDP concentrations used. These effects changed from possibly synergistic to explicitly synergistic at CDDP concentrations above 2.0 μmol/L (Table 2A). Differently, the overall effect remained additive with gemcitabine plus photodynamic therapy. The CI was 1 both when the drug was increased from 2 to 8 nmol/L and the light fluence was fixed at 0.28 J/cm^2 (Table 2B) and with gemcitabine fixed at 4 nmol/L and light fluences were between 0.18 and 0.54 J/cm^2 (Table 2C).

Cell Cycle and Protein Expression

To investigate the mechanisms by which Photofrin/photodynamic therapy and the cytotoxic drugs exert their effects when used alone or in combination, we analyzed the H1299 cell cycle and the expression levels of the Bcl-2, Bcl-XL, Bax, caspase-3, p21, pRb, cyclin A, Cdk2, HSP60, and HSP70 proteins (Fig. 5), which are related to apoptosis, cell cycle, and stress. Figure 1 shows the schedules of single-agent and combination treatments. The cytofluorimetric profiles obtained after the release of cells in drug-free medium for an additional 24 hours represents the distribution that would be found in the event of ineffective photodynamic therapy.

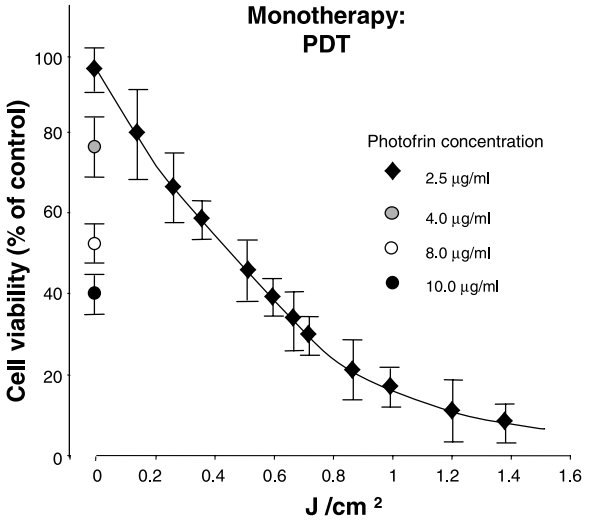

Figure 3. H1299 cells were incubated in the dark for 16 h with Photofrin (2.5, 4.0, 8, or 10 μg/mL). Dark toxicity was low (<5%) with 2.5 μg/mL Photofrin and high with 4 to 10 μg/mL (*circles*). Cell viability on irradiation was measured by the trypan blue exclusion test with a Photofrin concentration of 2.5 μg/mL. *Points,* average of three determinations; *bars,* SD. *PDT,* photodynamic therapy.

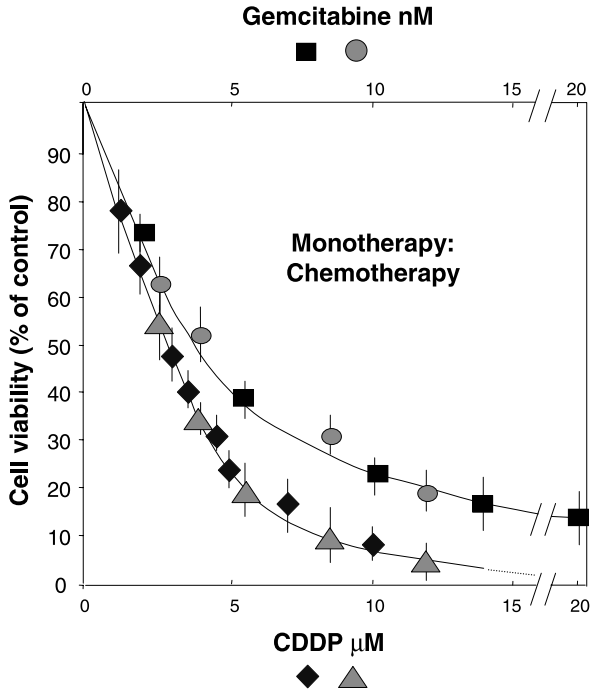

Figure 2. Effect of increasing concentrations of CDDP (*bottom curve*; 0–15 μmol/L) and gemcitabine (*top curve*; 0–12 nmol/L) on the viability of H1299 cells. Two sets of data from separate experiments are reported. Cells were incubated at the indicated CDDP or gemcitabine concentrations for 24 h, washed, and incubated for 24 h in fresh medium. Cell viability was measured by counting cells negative to trypan staining. Residual viability was expressed as percentage of untreated cells (controls). *Triangles* and *diamonds,* CDDP; *squares* and *circles,* gemcitabine. *Points,* average of three determinations; *bars,* SD.

CDDP. Using cytofluorimetry, we examined the H1299 cell cycle after 0, 8, 12, and 24 hours of incubation with 2.5 μmol/L CDDP (Table 1). After 24 hours, cells have accumulated in G_0-G_1 phase (see Table 1; Fig. 6) with a consequent loss of cells (~50%; trypan blue assay) in S phase. After exposure to CDDP for 24 hours, cells were released into fresh medium for ~3 and 24 hours. Synchronization in S phase was sustained for the first 3 hours, whereas cells approached the normal cycle at 24 hours (data not shown). This observation implies that the arrest in S phase was reversible. Protein expression studies (Western blot) support this notion. In fact, p21 protein expression was enhanced in H1299 cells exposed to 2.5 μmol/L CDDP for 24 hours (Fig. 5A, *lane 2*). However, p21 expression returned to basal levels within 24 hours (Fig. 5A, *lane 5*).

Surprisingly, although H1299 cells are p53 mutated (−/−), p21 protein expression seemed to be up-regulated at transcriptional level in the presence of CDDP. However, the p21 gene is also regulated by p53-independent factors, including growth promotion factors and differentiation-associated transcription factors (18). Moreover, CDDP concentration and incubation conditions may account for cytofluorimetric profile changes in various cells. In fact, whereas high CDDP concentrations cause cells to accumulate in the S-G_2 phases (13, 19–21), low CDDP doses induce

Table 2. Monotherapy versus combined therapy: median effect analysis and CI

A. Comparison of monotherapy (photodynamic therapy or CDDP) versus combined therapy (photodynamic therapy and CDDP) at a constant light fluence (CI < 1 indicates synergy)

Monotherapy			Combined therapy			
1	2	3	4	5	6	7
$(D_x)_1$ Fluence (J/cm2)	$(D_x)_2$ CDDP (μmol/L)	Observed effect cell viability (%)	D_1 fluence (J/cm^2)	D_2 CDDP (μmol/L)	CI	Combined effect
0	0	100	0.54	—	—	—
0.18	ND	82		—	—	—
0.36	1.5	68.5		—	—	—
0.54	2.5	50		0	1	Additive
0.61	3.0	45		0.25	1.02	Additive
0.73	4.0	36		0.50	0.96	Additive
0.81	1.5	33		1.00	1.04	Additive
0.99	5.0	25		1.50	0.90	Additive
1.08	6.0	20		2.00	0.85	Additive/synergistic
1.25	9.0	12		2.25	0.76	Synergistic
1.44	10.0	7		2.50	0.74	Synergistic

B. Comparison of monotherapy (photodynamic therapy or gemcitabine) versus combined therapy (photodynamic therapy and gemcitabine) at a constant light fluence (CI = 1 indicates an additive effect)

Monotherapy			Combined therapy			
1	2	3	4	5	6	7
$(D_x)_1$ Fluence (J/cm^2)	$(D_x)_2$ Gemcitabine (nmol/L)	Observed effect cell viability (%)	D_1 Fluence (J/cm^2)	D_2 Gemcitabine (nmol/L)	CI	Combined effect
0.28	1.5	80	0.28	0	1	—
0.38	2.0	72		2.0	1.03	Additive
0.60	5.5	44		4.0	1.06	Additive
0.80	8.0	30		6.0	0.97	Additive
0.92	12.5	22		8.0	0.99	Additive

C. Comparison of monotherapy (photodynamic therapy or gemcitabine) versus combined therapy (photodynamic therapy and gemcitabine) at a constant gemcitabine concentration (CI = 1 indicates additivity)

Monotherapy			Combined therapy			
1	2	3	4	5	6	7
$(D_x)_1$ Fluence (J/cm^2)	$(D_x)_2$ Gemcitabine (nmol/L)	Observed effect cell viability (%)	D_1 Fluence (J/cm^2)	D_2 Gemcitabine (nmol/L)	CI	Combined effect
0.54	4.0	50	0	4.0	1	—
0.65	6.0	41	0.18		1.05	Additive
0.72	6.5	37	0.28		1.01	Additive
0.98	11.0	21	0.36		0.99	Additive
1.2	14.5	15	0.54		0.98	Additive

NOTE: $(D_x)_1$ and $(D_x)_2$ are the doses of light or drug necessary to obtain a given effect when used alone; (D_1) and (D_2) are the doses of light and drug needed to obtain the same effect when used in the combination. Column 3 shows the residual cell viability on irradiation at the indicated light fluences [column 1, $(D_x)_1$] or drug treatment at the indicated concentrations [column 2, $(D_x)_2$], respectively. Columns 4 and 5 (D_1 and D_2) report the light fluences and drug concentrations used in combination. Columns 6 and 7 show the CI and the type of effect ensuing from combination. Monotherapy data in Table 2A–C are taken from Figs. 2 and 3, which provide the relative SD. Combined therapy data were obtained in separate experiments (data not shown).

an increase in p21 expression unaccompanied by bromodeoxyuridine incorporation (21), which suggests an arrest in G_1. A G_1 arrest has also been reported in other cell lines at high CDDP concentrations (50 μmol/L) but with short-term (2 hours) exposure (22). Also in our hands, 24-hour incubation with CDDP concentrations as high as 8 μmol/L caused cells to accumulate in G_2 (from <14% at 2.5 μmol/L to >31% at 8 μmol/L; data not shown). In conclusion,

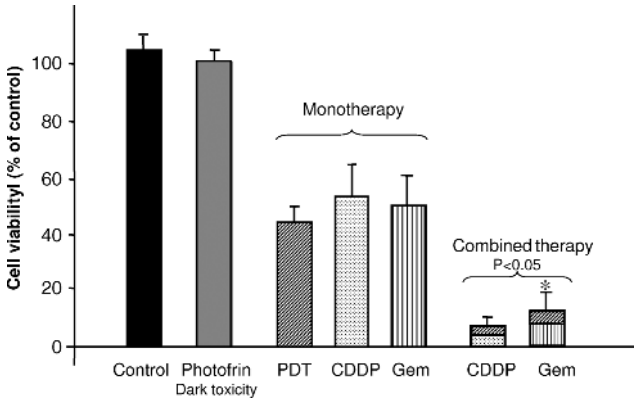

Figure 4. Effect of single versus combined treatment on the viability of H1299 cells. Viability was evaluated by the trypan blue assay in control cells, and cells incubated in the dark with Photofrin (2.5 μg/mL), after monotherapy with CDDP (2.5 μmol/L), gemcitabine (*Gem*; 4 nmol/L), or photodynamic therapy (0.54 J/cm^2), or combined therapy with 2.5 μmol/L CDDP and photodynamic therapy (0.54 J/cm^2) or 4 nmol/L gemcitabine and photodynamic therapy (0.54 J/cm^2). *Columns,* average of four determinations (trypan blue exclusion assay); *bars,* SD.

it seems that exposure of H1229 cells to sublethal doses of CDDP for 24 hours was detrimental for cells in S phase and caused cells to accumulate in G_0-G_1. This cytofluorimetric scenario is mirrored by the results of Western blot experiments.

Gemcitabine. The cytofluorimetric profile of H1299 cells after incubation for 24 hours with low doses of gemcitabine indicates a significant accumulation of cells in S phase (Table 1; Fig. 6), resulting from a massive (50%; trypan blue assay) loss of cells in the G_0-G_1 phase. The cell cycle was profoundly altered when cells were exposed to gemcitabine (4 nmol/L) for 8, 12, and 24 hours. At 24 hours, most cells were synchronized in S phase (Table 1). Synchronization in S phase was sustained for at least 3 hours after drug removal and the release of cells into fresh medium (data not shown). The arrest in S phase was not permanent as indicated by the fact that surviving cells reverted to the original (control) profile within 24 hours (data not shown). Cell accumulation in S phase after 24-hour incubation with gemcitabine, as shown by cytofluorimetry, was also consistent with an increase in cyclin A expression (Fig. 5B, *lane* 2) and in line with previous observations (23, 24). In conclusion, treatment for 24 hours of H1299 with sublethal gemcitabine doses was detrimental for cells in the G_0-G_1 phase and induced an accumulation of cells in S phase. This interpretation is supported by both Western blot experiments and cytofluorimetric profiles. The altered expression profiles were totally reverted 24 hours after drug removal.

Photodynamic Therapy. Photodynamic therapy with 2.5 μg/mL Photofrin (i.e., at a concentration that does not present ''dark toxicity'') induced cellular damage proportional to light fluence. Cell injury went from reversible, with rapid recovery of cellular functions and growth, to profound and irreversible. At concentrations ~10 μg/mL Photofrin, photodynamic therapy causes cell death, apoptosis, or necrosis depending on such factors as light

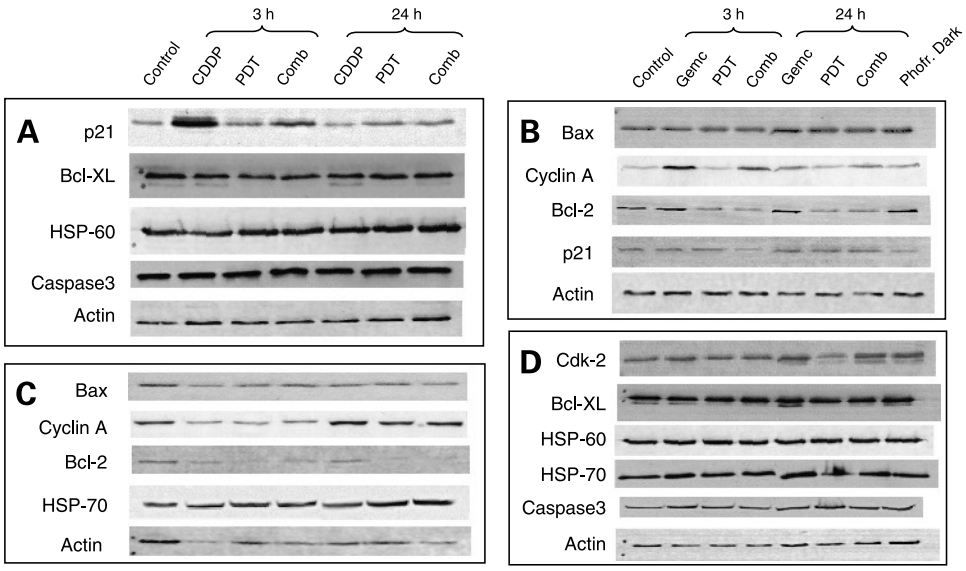

Figure 5. Protein expression in cells treated with monotherapy or combined therapy. Protein extracts were analyzed 3 or 24 h after cells were placed in fresh medium after individual or combined treatments (see Fig. 4). **A** and **C**, CDDP; **B** and **D**, gemcitabine. Actin was always used as loading control. Further observations: photodynamic therapy increased the expression of p21 (1 – 3 h), split the Bcl-XL electrophoretic band in a doublet (see also **D**), and seemed to destroy Bcl-2 (**B**). Photodynamic therapy also caused a detectable increase in HSP60 and HSP70 expression. Indeed, although the expression of actin in **C** is highly variable, the expression of HSP70 on photodynamic therapy (alone or in combination) is clearly increased, whereas the questionable fading of Bcl-2 is confirmed by inspection of **B**. Gemcitabine significantly affected cyclin A expression (**B**). Treatment did not affect Bax and caspase-3 expression (**C, B** and **A, D**). Photofrin in the absence of light (dark effect) did not affect cells as shown by two experiments shown in **B** and **D**.

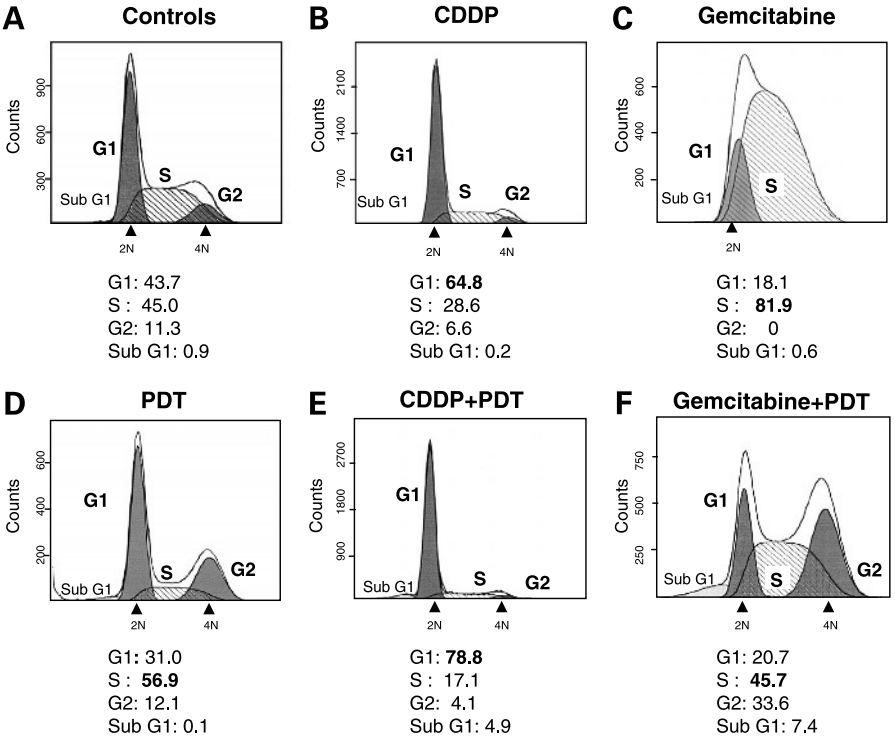

Figure 6. Representative experiments depicting the cell cycle distribution of H1299 cells as measured by flow cytometric analysis of DNA content before (**A**, controls) and after treatment with CDDP (**B**), gemcitabine (**C**), photodynamic therapy alone (**D**), or in sequential combination (**E** and **F**). In these cases, cells were analyzed 24 h after photodynamic therapy. The FACScan software assigns apoptotic cells and large cell debris to sub-G_1 phase. *Gray histograms,* G_0-G_1 and G_2-M phases; *dashed histograms,* S phase.

fluence, photosensitizer concentration, and cell type (25). The Photofrin incubation protocol has also been implicated in the cell death pathway (26). Although we focused on the effects of a single light dose (0.54 J/cm^2), after 16 hours of incubation with 2.5 μg/L Photofrin, few H1299 cells underwent apoptosis (sub-G_1; Fig. 6). Indeed, the expression of Bax (Fig. 5B and C) and caspase-3 (Fig. 5A and D) was unchanged 3 and 24 hours after photodynamic therapy. Differently, Bcl-2 expression was significantly reduced. This coincides with the finding that some photosensitizers induce Bcl-2 degradation (27). Moreover, Hypericin/photodynamic therapy alters the expression and function of Bcl-2 and delays the onset of apoptosis (28). Here, we show that also Photofrin/photodynamic therapy causes Bcl-2 degradation. This degradation, which can only be inferred from Fig. 5C (*lane 3*; because of the large actin control variability), clearly emerges in Fig. 5B (i.e., *lane 3*). Finally, Photofrin photodynamic therapy caused changes in the electrophoretic profile of Bcl-XL as indicated by the disappearance of the faster-migrating Bcl-XL isoform (Fig. 5A, *lane 3*, and D, *lane 3*). Pc 4 photodynamic therapy has been shown to damage Bcl-XL isoforms in several other human cancer cells (29). Although Hanlon et al. (30) reported a very important increase in the expressions of HSP60 and HSP70 proteins, they were only modestly, albeit clearly, enhanced by photodynamic therapy in our conditions (Fig. 5A, B and C, D, respectively). However, Hanlon et al. used different cell lines as well as much higher Photofrin concentrations. Indeed, Photofrin concentrations higher than 5 μg/mL are per se highly toxic for H1299 cells even in the dark.

We used Western blotting to evaluate changes in protein expression after monotherapy (i.e., individual drugs or photodynamic therapy) and after combined treatments (i.e., each drug + photodynamic therapy). It is noteworthy that with time most protein expression profiles tended to revert to their original qualitative and quantitative patterns (Fig. 5A–D). The apparent ''increase'' in cyclin A expression (Fig. 5C, *lanes 5–7*) may represent an experimental artifact given the large variability of the actin control. As stated, the expression of HSP60 and HSP70 proteins was enhanced after 24 hours albeit to a lesser extent versus cyclin A (Fig. 5A, C, and D). The cell cycle patterns after combined therapy (Fig. 6E and F) are not in disagreement with the protein expression profiling data.

Figure 6 is representative of various experiments concerning the effects of combined treatment. Within 24 hours, 2.5 μmol/L CDDP killed ~50% of cells, most of which were in S phase (Fig. 6B). At variance, photodynamic therapy (0.54 J/cm^2) eliminated mainly G_0-G_1 cells (Fig. 6D), and most of the remaining cells were in S phase. In conclusion, CDDP, at a low concentration, killed cells in S phase, and surviving cells occurred mainly in G_0-G_1, a phase in which cells are susceptible to photodynamic therapy (Table 2A).

Gemcitabine alone, at a concentration as low as 4 nmol/L, killed ~50% of cells (most of which were in G_0-G_1 phase) and induced a pronounced accumulation of cells in S phase (Fig. 6C). It seems that gemcitabine at this concentration enhances photodynamic therapy cytotoxicity, but to a much lesser extent than CDDP, and the effect is essentially additive (Table 2B and C). In controls, 44.2% were in G_0-G_1, 44.6% were in S, and 11.2% were in G_2-M. After photodynamic

therapy (0.54 J/cm^2) or 24 hours of incubation with CDDP (2.5 μmol/L) or gemcitabine (4 nmol/L; all conditions that kill ~50% of cells), 31.2%, 76.1%, and 18.0% of cells were in G_0-G_1, 56.7%, 10.5%, and 82.0% were in S, and 12.1%, 13.4%, and ~0% were in G_2-M, respectively. Hence, photodynamic therapy and gemcitabine preferentially damage cells in G_0-G_1, whereas CDDP targets cells in S phase. In conclusion, it seems that the targeting of cells in different phases results in an accumulation of death signals caused separately and independently by photodynamic therapy and a suitable cytotoxic drug.

Photodynamic therapy is a well-established stand-alone therapy (9) in which the photosensitizer can be administered by i.v. injection or applied on the skin and selectively targets cancer cells. Its effectiveness increases when combined with other therapeutic measures. Here, we describe a way to exploit mutual reinforcement of two independent therapeutic modalities: Photofrin/photodynamic therapy and chemotherapy. Photofrin and porphyrin derivatives, in general, are the photosensitizers most widely used in photodynamic therapy. At variance with gemcitabine, which to our knowledge has never been used with Photofrin/photodynamic therapy, CDDP has been used in combination with various photosensitizers, including porphyrin derivatives (11, 31–35). However, previous studies were mainly descriptive and were limited to observations about the effects exerted on cell mortality. No reasons were advanced to account for the greater efficacy of combined treatment, nor did those studies report changes in protein expression and related cell cycle changes. Our study shows that doses of CDDP or gemcitabine and light/Photofrin that were partially effective in killing H1299 cells when given singly were remarkably more effective when used in combination. These effects span from additive to synergistic. Additivity occurred with both drugs, but the effect was synergistic when the drug (CDDP) exerted its activity disjointed, in terms of cell cycle, from those of photodynamic therapy. Under the conditions we used, not all metastatic cells were killed. However, preincubation of H1299 cells with the low CDDP dose (2.5 μmol/L) followed by their exposure to a light fluence only 1.5-fold higher (i.e., ~0.80 J/cm^2) than that used in most experiments described herein (~0.54 J/cm^2) resulted in the rapid death of all cells.

In conclusion, selectively localized photosensitizers and appropriate doses of light combined with low doses of chemotherapeutic drugs represent a promising treatment strategy for cancer. In principle, combinations of photodynamic therapy and drugs would not only destroy cancer cells more efficiently but would also reduce the noxious side effects of chemotherapy.

Acknowledgments

We thank Jean Ann Gilder for text editing.

References

1. Dougherty TJ, Gomer CJ, Henderson BW, et al. Photodynamic therapy. J Natl Cancer Inst 1998;90:889–905.

2. Gossner L. Photodynamic therapy: esophagus [review]. Can J Gastroenterol 2002;16:642–4.

3. Gomer TJ, Dougherty TJ. Determination of ^{3}H and ^{14}C hematoporphyrin derivative distribution in malignant and normal tissues. Cancer Res 1979;39:146–51.

4. Oleinick NL, Morris RL, Belichenko I. The role of apoptosis in response to photodynamic therapy: what, where, why, and how. Photochem Photobiol Sci 2002;1:1–21.

5. Roninson IB, Broude EV, Chang BD. If not apoptosis, then what? Treatment-induced senescence and mitotic catastrophe in tumor cells [review]. Drug Resist Updat 2001;4:303–13.

6. Crul M, van Waardenburg RCA M, Beijnen JH, Schellens JHM. DNA-based drug interactions of cis-platin. Cancer 2002;28:291–303.

7. Mackey JR, Mani RS, Selner M, et al. Functional nucleoside transporters are required for gemcitabine influx and manifestation of toxicity in cancer cell lines. Cancer Res 1998;58:4349–57.

8. Shewach DS, Reynolds KK, Hertel L. Nucleotide specificity of human deoxycytidine kinase. Mol Pharmacol 1992;42:518–24.

9. Dolmans DE, Fukumura D, Jain RK. Photodynamic therapy for cancer [review]. Nat Rev Cancer 2003;3:380–7.

10. Doyle A, Griffiths JB, Newell DG. Trypan blue exclusion method for cell viability estimation. In: Cell and tissue culture: laboratory procedures. London: Wiley; 1993; 4:5.2.

11. Crescenzi E, Varriale L, Iovino M, Chiaviello A, Veneziani BM, Palumbo G. Photodynamic therapy with indocyanine green complements and enhances low-dose cisplatin cytotoxicity in MCF-7 breast cancer cells. Mol Cancer Ther 2004;3:537–44.

12. Chou TC, Talalay P. A Quantitative analysis of dose-effect relationships: the combined effects of multiple drugs or enzyme inhibitors. Adv Enzyme Regul 1984;22:27–55.

13. Mack PC, Gandara DR, Lau AH, Lara PN, Jr., Edelman MJ, Gumerlock PH. Cell cycle-dependent potentiation of cisplatin by UCN-01 in non-small-cell lung carcinoma. Cancer Chemother Pharmacol 2003;51:337–48.

14. Bradford M. A rapid and sensitive method for the quantitation of microgram quantities of protein utilizing the principle of protein-dye binding. Anal Biochem 1976;72:248–54.

15. Laemmli UK. Cleavage of structural proteins during the assembly of the head of bacteriophage T4. Nature 1971;227:680–5.

16. Fisher AM, Ferrario A, Rucker N, Zhang S, Gomer CJ. Photodynamic therapy sensitivity is not altered in human tumor cells after abrogation of p53 function. Cancer Res 1999;59:331–5.

17. Itahana K, Dimri G, Campisi J. Regulation of cellular senescence by p53. Eur J Biochem 2001;268:2784–91.

18. Agami R, Bernards R. Distinct initiation and maintenance mechanisms cooperate to induce G_1 cell cycle arrest in response to DNA damage. Cell 2000;102:55–66.

19. Chang BD, Swift ME, Shen M, Fang J, Broude EV, Roninson IB. Molecular determinants of terminal growth arrest induced in tumor cells by a chemotherapeutic agent. Proc Natl Acad Sci U S A 2002;99:389–94.

20. Sekiguchi I, Suzuki M, Tamada T, Shinomiya N, Tsuru S, Murata M. Effects of cisplatin on cell cycle kinetics, morphological change, and cleavage pattern of DNA in two human ovarian carcinoma cell lines. Oncology 1996;53:19–26.

21. Lanzi C, Perego P, Supino R, et al. Decreased drug accumulation and increased tolerance to DNA damage in tumor cells with a low level of cisplatin resistance. Biochem Pharmacol 1998;55:1247–54.

22. Miyaji T, Kato A, Yasuda H, Fujigaki Y, Hishida A. Role of the increase in p21 in cisplatin-induced acute renal failure in rats. J Am Soc Nephrol 2001;12:900–8.

23. Erlandsson F, Wählby C, Ekholm S, Bengtsson E, Zetterberg A. A detailed analysis of cyclin A accumulation at the G([1])/S border in normal and transformed cells. Exp Cell Res 2000;259:86–95.

24. Shi Z, Azuma A, Sampath D, Li YX, Huang P, Plunkett W. S-Phase arrest by nucleoside analogues and abrogation of survival without cell cycle progression by 7-hydroxy-stauro-sporine. Cancer Res 2001;61:1065–72.

25. Marcinkowska A, Malarska A, Saczko J, et al. Photofrin-factor of photodynamic therapy induces apoptosis and necrosis. Folia Histochem Cytobiol 2001;Suppl 2:177–8.

26. Dellinger M. Apoptosis or necrosis following Photofrin photosensitization: influence of the incubation protocol. Photochem Photobiol 1996; 64:182 – 7.

27. Xue LY, Chiu SM, Oleinick NL. Photochemical destruction of the Bcl-2 oncoprotein during photodynamic therapy with the phthalocyanine photosensitizer Pc 4. Oncogene 2000;20:3420 – 7.

28. Vantieghem A, Xu Y, Assefa Z, et al. Phosphorylation of Bcl-2 in G_2-M phase-arrested cells following photodynamic therapy with hypericin involves a CDK1-mediated signal. J Biol Chem 2002;277:37718 – 31.

29. Xue LY, Chiu SM, Fiebig A, Andrews DW, Oleinick NL. Photodamage to multiple Bcl-XL isoforms by photodynamic therapy with the phthalocyanine photosensitizer Pc-4. Oncogene 2003;22:9197 – 204.

30. Hanlon JG, Adams K, Rainbow AJ, Gupta RS, Singh G. Induction of Hsp60 by Photofrin-mediated photodynamic therapy. J Photochem Photobiol B 2001;64:55 – 61.

31. Zimmermann A, Walt H, Haller U, Baas P, Klein SD. Effects of chlorin-mediated photodynamic therapy combined with fluoropyrimidines *in vitro* and in a patient. Cancer Chemother Pharmacol 2003;51: 147 – 54.

32. Canti G, Nicolin A, Cubeddu R, Taroni P, Bandieramonte G, Valentini G. Antitumor efficacy of the combination of photodynamic therapy and chemotherapy in murine tumors. Cancer Lett 1998;125: 39 – 44.

33. Nahabedian MY, Cohen RA, Contino MF, et al. Combination cytotoxic chemotherapy with cisplatin or doxorubicin and photodynamic therapy in murine tumors. J Natl Cancer Inst 1988;80:739 – 43.

34. Sharkey SM, Wilson BC, Moorehead R, Singh G. Mitochondrial alterations in photodynamic therapy-resistant cells. Cancer Res 1993;53: 4994 – 9.

35. Ma LW, Moan J, Berg K, Peng Q, Steen HB. Potentiation of photodynamic therapy by mitomycin C in cultured human colon adenocarcinoma cells. Radiat Res 1993;134:22 – 8.

Photodynamic therapy with indocyanine green complements and enhances low-dose cisplatin cytotoxicity in MCF-7 breast cancer cells

Elvira Crescenzi, Linda Varriale, Mariangela Iovino, Angela Chiaviello, Bianca Maria Veneziani, and Giuseppe Palumbo

Dipartimento di Biologia e Patologia Cellulare e Molecolare ''L. Califano,'' University of Naples, Federico II, Naples, Italy

Abstract

Objective: We investigated the effects of photodynamic therapy (PDT) combined with low-dose chemotherapy on breast cancer cells. Photodynamic treatment was administered by irradiating indocyanine green-preloaded MCF-7 cells with an IR diode laser source at 805 nm; cisplatin was used for chemotherapy. Methods: The dose-response phenomena associated with the two treatments administered individually and together were evaluated with the following tests: trypan blue dye exclusion, 3-(4,5-dimethylthiazol)-2,5-diphenyltetrazolium bromide (MTT) assay, clonogenic survival, thymidine and methionine incorporation, and insulin-dependent and insulin-independent glucose transport. Results: Viability and metabolic data demonstrated mutual reinforcement of therapeutic efficacy. However, isobolographic analysis of quantal and variable data indicated that reinforcement was additive according to trypan blue data and synergistic according to MTT data. To investigate the molecular mechanisms underlying alterations in cell proliferation and apoptosis, we evaluated (by Western blotting) the expression of proteins Bcl-2, Bax, Bcl-X_L, p21, p53, and poly(ADP-ribose) polymerase. Photodynamic treatment caused transient selective destruction of Bcl-2 and up-regulation of Bax. It also induced apoptosis in a limited fraction of cells (10–12%). Flow cytometry data showed that PDT killed mostly G_1-phase cells, whereas cisplatin killed mostly S-phase cells. This disjointed phase-related effect may account for the favorable effects exerted by combined treatment. Conclusions: Our findings imply that low doses of cytostatic drugs may be as effective or even more effective than currently used doses if appropriately combined with PDT. [Mol Cancer Ther 2004;3(5):537–44]

Introduction

Photodynamic therapy (PDT) is a relatively new and effective treatment for human tumors (1). It entails local or systemic administration of a photosensitizer and subsequent exposure of the neoplastic area to a light of suitable wavelength. The rationale is that, on exposure to light, the photosensitizer, which is absorbed by all cells and selectively retained by malignant tissue (2, 3), is promoted to an excited state and then, as it decays, induces local release of cytotoxic reactive oxygen species. Depending on the experimental conditions and cell sensitivity, the cytotoxic molecular species resulting from PDT may trigger cell apoptosis or induce necrosis (4).

The near-IR spectral region is particularly suitable for PDT because it penetrates deep into tissues without causing significant heating. To date, the most suitable IR-photosensitizable molecule is indocyanine green dye (ICG). In fact, ICG is not toxic, is widely used in humans as a diagnostic tool in hemodynamics (5, 6), has an absorption peak between 775 and 810 nm (7, 8), and is a photosensitizer.

Cisplatin [*cis*-diammine-dichloroplatinum (II)] is used in the management of various cancers. By forming adducts to DNA, cisplatin inhibits DNA replication and chain elongation, which accounts for its antineoplastic activity. In clinical practice, cisplatin is often combined with other chemotherapeutic agents. Synergy between cisplatin and other chemotherapeutic agents occurs by various pathways: increased intracellular drug accumulation, enhanced binding to DNA, and decreased DNA repair (9).

The MCF-7 cell line was established 30 years ago from the pleural effusion of a patient with a breast carcinoma (10). These malignant cells have functional p53, lack caspase-3 activity, maintain a functionally intact estrogen receptor, and have constitutively high levels of Bcl-2, a protein endowed with cytostatic and antiapoptotic activities (11, 12). The latter two features are probably closely related because, as we have recently shown, the coding sequence of the *bcl-2* gene includes a functioning estrogen-responsive element (13).

MCF-7 cells are remarkably resistant to various treatments including cisplatin and some types of PDT but not to tumor necrosis factor or staurosporin (14). However, the cells become sensitive to cisplatinum on p53 disruption (15). In contrast, parental MCF-7 cells and p53-abrogated cells are equally sensitive to photofrin/PDT (16).

In an attempt to identify treatment combinations in which the dose of the toxic compound could be decreased without reducing efficacy, we examined the effects of

Received 2/2/04; revised 3/16/04; accepted 3/22/04.

Grant support: MIUR-COFIN 2002 program and Agenzia Spaziale Italiana (Rome, Italy).

The costs of publication of this article were defrayed in part by the payment of page charges. This article must therefore be hereby marked advertisement in accordance with 18 U.S.C. Section 1734 solely to indicate this fact.

Note: E. Crescenzi and L. Varriale contributed equally to this study.

Requests for Reprints: Giuseppe Palumbo, Dipartimento di Biologia e Patologia Cellulare e Molecolare ''L. Califano,'' University of Naples, Federico II, Via S. Pansini 5, 80131 Naples, Italy. Phone: 39-81-7463249; Fax: 39-81-7701016. E-mail: palumbo@unina.it

moderately toxic doses of cisplatin and ICG/PDT, administered separately and together, on various metabolic and proliferative parameters of MCF-7 cells. We also describe changes in the expression profile of some proteins involved in the control of the cellular proliferative status and apoptosis.

Materials and Methods

Cells

Human breast cancer MCF-7 cells were grown at 37°C in a humidified atmosphere (95% air and 5% CO_2), DMEM supplemented with phenol red, L-glutamine (2 mM), penicillin (100 units/ml), streptomycin (100 μg/ml), gentamicin (50 μg/ml), and 10% FCS. Fresh medium was provided every 3 days.

Laser Source

The laser source was a diode array laser from Quanta System (Milan, Italy) emitting at 805 nm. The nominal output energy (continuous wave) was 0.65 W. The laser was equipped with an adjustable (0.1 s) time shutter.

Photosensitizer and Photosensitization

The ICG (M_r = 775.0) preparation (Sigma Chemical Co., St. Louis, MO) was iodide free, unlike the ICG preparations used for most previous studies (7, 17). The ICG stock solution was obtained by dissolving the deep green powder (~1 mg/ml) in 100 mM sodium phosphate (pH 7.2). Before measurements, appropriate aliquots of this solution were diluted to the desired concentration. The purity of the commercial product was checked by isocratic high-performance liquid chromatography in 10 mM sodium phosphate in 47% acetonitrile, 3% methanol using a C18 reverse-phase column equipped with a UV detector set at 230 nm. Aqueous ICG samples at various concentrations (between 10 and 400 μM) were analyzed by high-performance liquid chromatography immediately after their preparation and after extensive irradiation (>1000 J cm^{-2}). The resulting chromatograms did not differ from that of nonirradiated ICG, except for a significant decrease in the relative height (and areas) of the ICG peaks, which indicates extensive photobleaching of the dye.

Photosensitization experiments were performed with MCF-7 cells incubated in 20 μM ICG for 24 h. Because of the low concentration of ICG used, we did not measure uptake of the dye by MCF-7 cells in these conditions. However, the ICG uptake in keratinocytes under similar experimental conditions was about 3–5 nmol/10^5 cells (17). Plates were washed twice with ICG-free medium and positioned under the laser beam at the appropriate distance. The temperature of plates during irradiation was controlled by their partial immersion in a water bath heated at 35°C. Except for the dose-response curves shown in Fig. 1, cells were routinely irradiated with light doses of 25 J cm^{-2}. After exposure(s), cells (normally quadruplicates) were incubated in the dark at 37°C for an additional 5 h (or >10 h in some cases) before further analysis.

Sample Treatment Schedules

All experiments reported herein included several controls (*i.e.*, untreated cells, ICG-loaded but not light-sensitized cells, and cells exposed to light in the absence of ICG). The various parameters evaluated under these conditions did not differ and are not reported herein.

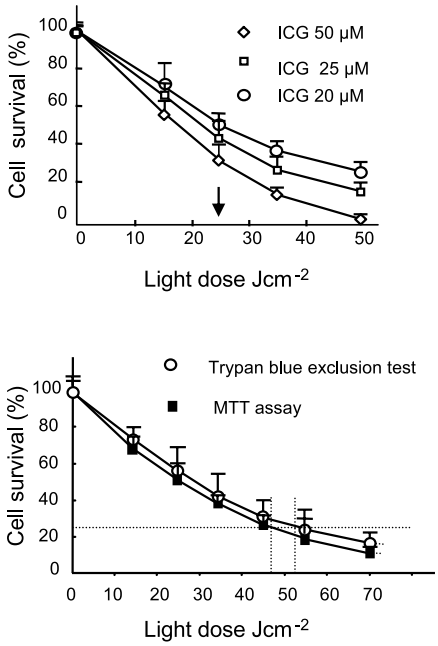

Figure 1. Effect of three doses of ICG photosensitization at 805 nm on MCF-7 cells. Five hours after each irradiation, cell viability was assessed by the trypan blue exclusion test. *Points,* average of four determinations; *bars,* SD. Combination treatments were performed at a light fluence of 25 J cm^{-2} and an ICG concentration of 20 μM (*hatched line*).

Cell Viability, Cytotoxicity, and Survival Assays

Trypan Blue Dye Exclusion Assay. Cell viability after treatment (irradiation, cisplatin, or both) was determined by the trypan blue dye exclusion test 5 h after each treatment (unless indicated otherwise). All assays were performed in quadruplicate and results are reported as the mean ± SD.

3-(4,5-Dimethylthiazol)-2,5-Diphenyltetrazolium Bromide Assay. Cell viability after each treatment (irradiation, cisplatin, or both) was determined by the 3-(4,5-dimethylthiazol)-2,5-diphenyltetrazolium bromide (MTT) assay (18). MCF-7 cells (2×10^4 cells/0.2 ml) were seeded in 96-well plates and kept in the incubator at 37°C overnight. Cells were then treated with ICG alone, cisplatin alone, or ICG plus cisplatin and incubated for a further 24 h. After incubation, cells containing ICG were irradiated with a fluence of 25 J cm^{-2}. Five hours later, cells were washed, collected in tubes, and centrifuged at 1000 rpm for 5 min. Supernatants were removed and the cells were resuspended in ICG-free medium. Control cells were processed in the same way. A MTT stock solution was made by dissolving the crystals in a phenol red-free culture medium to a final concentration of 0.5 mg/ml. Typically, 50 μl of this solution were added to each well containing suspended cells in 200 μl of medium. After an additional 4 h incubation at 37°C, cells were collected by aspiration and

centrifuged at 1500 rpm for 7 min. The converted dye was extracted from the supernatant obtained by adding acidic (0.1 M HCl) isopropanol to the pelleted cells. Absorbance of the samples, read with a Titertek-Multiscan photometer (Huntsville, AL) equipped with a 532 nm filter, of converted dye in stimulated cells *versus* untreated controls is called MCF-7 viability. Quadruplicate samples were used in each experiment.

Clonogenic Survival Assay. The assay was performed exactly as described by Theodossiu *et al.* (19). Cells were seeded in 100 mm Petri dishes at low density ($\sim 3 \times 10^4$/dish) and left to adhere for 24 h in a standard medium. ICG (20 μM) and/or cisplatin (8 μM) were added where appropriate. Twenty-four hours later, samples intended for PDT, alone or in combination, were irradiated (fluence of 25 J cm^{-2}).

After irradiation, cells were washed, immediately trypsinized, resuspended in single-cell suspension, and plated for the determination of macroscopic colony formation. After 6 days of growth, colonies were fixed with a 3:1 mixture of methanol/acetic acid and stained with crystal violet. Only colonies constituted by more than 50 cells were scored (19). Two separate experiments were performed using duplicate samples.

Flow Cytometry

Plates containing 5×10^5 MCF-7 cells were incubated for 24 h at 37°C in 2 ml complete medium (controls) or medium supplemented with ICG (20 μM), cisplatin (8 μM), or both (ICG and cisplatin). Photodynamic treatment of cells was performed as reported under Photosensitizer and Photosensitization. Cells were detached by trypsinization from 10 cm plates, suspended in serum-rich medium, centrifuged, washed twice with 1 ml PBS, and resuspended for storage (4°C) in absolute ethanol. Before analysis, fixed cells were washed twice, centrifuged, and resupended in 1 ml PBS containing 5 μg RNase and 100 μg propidium iodide. Samples were stored in the dark for 20 min at room temperature before final readings. The cellular orange fluorescence of propidium iodide was detected on a linear scale using a flow cytometer (FACScan, Becton Dickinson, Mountain View, CA) equipped with an excitation laser line at 488 nm. At least 20,000 events were collected for each sample. The cell cycle was examined 5 h after each single or combined treatment. Four separate experiments were performed.

Thymidine Incorporation

Thymidine incorporation experiments were performed in 24-well plates according to Love-Schimenti *et al.* (20) with minor modifications. In brief, cells (3×10^4 cells/well) were incubated at 37°C in 2 ml complete medium (controls) or medium supplement with ICG (20 μM), cisplatin (8 μM), or both. All samples were run in triplicate. After 24 h incubation, each well was washed with 1 ml warm medium. ICG-loaded cells were then irradiated at 25 J cm^{-2}. After irradiation, the medium was replaced (all samples) with fresh culture medium containing labeled [^{3}H]thymidine (0.5 μCi/ml; Amersham, Buckinghamshire, UK). After 5 h at 37°C, incorporation was blocked by extensive washing with warm serum-free medium. NaOH (0.1 M) was added to all wells (1 ml) and the plates were left at 37°C for 1 h under constant agitation. Solutions (100 μl) were used to measure the protein content (21) and the remainder was used to measure the incorporated thymidine with the semiautomatic Harvester 96 (Skatron Instruments, Lier, Norway). Thymidine counts were expressed as a fraction of counts found in controls.

Methionine Incorporation

We used six-well plates for methionine incorporation experiments as described by Consiglio *et al.* (22). Cells (10^5 cell/well) were incubated at 37°C in 2 ml complete medium (controls) or medium supplemented with ICG (20 μM), cisplatin (8 μM), or both (ICG and cisplatin). All samples were run in triplicate. After 24 h incubation under these conditions, each well was washed with 1 ml warm medium and irradiated at 25 J cm^{-2} (ICG-loaded cells only). Four hours later, the medium of each well was replaced with 1 ml medium containing 30 μCi [^{35}S]methionine (specific activity 1000 Ci/mmol; Amersham, United Kingdom). After 60 min, labeling was terminated by three consecutive washings with 1 ml cold PBS. Cells were finally scraped and lysed by keeping them for 15 min on ice with 0.45 ml lysis buffer consisting of 137 mM NaCl, 4 mM KCl, 1 mM $MgCl_2$, 1% Triton X-100, 0.1% BSA and protease inhibitors, 50 μg/ml leupeptin, and 50 μg/ml aprotinin. Aliquots (100 μl) of cell lysates were precipitated in triplicate on GFC Whatman (Springfield Mill, UK) filters by soaking them in 10% trichloroacetic acid (TCA) on ice for 10 min. Filters were washed thrice for 10 min in 5% TCA and then rinsed twice in 95% ethanol and acetone. Finally, filters were dried at 60°C and counted in a Beckman (Fullerton, CA) liquid scintillator.

Increasing the time of lysis from 30 min to 2 h did not affect the TCA-precipitable counts. Aliquots of 100 μl were used to measure protein contents according to the procedure of Bradford (21).

Deoxyglucose Uptake

Glucose uptake was determined according to Singh *et al.* (23). Twenty-four plates (3.5 cm) containing MCF-7 cells (2×10^5 cells/well) were incubated for 24 h at 37°C in 2 ml complete medium (controls) or medium supplemented with ICG (20 μM), cisplatin (8 μM), or both. The cells were then washed with fresh medium. The plates intended for PDT (alone or in combination) were irradiated as usual. Five hours later, all cells were washed thrice again with PBS and divided into two groups of 12 plates each (four samples, each sample in triplicate). The two groups of 12 plates each (*i.e.*, three controls, three plates treated with cisplatin alone, three plates treated with ICG/PDT alone, and three plates treated with cisplatin and ICG/PDT) were incubated for 30 min at 37°C in a buffer containing 1 μCi [^{14}C]deoxyglucose (specific activity 200 μCi/ml) in the absence or presence of 1 μM insulin. Uptake was terminated in all plates by extensively washing cells with ice-cold PBS. Cell monolayers were finally solubilized with 1 ml 0.01% Triton X-100 in 0.01 M NaOH. Aliquots of 100 μl served for protein determination (21) and the rest was used for liquid scintillation counting.

Isobolographic Analysis

Isobolograms were constructed according to a ''fixed dose method'' (24, 25). Firstly, the responses in a fraction x of the cells were evaluated after treatment with PDT or cisplatin. A fraction corresponding to 75% was found to be suitable and is called ED_{75}. Cells were then assigned to receive treatment consisting of a fixed dose of cisplatin (8 μM) combined with PDT of increasing potency by varying light fluence from 0 to 60 J cm^{-2}, the ICG concentration remaining fixed at 20 μM. The aim of this analysis was to ascertain experimentally the light dose necessary to attain the prefixed effect in the presence of the prefixed concentration of cisplatin.

In a typical isobologram, the ED_x, computed by the individual dose-response curves, was plotted on the vertical and horizontal axes, respectively. The theoretical dose-additive line, including its 95% fiducial limits (calculated by the SE multiplied by 1.96), was attained by joining the two ED_x of choice. If the experimental ED_x of the combination is within the boundary of the dose-additive line and the confidence interval (*i.e.*, the experimental point is nearly coincident with the theoretical point), then the specific combination of PTD with a fixed concentration of cisplatin exerts a dose-additive effect. The effect is synergistic if the experimental point and theoretical point are below the boundaries and antagonistic if they are above the boundaries.

PAGE and Western Blotting

Polyacrylamide gels (15% or 7.5%) were prepared essentially as described by Laemmli (26). Proteins separated on the polyacrylamide gels were blotted onto nitrocellulose filters (Hybond-C pure; Amersham, Milan, Italy) and immunorevealed with specific primary monoclonal antibodies (Santa Cruz Biotechnology, Santa Cruz, CA). Filters were washed and treated with horseradish peroxidase-linked antibodies and the blots were revealed autoradiographically with enhanced chemiluminescence detection reagents (Amersham, Milan, Italy). The entire procedure has been described elsewhere (27). Blots were reprobed with β-actin antibody as loading control. Autoradiographs were scanned with a Discover Pharmacia Scanner equipped with a Sun Spark Classic Workstation and appropriate software (*pdi*, RFL print, version 2; Oakwood, Huntington Station, NY).

Results and Discussion

We have evaluated if treatment with ICG/PDT plus cisplatin results in an effective outcome (additive or even synergistic) so that the dose of the two components or at least of the most toxic one (*i.e.*, cisplatin) can be reduced. We analyzed (*a*) the response of ICG-treated cells to increasing light doses and (*b*) the response of MCF-7 cells to cisplatin administered alone (at increasing concentrations) or combined with ICG/PDT. In all the combined treatment experiments, we used a low cisplatin concentration (8 μM) and rather mild PDT conditions (20 μM ICG, light fluence of 25 J cm^{-2}).

Individual Treatments

Dose-Response Effects of ICG/PDT on Cell Viability. As shown in Fig. 1 (*upper panel*), both ICG concentration and light dose affected the magnitude of cell injury. At a fluence of 50 J cm^{-2}, about 30% of cells survived exposure to 20 μM ICG, much less survived exposure to 25 μM ICG, and no cells survived exposure to 50 μM ICG. To ascertain the effect of combined treatment, we administered PDT at sublethal doses using an ICG concentration of 20 μM. Figure 1 (*lower panel*) shows the dose-response curves obtained with this ICG concentration. Apparently, the ED_{75} as measured by MTT assay and the trypan blue exclusion test are not superimposable because they span from ~47 to ~52 J cm^{-2}, respectively. Except where specifically indicated, all experiments reported hereafter were conducted with cells preloaded with 20 μM ICG and a light fluence of 25 J cm^{-2}.

Dose-Response Effects of ICG/PDT on Protein Expression. To test whether ICG/PDT altered the expression of proteins related to cell death, we measured the expression of proteins Bcl-2, Bax, Bcl-X_L, p21, poly(ADP-ribose) polymerase (PARP), and p53 by Western blot analysis. The analyses were performed 5 and >10 h after irradiation with either 15 or 25 μM ICG and two different fluences (*i.e.*, 15 or 25 J cm^{-2}). Figure 2 shows that Bcl-2 expression decreased while Bax expression increased as the fluence increased from 15 to 25 J cm^{-2}. PARP cleavage is clearly visible only at most effective conditions. Such increase in PDT efficacy caused also an increase in the expression of p21 and p53 proteins; at variance, no changes were observed in the expression of Bcl-X_L. Indeed, time course experiments demonstrated that the expression profiles of Bcl-2, Bax, and other proteins analyzed returned to basal levels in about 10 h (data not shown). Possibly, the PDT-driven Bcl-2 disruption transiently deranged the equilibrium between

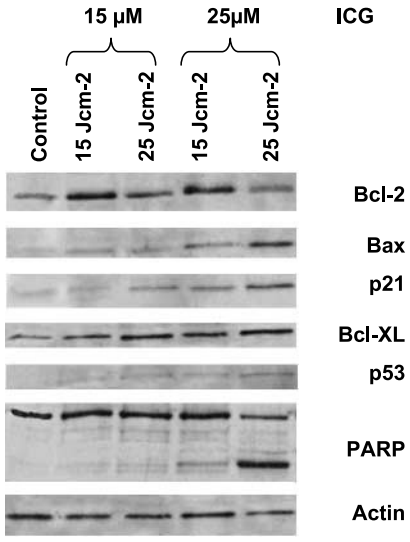

Figure 2. Expression of various proteins at different ICG concentrations and light fluence rates. Proteins were extracted 5 h after PDT. Note the effects on Bcl-2 (fading), Bax (increase), and PARP (fragmentation) at most drastic conditions.

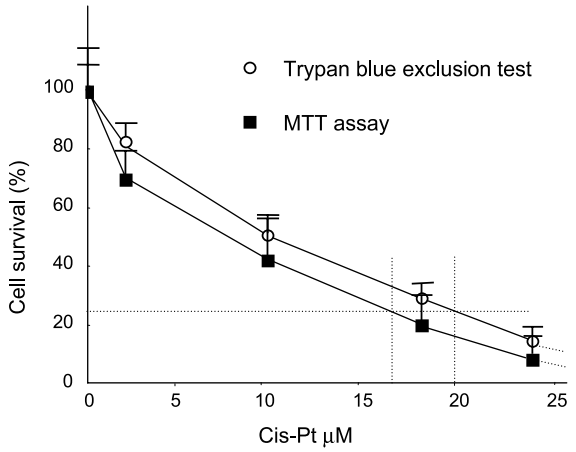

Figure 3. Effect of increasing concentrations of cisplatin (15 – 15 μM) on MCF-7 viability. Cells were incubated at the indicated cisplatin concentrations for 24 h. Cells were then washed with complete medium and left to stand for 5 h. Cell viability was measured by the trypan blue exclusion test (*open circles*) and MTT assay (*filled squares*). *Points,* average of four determinations; *bars,* SD.

proapoptotic and antiapoptotic proteins, thereby resulting in apoptosis of a small fraction of cells. The PARP fragmentation shown in Fig. 2 was unexpected because MCF-7 cells do not express caspase-3, the activation of which is a prerequisite for PARP degradation. However, apoptotic pathways that involve caspases (caspase-6 and/or caspase-7) other than caspase-3 have been described in MCF-7 cells (28, 29). MCF-7 human breast cancer cells are p53 positive and highly resistant to many harmful agents. The scarce sensitivity of MCF-7 cells to cisplatin-induced apoptosis has been ascribed to a functioning p53 because apoptosis was greater in cisplatin-treated cells in which p53 was abrogated (15). The effect of the antiapoptotic protein Bcl-2, the transcription of which is up-regulated in MCF-7 cells via two estrogen-responsive elements (13), may be an additional protective factor. However, apoptosis could not be elicited in these cells by photofrin/PDT even on p53 abrogation (16). Here, we report a similar observation with ICG/PDT. Although p53 and p21 expression was enhanced in relation to photosensitizer concentration and light dose (Fig. 2), only a limited fraction of cells may undergo apoptosis. The photodynamic destruction of the Bcl-2 protein, accompanied by Bax up-regulation, has already been reported in MCF-7 cells (30) although with a different photosensitizer (phthalocyanine Pc 4). Thus, Bcl-2 may also be a preferential target of ICG/PDT, and PDT-induced damage to Bcl-2 may explain the death of a fraction (10–12%) of MCF-7 cells. It is noteworthy that Bax expression increased as Bcl-2 expression declined. At present, we are unable to explain this increase. It was interesting to observe PARP fragmentation in the MCF-7 cells that lacked caspase-3; it is conceivable that ICG/PDT would trigger greater apoptosis in caspase-3-positive cells. This has indeed been shown in human retinal pigment epithelial cells (31) and in a human leukemic cell strain from a histiocytic lymphoma (8).

Dose-Response Effects of Cisplatin. Figure 3 shows the results of the trypan blue dye exclusion and MTT assays of cells treated with increasing concentrations of cisplatin (1.5–20.0 μM). The trypan blue assay reveals cells with intact membrane; the MTT assay is a measure of the reductive potential of mitochondrial enzymes. The cisplatin dose required to kill 75% of cells (ED_{75}) was near 20 μM according to the trypan blue exclusion test and 17 μM according to MTT data. With 8.0 μM cisplatin, almost 50–60% of cells were viable 5 h after withdrawal of the chemotherapeutic agent. Consequently, we used this sublethal cisplatin dose in the combined experiments reported hereafter.

Combined Treatments

In the experiments of combined treatment, we used 8 μM cisplatin and 20 μM ICG at a light fluence of 25 J cm^{-2}. Administered singly, these treatments were not lethal for MCF-7 cells. As shown in Fig. 4, cell viability as assessed by trypan blue assay (membrane integrity) was reduced by a factor of ~1.6 with 8 μM cisplatin, ~2.0 with ICG/PDT (20 μM/25 J cm^{-2}), and ~4 with combined treatment (cisplatin plus ICG/PDT) as compared with untreated controls. Similar results were obtained with the clonogenic assay (same figure), which measures the ability of each cell in the culture to maintain all the functions needed to divide and form a colony. The MTT assay gave somewhat different results: the reduction in cell viability was much greater with cisplatin plus PDT (~10-fold) than with the two treatments administered separately (~1.5- and ~2.0-fold, respectively).

Finally, we found that ICG/PDT and cisplatin target different phases of the cell cycle. In fact, only about 40% of the G_1 cell population survived ICG/PDT *versus* 65% of control cells. Differently, after cisplatin treatment, 85% of the surviving cells accumulated in the G_1 phase. This finding coincides with the observation that cisplatin induces cell cycle arrest and death in the S-G_2 phase (32). The cell cycle-related effect of ICG/PDT and cisplatin on MCF-7 cells ensures continuous apoptotic coverage throughout the cell cycle, thereby potentiating the overall lethal output.

Individual and Combined Treatments: Effects on Cell Metabolism

DNA Synthesis. The impairment of cellular function may be also measured by evaluating the ability of cells to incorporate thymidine into nuclear DNA. We assessed DNA synthesis in control and treated cells by measuring incorporation of thymidine into DNA. As expected, both chemotherapy and PDT significantly inhibited DNA synthesis. The residual capacity of cells to incorporate thymidine (Fig. 5, *hatched bars*) into DNA after individual treatments was reduced by a factor of ~1.3 in the presence of 8 μM cisplatin and by a factor of ~2 with ICG/PDT. As compared with untreated controls, DNA synthesis was reduced by ~10-fold with ICG/PDT plus cisplatin.

***De Novo* Synthesis of Proteins.** To evaluate whether protein synthesis was altered in the cells treated with ICG/PDT and cisplatin, we measured the percentage change in

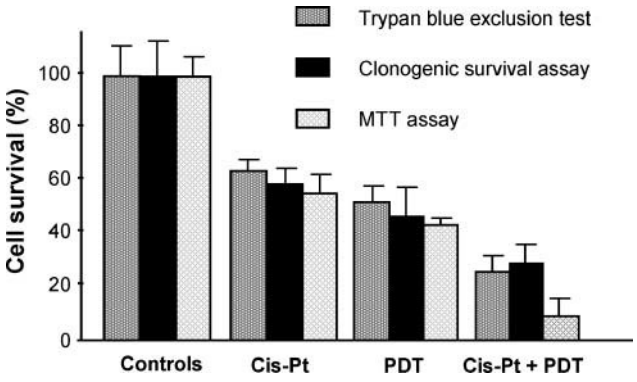

Figure 4. Viability of MCF-7 cells was estimated after single (8 μM cisplatin or 20 μM ICG/25 J cm^{-2}) or combined (8 μM cisplatin and 20 μM ICG/25 J cm^{-2}) treatments. Viability was measured with the trypan blue assay exclusion test, colony-forming assay (quantal responses), or MTT assay (variable response). *Columns,* average of four (trypan blue exclusion test and MTT assay) or two (colony-forming assay) determinations; *bars,* SD.

labeled methionine incorporated into neosynthesized proteins in normally growing cells (controls), in cells exposed for 24 h to cisplatin (8 μM), in cells irradiated at a fluence of 25 J cm^{-2} after 24 h incubation in a medium containing ICG (20 μM), and in cells exposed to both treatments (Fig. 5, *filled bars*). As expected, both chemotherapy and PDT significantly inhibited protein synthesis. The residual capacity of viable cells to incorporate methionine into their proteins after individual treatments was reduced by factors of ~1.6 and ~2.7, respectively, with respect to controls. On combined treatment, the capacity of cells to incorporate methionine approached 0.

Glucose Uptake. Glucose uptake and metabolism are increased in most cancer cells. It is well known that malignant cancer cells are unable to store glucose and depend on constant refurbishment to meet their energy requirements (33). It is also known that GLUT-1 expression is enhanced in malignant cells (34). Therefore, inhibition of deoxyglucose uptake, either basal or insulin stimulated, may give a measure of cell fitness. We found that single and combined treatments caused a significant reduction in (deoxy)glucose uptake (Fig. 6). The decrease paralleled the decrease in thymidine and methionine incorporation on similar treatments. Glucose transport was increased by 25–30% in control insulin-treated MCF-7 cells (Fig. 6). Both individual and combined treatment inhibited this response to insulin. The changes in DNA synthesis, protein synthesis, and glucose transport in surviving cells evaluated 5 h after treatment reflected the general trend of changes revealed by cell viability assays; moreover, they were very similar to the changes revealed by the MTT assay.

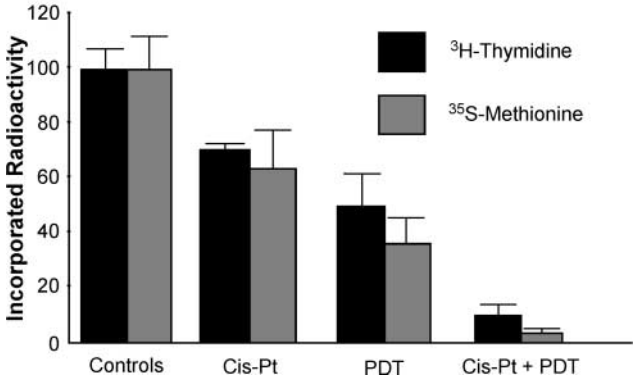

Figure 5. [^{3}H]Thymidine (*black bars*) and [^{35}S]methionine (*gray bars*) incorporation into MCF-7 cells after single (8 μM cisplatin or 20 μM ICG/25 J cm^{-2}) and combined (8 μM cisplatin and 20 μM ICG/25 J cm^{-2}) treatments. *Columns,* average of three determinations; *bars,* SD.

Isobolographic Assessment of the Effects of Combinations of PDT and Cisplatin

The effects of combined treatments may be evaluated by analyzing dose-response experimental data isobolographically. Dose-response phenomena can have either quantal or measurement values. Quantal responses are framed by questions about what fraction of exposed organisms showed the index response. Measurement responses are those with magnitude that usually increases or decreases as a continuous variable in response to mounting stimuli. In this regard, we constructed isobolograms with quantal data (trypan blue assay; Fig. 7, *upper panel*) and variable data (MTT assay; Fig. 7, *lower panel*). Dose-response curves were assessed by evaluating cell viability with the trypan blue or MTT assay at fixed cisplatin concentration (8 μM) followed by irradiation with fluences between 0 and 60 J cm^{-2} (20 μM ICG).

Based on MTT data, the fluence rate required to obtain 75% lethality (ED_{75}) was lower than that indicated by trypan blue assay data. In fact, as shown in Fig. 7, MTT was better than trypan blue in detecting cell viability. The first isobologram (trypan blue data) shows that PDT plus cisplatin had an additive effect, whereas the second

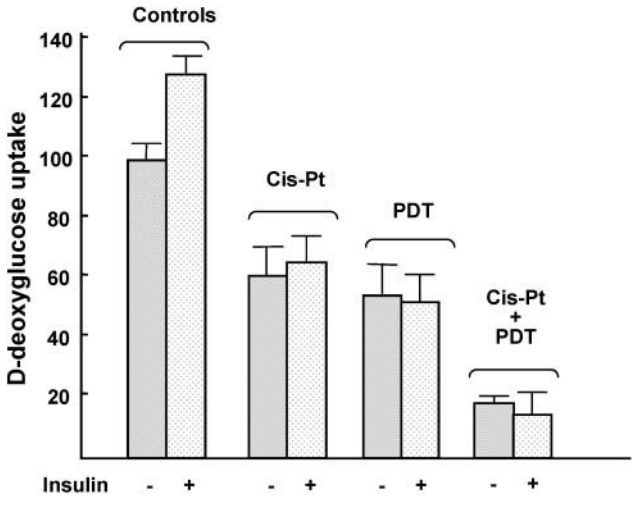

Figure 6. Basal *versus* insulin-stimulated [^{14}C]deoxyglucose incorporation into MCF-7 cells after single (8 μM cisplatin or 20 μM ICG/25 J cm^{-2}) and combined (8 μM cisplatin and 20 μM ICG/25 J cm^{-2}) treatments. *Columns,* average of three determinations; *bars,* SD.

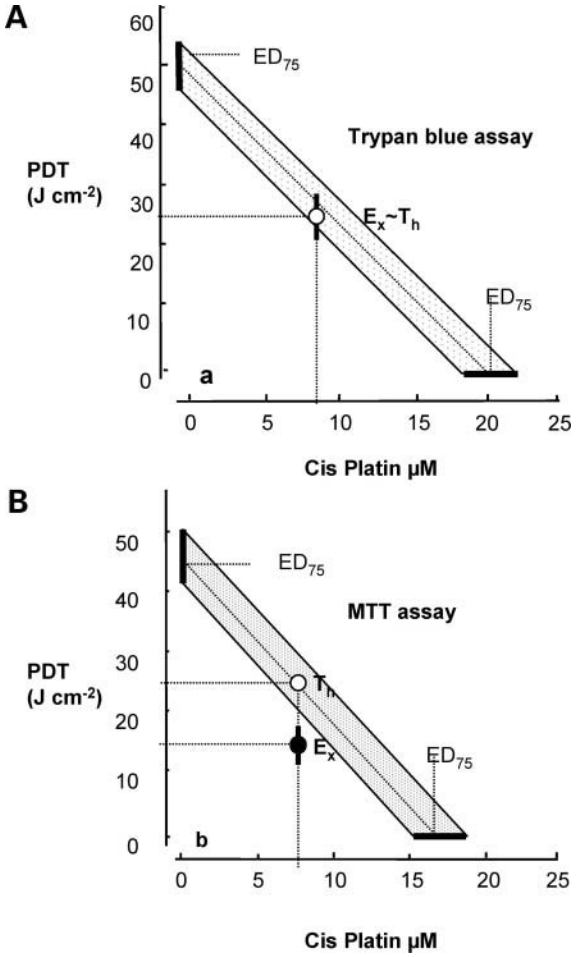

Figure 7. Isobolographic analysis of data obtained with combined treatments. **A,** isobologram constructed with E_{75} data measured by the trypan blue assay. The theoretical light fluence (T_h) that must be used with 8 μM cisplatin to obtain an E_{75} coincides with the experimental value (E_x). The effect is additive. **B,** isobologram constructed with E_{75} data measured by MTT assay. The theoretical light fluence (T_h) that must be used with 8 μM cisplatin to obtain an E_{75} is about 10 J cm^{-2} higher than the experimental value (E_x). The effect is synergistic.

isobologram (MTT data) shows that it had a synergistic effect. This observation is in line with the possibility that metabolic impairment of cells (measured by MTT), which occurs well before cells are irreversibly damaged (detected by trypan blue), is a more sensitive indicator of cell fitness.

Although the response to the various treatments, as assessed by trypan blue and MTT data, was similar, the magnitude of change differed between the two techniques. In fact, the response was additive based on trypan blue data and quasi-synergistic based on MTT data. In both cases, combined treatment resulted in mutual reinforcement of destructive efficacy. This observation is supported by the cell cycle analysis of cells exposed to PDT, cells incubated with low-dose cisplatin, and cells exposed to PDT after incubation with low-dose cisplatin. In fact, cisplatin killed mostly S-phase cells, whereas ICG/PDT killed mostly G_1-phase cells. Only a small fraction of cells survived combined treatment, although cisplatin and ICG/PDT administered singly would kill only a limited number of cells. Obviously, preincubation of MCF-7 cells with the usual cisplatin dose (8 μM) followed by their exposure to higher light fluences (*e.g.*, 40 J cm^{-2}) results in the rapid death of all cells. Therefore, in principle, a combination consisting of a low dose of cisplatin and appropriately adjusted ICG/PDT dosage (*i.e.*, higher light fluence and/or photosensitizer concentration) would be effective. This strategy was among those listed by Dolmans *et al.* (35) in their review of PDT for cancer treatment. Our study supports the validity of this strategy and provides a clinical perspective. In fact, it appears from our data that the adverse effects of chemotherapy can be partially abated without reducing the efficacy of treatment. Obviously, this hypothesis should be tested in *in vivo* models before being applied in human therapy.

Acknowledgments

We thank Jean Ann Gilder for text editing.

References

1. Oleinick NL, Morris RL, Belichenko I. The role of apoptosis in response to photodynamic therapy: what, where, why, and how. Photochem Photobiol Sci 2002;1(1):1 – 21.

2. Gomer CJ, Dougherty, TJ. Determination of ^3H and ^{14}C hematoporphyrin derivative distribution in malignant and normal tissues. Cancer Res 1979;39(1):146 – 51.

3. Dougherty TJ, Gomer CJ, Henderson BW, et al. Photodynamic therapy [review]. J Natl Cancer Inst 1998;90(12):889 – 905.

4. Wyld L, Reed MW, Brown NJ. Differential cell death response to photodynamic therapy is dependent on dose and cell type. Br J Cancer 2001;84(10):1384 – 6.

5. Nahimisa T. Indocyanine green test and its development. Tokai J Exp Clin Med 1982;7(4):419 – 23.

6. Fox IJ, Wood WH. Indocyanine green: physical and physiologic properties. Mayo Clin Proc 1960;35:732 – 44.

7. Bäumler W, Abels C, Karrer S, et al. Photo-oxidative of human colonic cancer cells using indocyanine green and infrared. Br J Cancer 1999; 80(3 – 4):360 – 3.

8. Varriale L, Crescenzi E, Paba V, Mazziotti di Celso B, Palumbo G. Selective light-induced modulation of Bcl-X_L and Bax expressions in indocyanine green-loaded U937 cells: effects of continuous or intermittent photo-sensitization with low IR-light using a 805-nm diode laser. J Photochem Photobiol B Biol 2000;57(1):66 – 75.

9. Crul M, van Waardenburg RCA, Beijnen JH, Schellens JHM. DNA-based drug interactions of cis-platin. Cancer Treat Rev 2002;28(6):291 – 303.

10. Soule HD, Vazquez J, Albert S, Brennan MJ. A human cell line from a pleural effusion derived from a breast carcinoma. J Natl Cancer Inst 1973; 51(6):1409 – 16.

11. Vairo G, Soos TJ, Uoton TMV, et al. Bcl-2 retards cell cycle entry, through p27(kip1), pRb relative p130, and altered E2F regulation. Mol Cell Biol 2000;20(13):4745 – 53.

12. Zamzami N, Brenner C, Marzo I, Susin SA, Kroemer G. Subcellular and submitochondrial mode of action of Bcl-2-like oncoprotein. Oncogene 1998;16(17):2265 – 82.

13. Perillo B, Sasso A, Abbondanza C, Palumbo G. 17-β-estradiol inhibits apoptosis in MCF-7 cells, inducing Bcl-2 expression via two estrogen-responsive elements present in the coding sequence. Mol Cell Biol 2000; 8(8):2890 – 901.

14. Janicke RU, Sprengart ML, Wati MR, Porter AG. Caspase-3 is required for α-fodrin cleavage but dispensable for cleavage of other death substrates in apoptosis. J Biol Chem 1998;273(16):9357 – 60.

15. Fan S, Smith ML, Rivet DJ Jr, et al. Disruption of p53 function

sensitizes breast cancer MCF-7 cells to cisplatin and pentoxifylline Cancer Res 1995;55(8):1649 – 54.

16. Fischer AMR, Ferrario A, Rucher N, Zhang S, Gomer CJ. PDT sensitivity is not altered in human tumor cells after abrogation of p53 function. Cancer Res 1999;59(2):331 – 5.

17. Fickweiler S, Szeimies, RM Bäumler, W et al. Indocyanine green: intracellular uptake and phototherapeutic effects *in vitro*. J Photochem Photobiol B Biol 1997;38(2 – 3):178 – 83.

18. Yoshida Y, Hosokawa K, Dantes A, Tajima K, Kotsuji F, Amsterdam A. Theophylline and cisplatin synergize in down regulation of BCL-2 induction of apoptosis in human granulosa cells transformed by a mutated p53 (p53 val135) and Ha-ras oncogene. Int J Oncol 2000;17(2):227 – 35.

19. Theodossiu C, Cook JA, Fisher J, et al. Interaction of gemcitabine with paclitaxel and cis-platin in human tumor cell lines. Int J Oncol 1998; 12(4):825 – 32.

20. Love-Schimenti CD, Gibson DF, Ratnam AV, Bikle DD. Antiestrogen potentiation of antiproliferative effects of vitamin D3 analogues in breast cancer cells. Cancer Res 1996;56(12):2789 – 94.

21. Bradford MM. A rapid and sensitive method for the quantitation of microgram quantities of protein utilizing the principle of protein-dye binding. Anal Biochem 1976;72:248 – 54.

22. Consiglio R, Rengo S, Liguoro D, et al. Inhibition by glass-ionomer cements of protein synthesis by human gingival fibroblasts in continuous culture. Arch Oral Biol 1998;43(1):65 – 71.

23. Singh A, Purohit A, Hejaz, HA, Potter, BV, Reed, MJ. Inhibition of deoxyglucose uptake in MCF-7 breast cancer cells by 2-methoxyestrone and 2-methoxyestrone-3-*O*-sulfamate. Mol Cell Endocrinol 2000;160 (1 – 2):61 – 6.

24. Wellman PJ, Tow S, McMahon L. Isobolographic assessment of the effects of combinations of phenylpropanolamine and fenfluramine on food intake in rats. Pharmacol Biochem Behavior 1995;50(2):287 – 91.

25. Gessner PK. Isobolographic analysis of interactions: an update on applications and utility. Toxicology 1995;105(2 – 3):161 – 79.

26. Laemmli UK. Cleavage of structural proteins during the assembly of the head of bacteriophage T4. Nature 1970;227(259):680 – 5.

27. Varriale L, Coppola E, Quarto M, Veneziani BM, Palumbo G. Molecular aspects of photodynamic therapy: low energy pre-sensitization of hypericin loaded human endometrial carcinoma cells enhances phototolerance, alters gene expression and affects cell cycle. FEBS Lett 2002; 512(1 – 3):287 – 90.

28. Mooney LM, Al-Sakkaf KA, Brown BL, Dobson PR. Apoptotic mechanisms in T47D and MCF-7 human breast cancer cells. Br J Cancer 2002;87(8):909 – 17.

29. Mc Gee MM, Hyland E, Campiani G, Ramunno A, Nacci V, Zisterer DM. Caspase-3 is not essential for DNA fragmentation in MCF-7 cells during apoptosis induced by the pyrrolo-1,5-benzoxazepine. FEBS Lett 2002;515(1 – 3):66 – 70.

30. Xue LY, Chiu SM, Oleinick NL. Photochemical destruction of the Bcl-2 oncoprotein during photodynamic therapy with the phthalocyanine photosensitizer Pc 4. Oncogene 2001;20(26):3420 – 7.

31. Yam HF, Kwok AK, Chan KP, et al. Effect of indocyanine green and illumination on gene expression in human retinal pigment epithelial cells. Invest Ophthalmol Vis Sci 2003;44(1):370 – 7.

32. Chou G. Cellular responses to cis-platin. The roles of DNA-binding proteins and DNA repair. J Biol Chem 1994;269(2):787 – 90.

33. Warburg O. On the origin of cancer cells. Science 1956;123(3191): 309 – 14.

34. Younes M, Lechago LV, Somoano JR, Mosharaf M, Lechago J. Wide expression of the human erythrocyte glucose transporter GLUT-1 in human cancers. Cancer Res 199;56(5):1164 – 7.

35. Dolmans DE, Fukumara D, Rakesh KJ. Photodynamic therapy for cancer. Nat Rev Cancer 2003 May;3(5):380 – 7.